Introduction to radio astronomy
Lectures 7 & 8

Miroslav Bárta
barta@asu.cas.cz

EUROPEAN ARC
ALMA Regional Centre || Czech

Astronomical Institute of the Czech Academy of Sciences

Outline – Part IV

- Interferometric imaging – aperture synthesis
  - Difference to phased arrays
  - Mathematical foundations: Van Cittert-Zernike theorem
  - Geometrical considerations and coordinate systems
  - From complex visibilities to image: Gridding, weighting, IFT & deconvolution
  - Dirty and clean images
  - Cleaning algorithms
- Calibration of interferometric spectral data
  - „System“ imperfectness: Atmosphere, pointing, antenna…
  - Total flux
  - Bandpass – spectral flattening
  - Amplitude & phase variations
  - Applying the calibration tables
- Modern frequency-agile interferometric arrays
  - LOFAR, SKA, MUSER
  - ALMA
  - ARCs: The ALMA user-support infrastructure

Interferometry: Basic approaches

Phased arrays

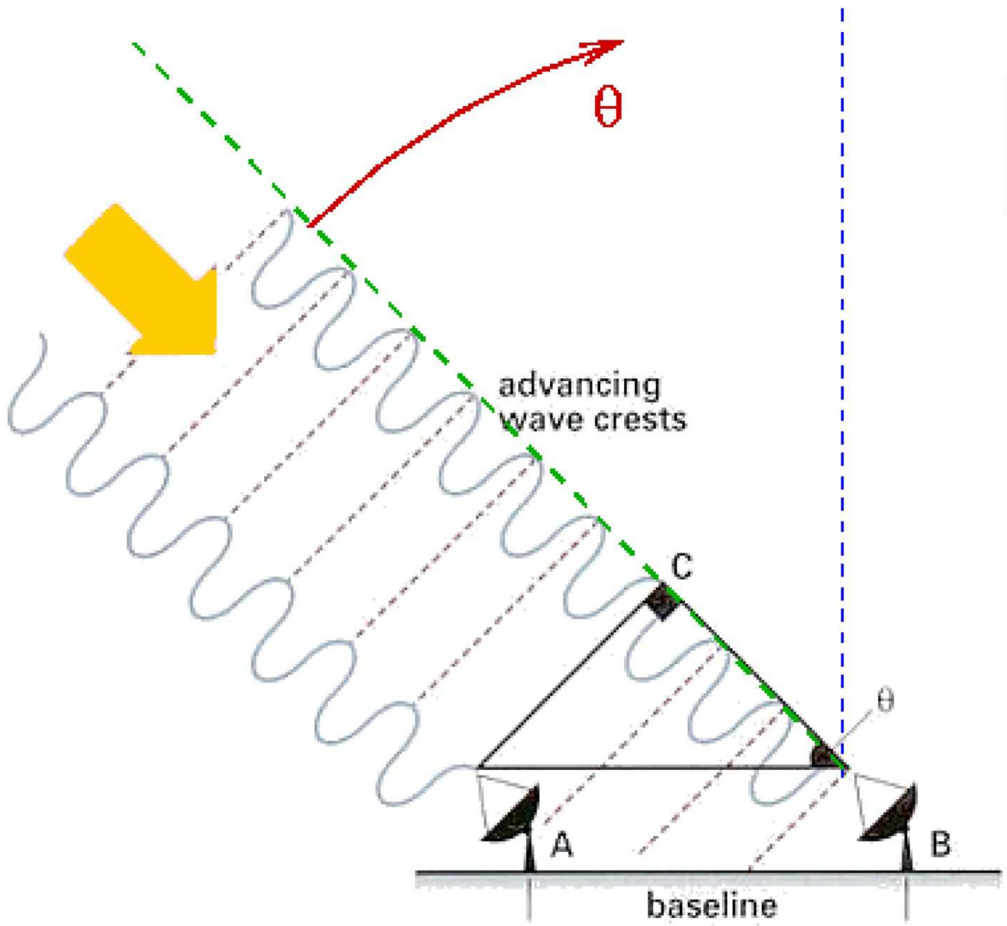

$$|I_{AB}(\theta)| = 1 + \cos\frac{2\pi D}{\lambda}\theta$$

Interferometry: Basic approaches

Phased arrays

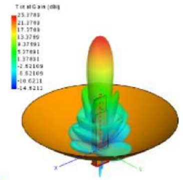

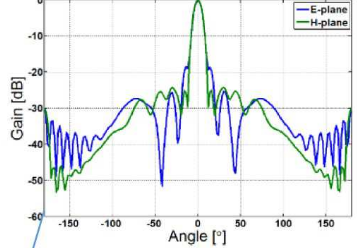

Old good times – sparse antenna rows / phased arrays (beam forming)

Analogy with optical gratings used in spectrographs

$$|I_\Sigma(\theta)| = \frac{1 - \cos \mathrm{N} \frac{2\pi D}{\lambda}\theta}{1 - \cos \frac{2\pi D}{\lambda}\theta}$$

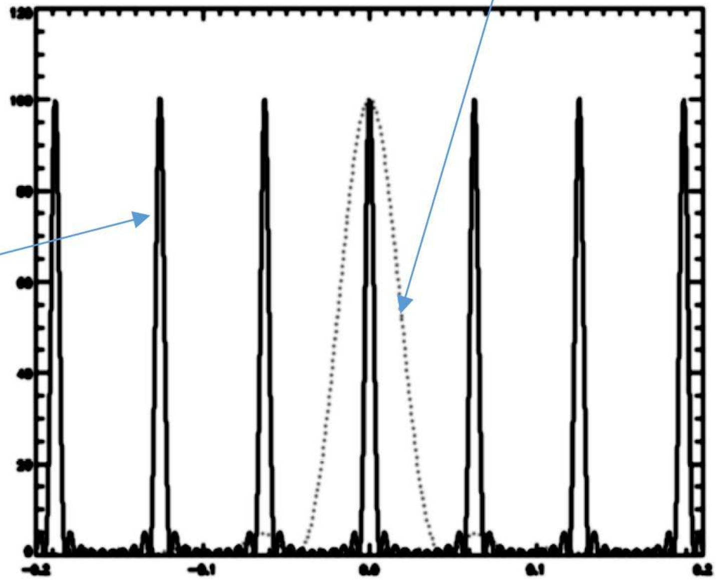

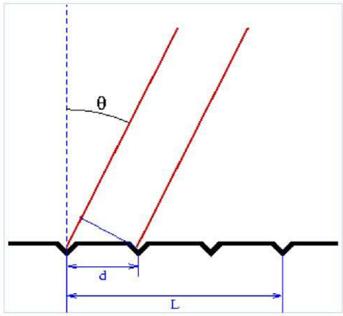

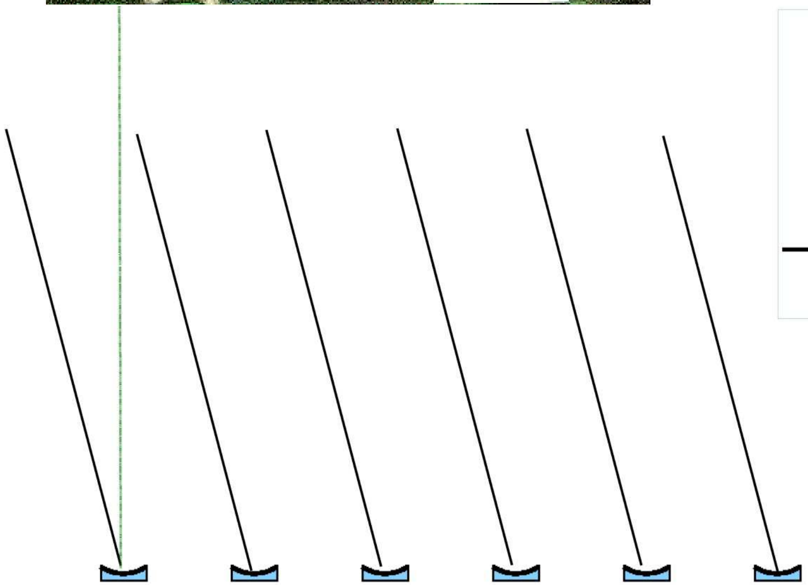

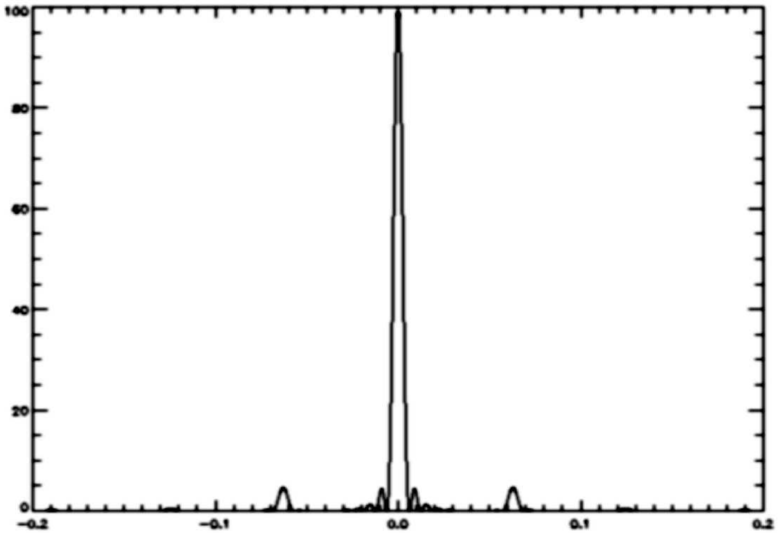

Interferometry: Basic approaches

Old good times – sparse antenna rows/ phased arrays

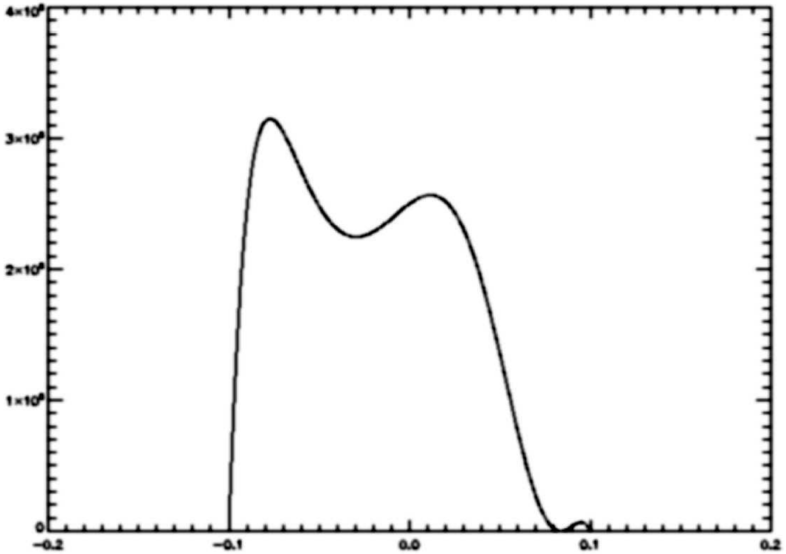

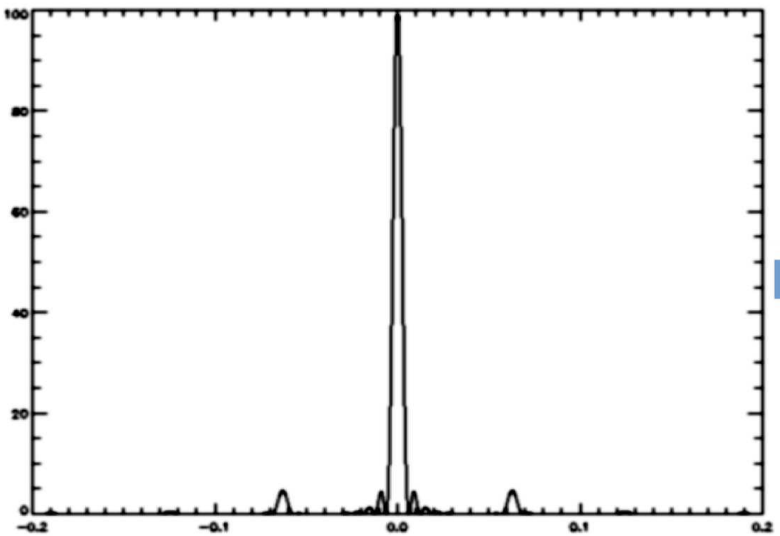

- Scanning with the beam
- Frequently supplied by MFI

Interferometry: Basic approaches

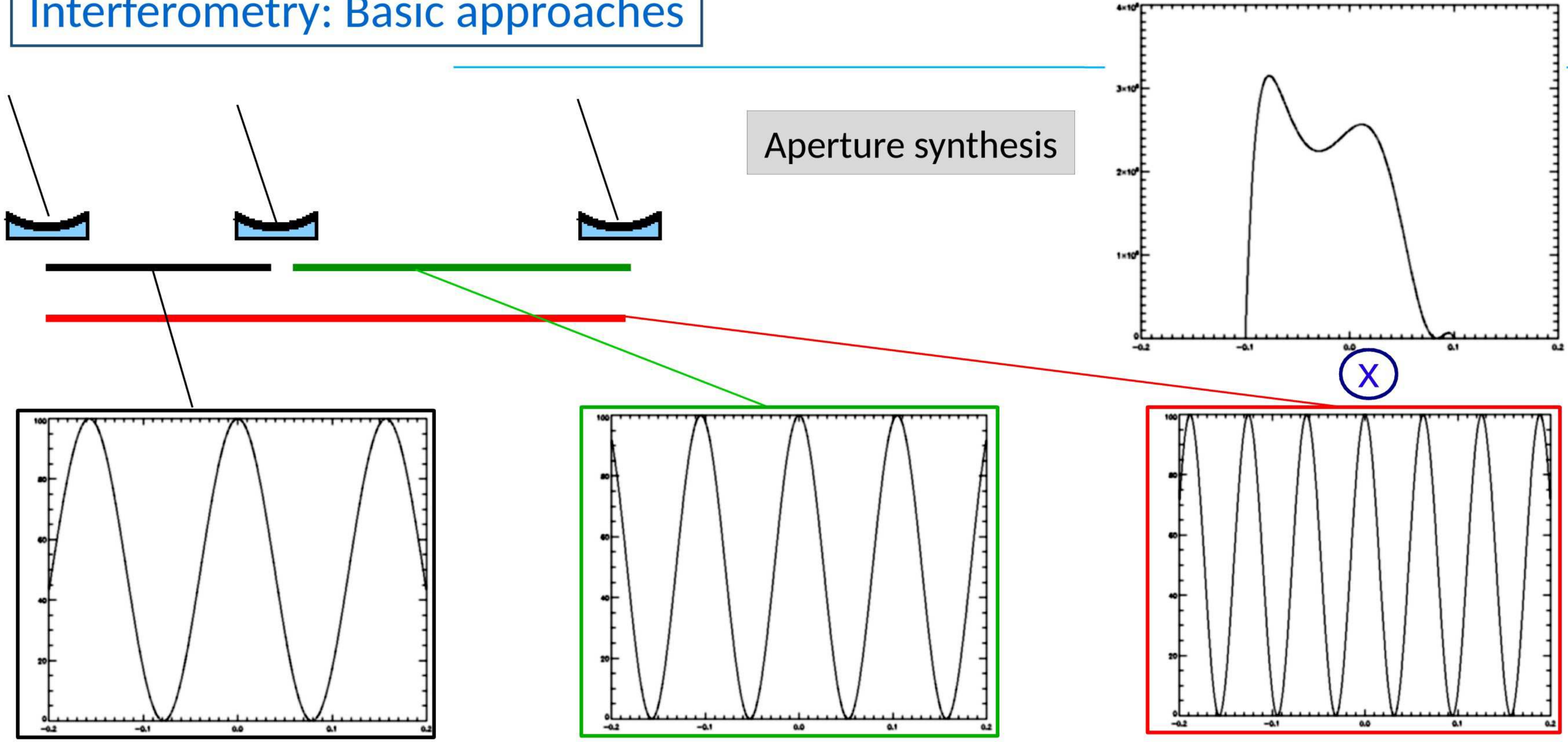

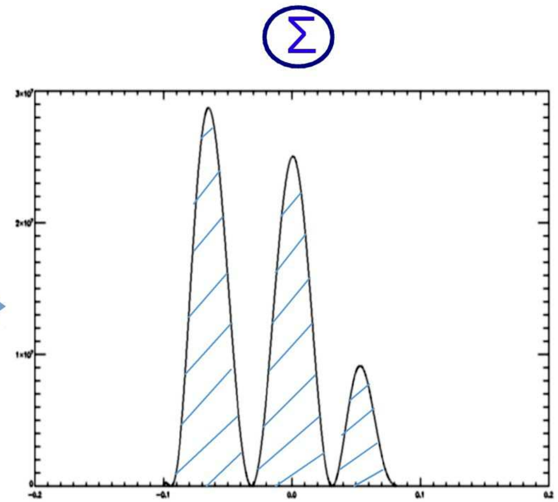

Nowadays: Aperture synthesis – decomposition of image to harmonics = Fourier transform

$$\langle I_{AB}(\theta)\rangle = \langle E_A\rangle.\overline{\langle E_B\rangle} = \int_{-\infty}^{+\infty} B(\theta)\exp\left(i\frac{2\pi D}{\lambda}\theta\right)d\theta$$

Cross-correlations – interferometric visibilities

Interferometry: Basic approaches

Aperture synthesis

$$\langle I_{AB}\rangle(\theta) = \int_{-\infty}^{+\infty} B(\theta)\exp\left(i\frac{2\pi D}{\lambda}\theta\right)d\theta$$

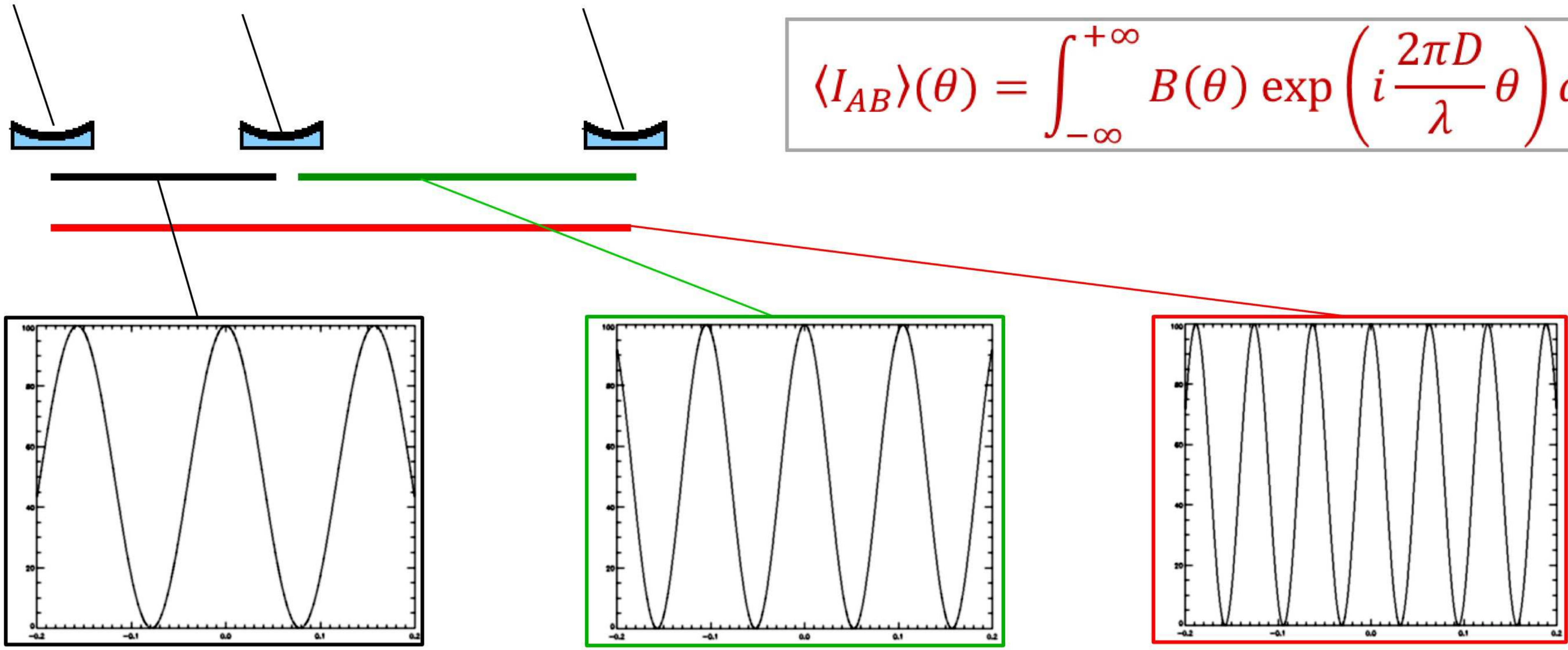

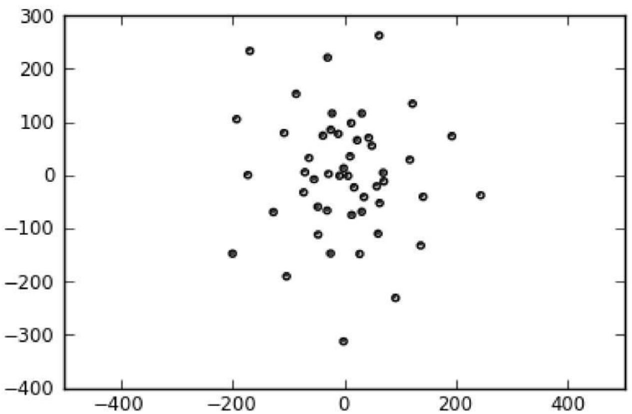

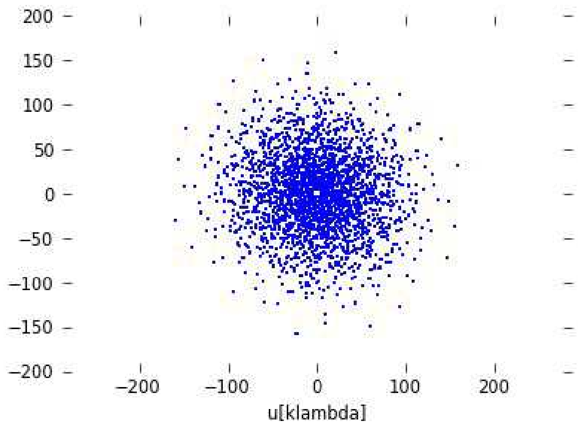

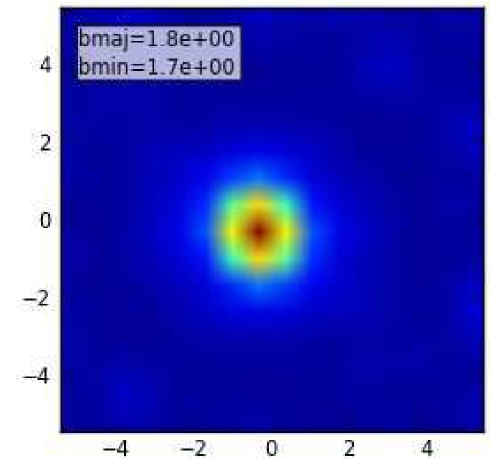

Aperture synthesis: Mathematical foundations

2-element interferometric correlator

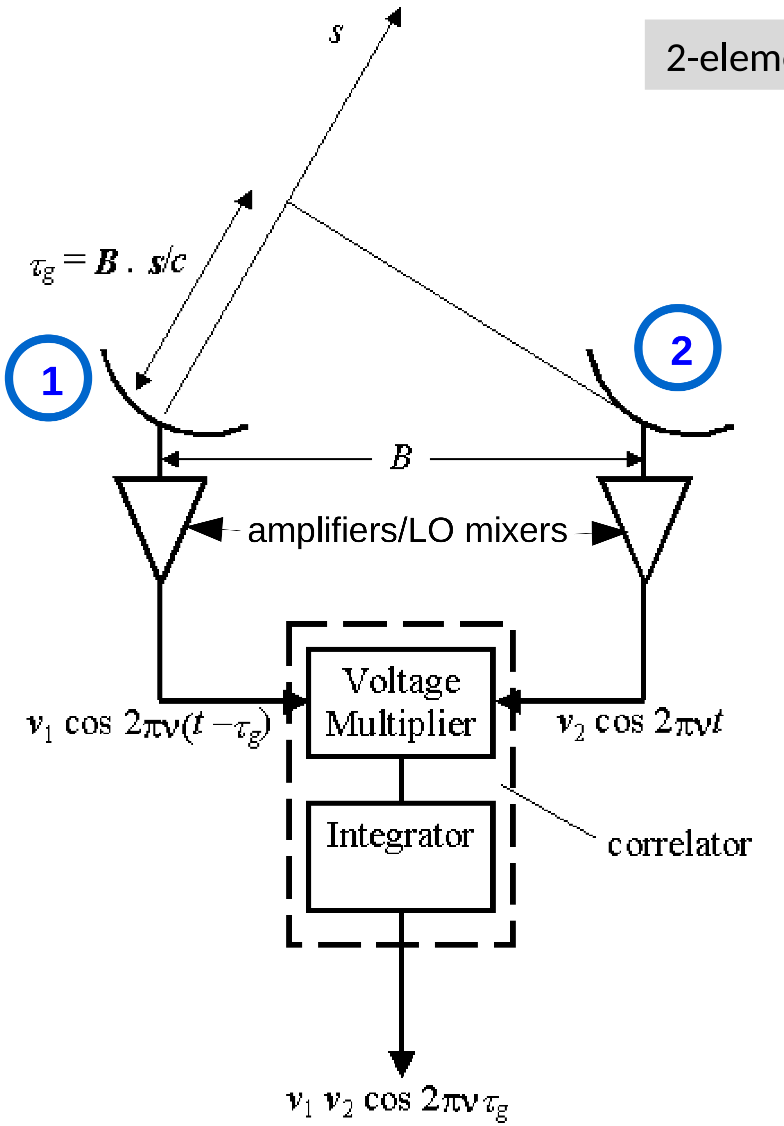

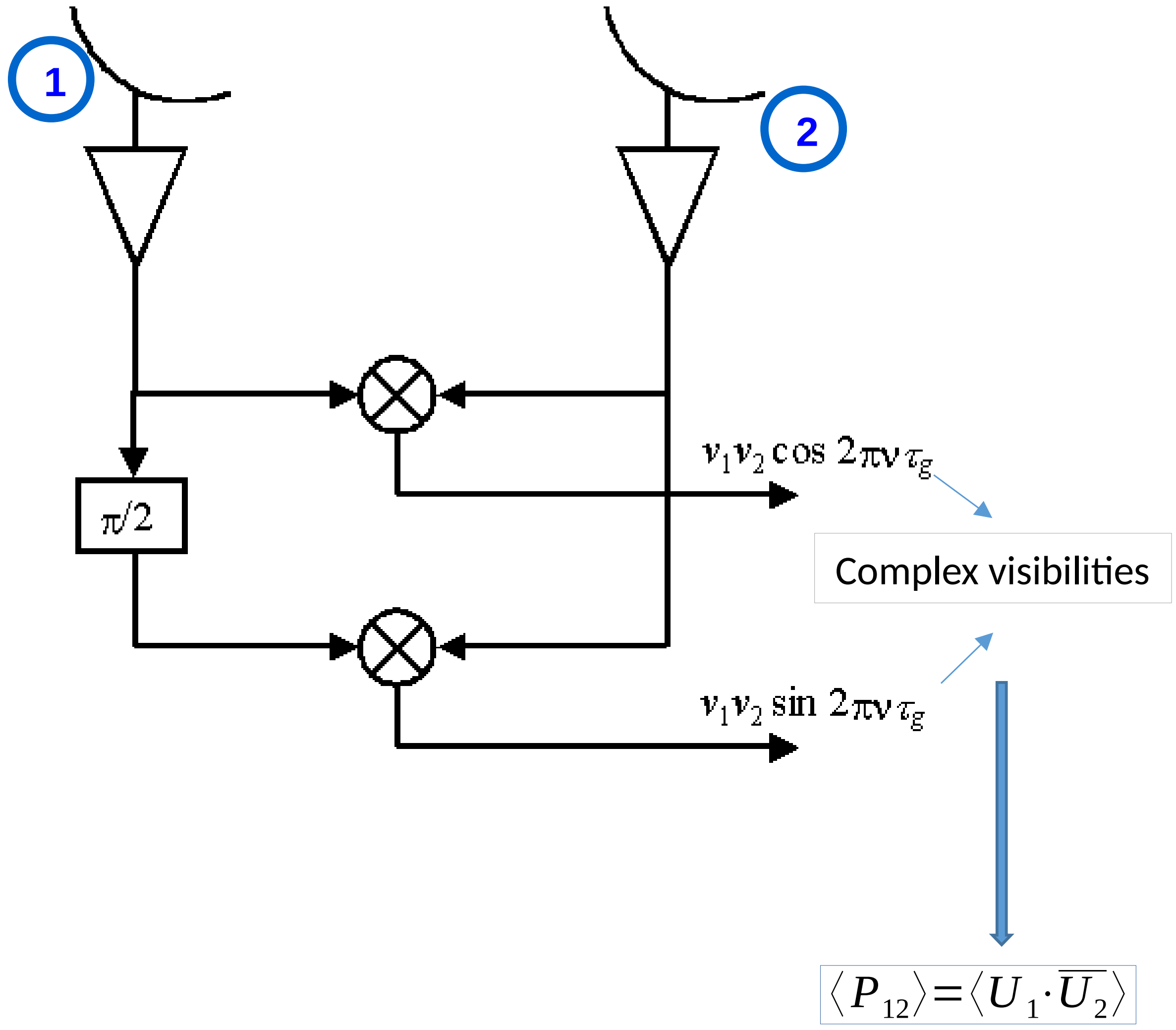

Aperture synthesis: Mathematical foundations

2-element interferometric correlator

1-D Geometry

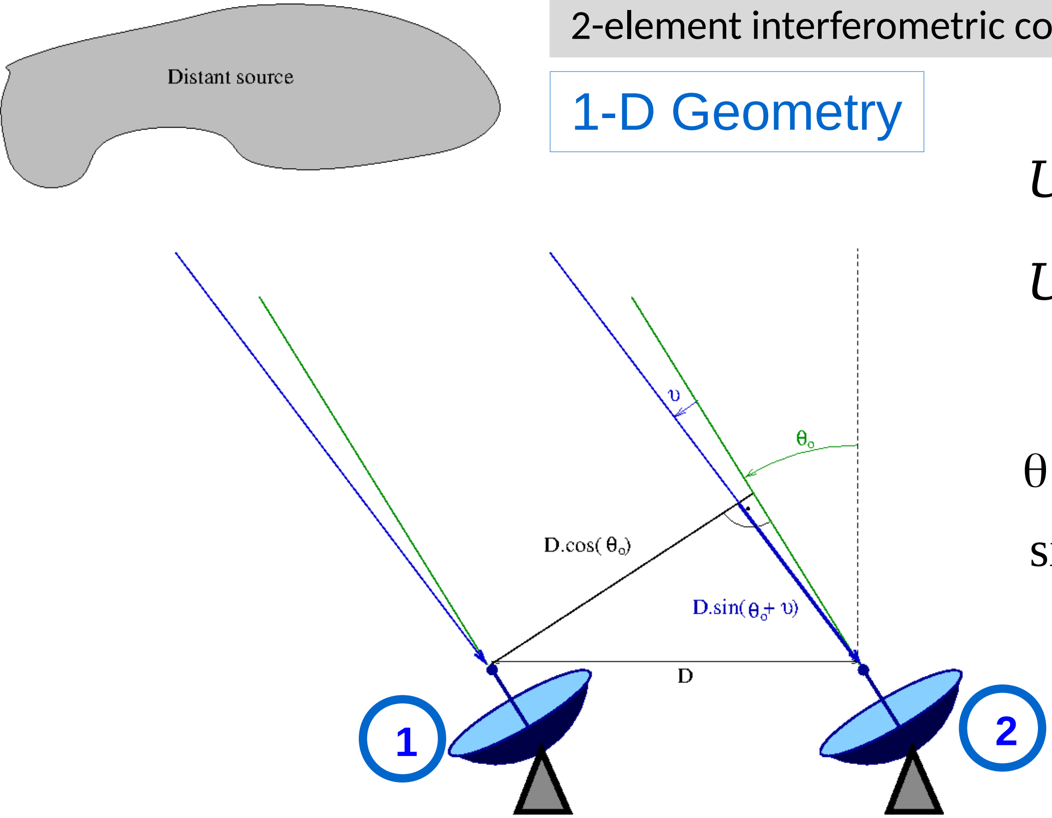

$$\langle P_{12}\rangle = \langle U_1 \cdot \overline{U_2}\rangle$$

$$U_1 = G_1 \cdot \int_{-\infty}^{+\infty} E(\theta)\cdot e^{i\varphi(\theta)}\cdot e^{-i\omega t}\, d\theta$$

$$U_2 = G_2 \cdot \int_{-\infty}^{+\infty} E(\theta)\cdot e^{i\varphi(\theta)}\cdot e^{-i\omega t}\cdot \exp\left(i\frac{2\pi D\sin\theta}{\lambda}\right) d\theta$$

"compact"-source assumption

$$\theta = \theta_0 + \vartheta$$

$$\sin(\theta_0+\vartheta) = \sin\theta_0\cos\vartheta + \cos\theta_0\sin\vartheta \approx \sin\theta_0 + \cos\theta_0\cdot\vartheta$$

$$U_1 = G_1 \cdot \int_{-\infty}^{+\infty} E(\vartheta)\cdot e^{i\varphi(\vartheta)}\cdot e^{-i\omega t}\, d\vartheta$$

$$U_2 = G_2 \cdot \int_{-\infty}^{+\infty} E(\vartheta)\cdot e^{i\varphi(\vartheta)}\cdot e^{-i\omega t}\cdot \exp\left(i\frac{2\pi D\sin\theta_0}{\lambda} + i\frac{2\pi D\vartheta\cdot\cos\theta_0}{\lambda}\right) d\vartheta$$

Pointing delay

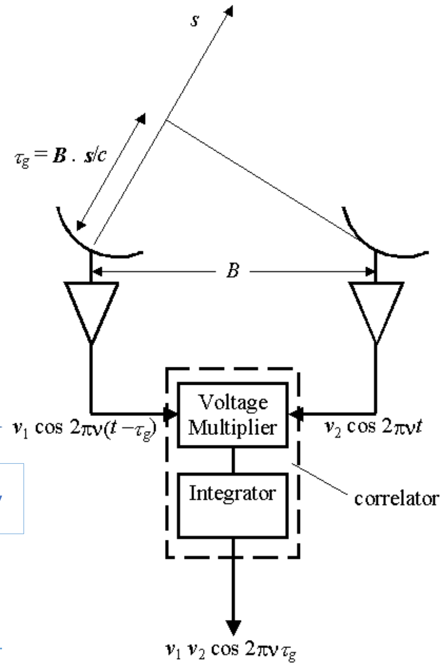

$$U_2 = G_2 \cdot \int_{-\infty}^{+\infty} E(\vartheta)\cdot e^{i\varphi(\vartheta)}\cdot e^{-i\omega t}\cdot \exp\left(i\frac{2\pi D\vartheta\cdot\cos\theta_0}{\lambda}\right) d\vartheta$$

Aperture synthesis: Mathematical foundations

2-element interferometric correlator

1-D Geometry

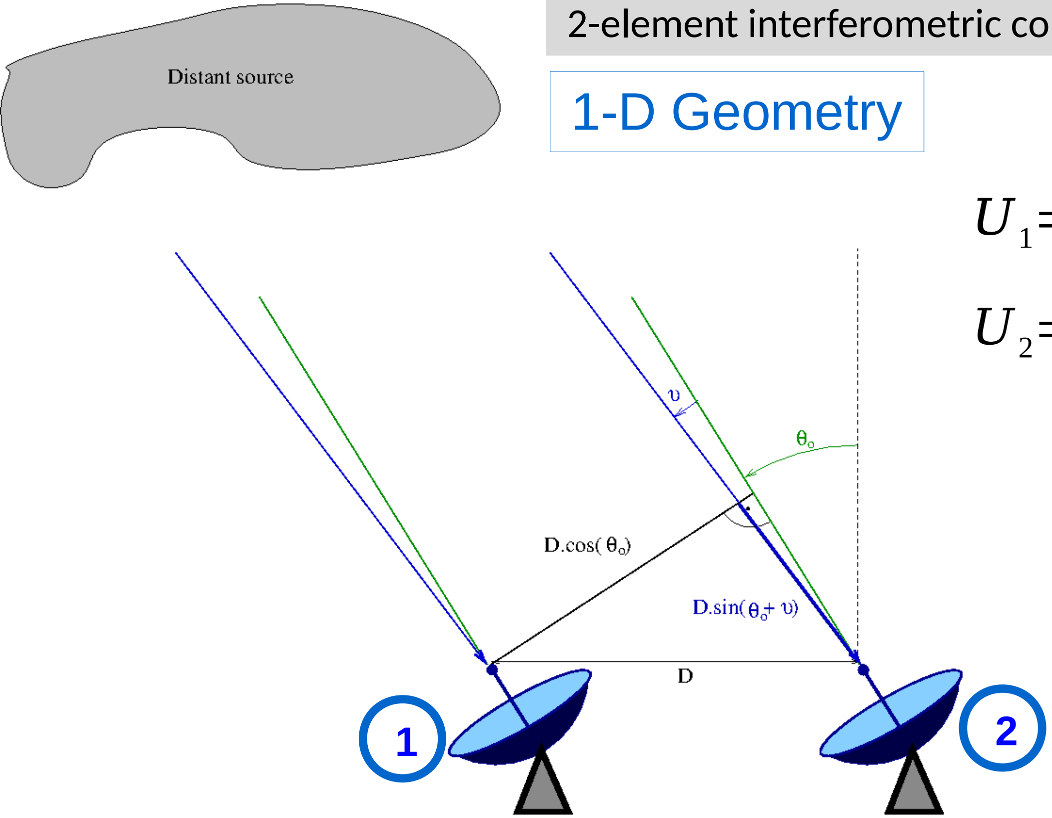

$$U_1 = G_1 \cdot \int_{-\infty}^{+\infty} E(\vartheta) \cdot e^{i\varphi(\vartheta)} \cdot e^{-i\omega t} d\vartheta$$

$$U_2 = G_2 \cdot \int_{-\infty}^{+\infty} E(\vartheta) \cdot e^{i\varphi(\vartheta)} \cdot e^{-i\omega t} \cdot \exp\left(i \frac{2\pi D \vartheta \cdot \cos\theta_0}{\lambda}\right) d\vartheta$$

$$\langle P_{12} \rangle = \langle U_1 \cdot \overline{U_2} \rangle = G_1 \overline{G_2} \cdot \left\langle \iint_{-\infty}^{+\infty} E(\vartheta) e^{i\varphi(\vartheta)} e^{-i\omega t} \cdot E(\vartheta') e^{-i\varphi(\vartheta')} e^{i\omega t} \cdot \exp\left(-i \frac{2\pi D \cos\theta_0 \cdot \vartheta'}{\lambda}\right) d\vartheta d\vartheta' \right\rangle$$

$$\langle P_{12} \rangle = G_1 \overline{G_2} \cdot \left\langle \iint_{-\infty}^{+\infty} E(\vartheta) \cdot E(\vartheta') e^{i\varphi(\vartheta) - i\varphi(\vartheta')} \cdot \exp\left(-i \frac{2\pi D \cos\theta_0 \cdot \vartheta'}{\lambda}\right) d\vartheta d\vartheta' \right\rangle$$

Aperture synthesis: Mathematical foundations

$$\langle P_{12}\rangle = G_1 \overline{G_2} \cdot \left\langle \iint_{-\infty}^{+\infty} E(\vartheta)\cdot E(\vartheta')\, e^{i\varphi(\vartheta)-i\varphi(\vartheta')} \cdot \exp\left(-i\,\frac{2\pi D\cos\theta_0 \cdot \vartheta'}{\lambda}\right) d\vartheta\, d\vartheta' \right\rangle$$

$$U = U_a + U_b$$

random-phase assumption

and the mutual coherence function (G.1) is

$$\begin{aligned}\langle U(P_1,t_1)U^*(P_2,t_2)\rangle &= \langle\{U_a(P_1,t_1)+U_b(P_1,t_1)\}\{U_a(P_2,t_2)+U_b(P_2,t_2)\}^*\rangle \\ &= \langle U_a(P_1,t_1)U_a^*(P_2,t_2)\rangle + \langle U_b(P_1,t_1)U_b^*(P_2,t_2)\rangle \\ &\quad + \langle U_a(P_1,t_1)U_b^*(P_2,t_2)\rangle \\ &\quad + \langle U_b(P_1,t_1)U_a^*(P_2,t_2)\rangle\,. \qquad \text{(G.7)}\end{aligned}$$

If we assume the two wave fields U_a and U_b are *incoherent*, we require that the field strengths U_a and U_b are uncorrelated even when measured at the same point, so that

$$\langle U_a(P_1,t_1)U_b^*(P_2,t_2)\rangle = \langle U_b(P_1,t_1)U_a^*(P_2,t_2)\rangle \equiv 0\,. \qquad \text{(G.8)}$$

$$\langle P_{12}\rangle = G_1 \overline{G_2} \cdot \iint_{-\infty}^{+\infty} I(\vartheta)\cdot \exp\left(-i\,\frac{2\pi D\cos\theta_0\cdot\vartheta}{\lambda}\right) d\vartheta$$

$$\langle P_{12}\rangle = G_1 \overline{G_2} \cdot \int_{-\infty}^{+\infty} I(\vartheta)\cdot \exp(-2\pi i u \vartheta)\, d\vartheta$$

$$u = \frac{D\cos\theta_0}{\lambda}$$

Aperture synthesis: Mathematical foundations

$$\langle P_{12}\rangle = G_1 \overline{G_2} \cdot \int_{-\infty}^{+\infty} I(\vartheta)\cdot \exp(-2\pi i u \vartheta)\, d\vartheta$$

2-element interferometric correlator

Van Cittert – Zernike theorem (1934)

Generalisation for 2D

$$\langle P_{12}\rangle = G_1 \overline{G_2} \cdot \iint_{-\infty}^{+\infty} I(l,m)\cdot \exp(-2\pi i (u\cdot l + v\cdot m))\, dl\, dm$$

distant-source assumption

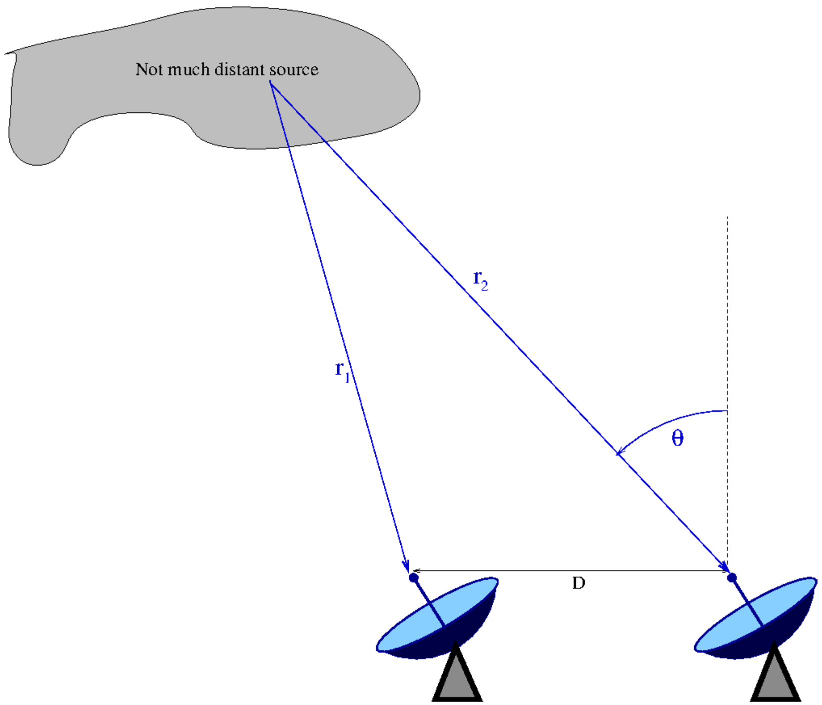

$$r_1^2 = r_2^2 + D^2 - 2 r_2 D\cos(\pi/2 - \theta)$$

$$(r_2 - r_1)(r_2 + r_1) = -D^2 + 2 r_2 D\sin\theta$$

$$r_2 - r_1 \approx D\sin\theta - \frac{D^2}{2r} \rightarrow \frac{D^2}{2r} \ll \lambda$$

considered phase delay

Generalisation – hetererogeneous arrays

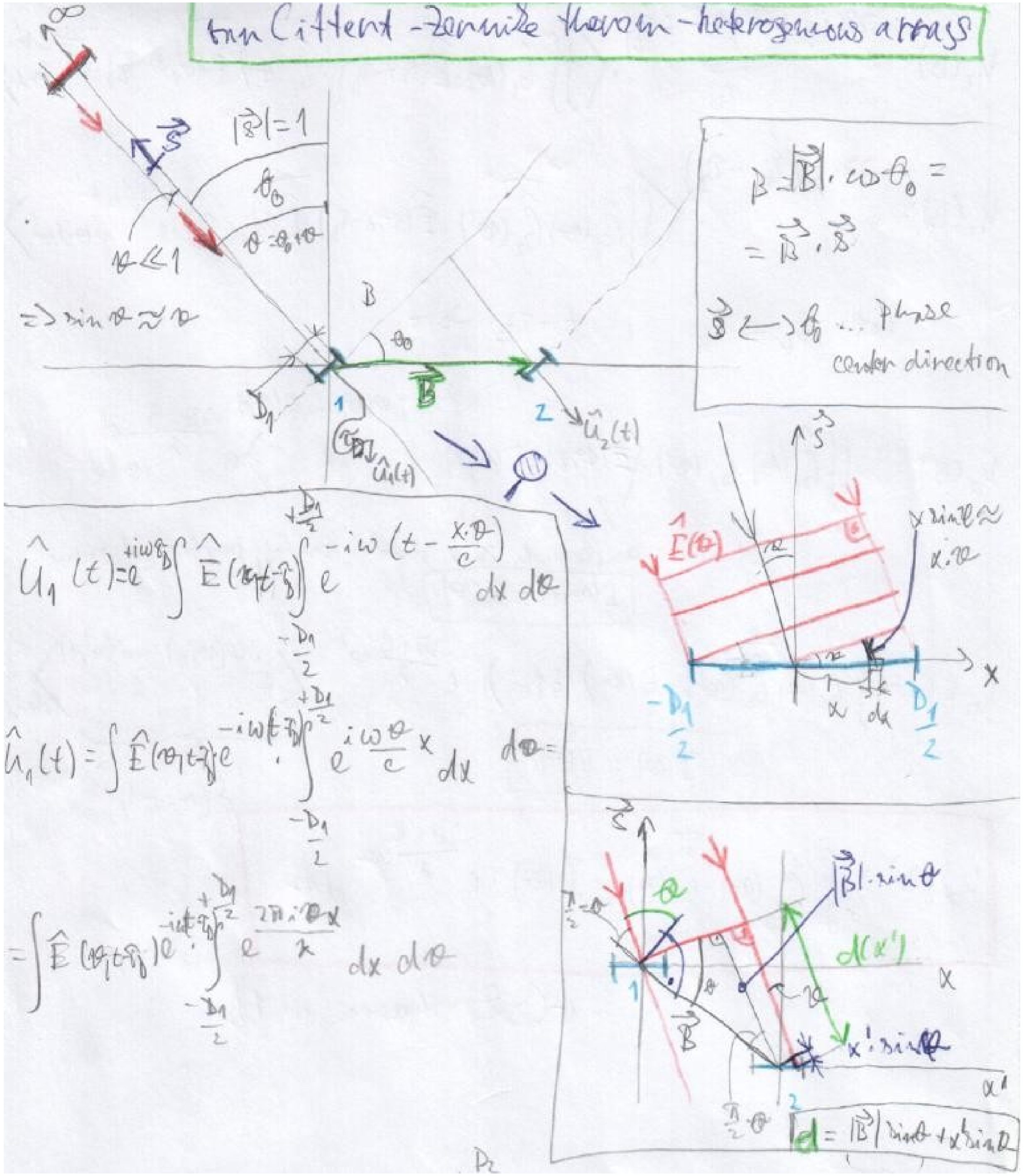

Generalisation – heterergeneous arrays

The (complex) voltage $U_1(t)$ at *Antenna 1* caused by incident radiation with the electric-field intensity $E(\upsilon,t)$ can be written as

$$\hat{U}_1(t) = K_1 \int_{source} \hat{E}(\vartheta, t-\tau_D) \int_{\frac{-D_1}{2}}^{\frac{+D_1}{2}} \exp[-i\omega(t - \frac{x\vartheta}{c} - \tau_D)]\, dx\, d\vartheta \quad ,$$

$$\hat{U}_1(t) = K_1 \int_{source} \hat{E}(\vartheta, t-\tau_D)\, e^{-i\omega(t-\tau_D)} \int_{\frac{-D_1}{2}}^{\frac{+D_1}{2}} \exp(\frac{2\pi i \vartheta x}{\lambda})\, dx\, d\vartheta$$

Generalisation – hetererogeneous arrays

For the *Antenna 2*, the voltage at the same time instant *t* reads:

$$\hat{U}_2(t)=K_2\int_{source}\hat{E}(\vartheta,t-\tau_B)e^{-i\omega t}\int_{\frac{-D_2}{2}}^{\frac{+D_2}{2}}\exp[\frac{2\pi i}{\lambda}(|\vec{B}|\sin\theta)+x\sin\vartheta]\,dx\,d\vartheta \quad .$$

Using the relation for sin*(x+y)* and, again, taking into account that *υ«1*, one can write

$\sin\theta=\sin(\theta_0+\vartheta)=\sin\theta_0\cos\vartheta+\cos\theta_0\sin\vartheta\approx\sin\theta_0+\cos\theta_0\,\vartheta$ and rewrite the above relation for $U_2(t)$ – with definition of *projected* baseline length (i.e., uv distance) $B\equiv|\mathbf{B}|\cos(\theta_0)$ – as

$$\hat{U}_2(t)=K_2\int_{source}\hat{E}(\vartheta,t-\tau_B)e^{-i\omega(t-t_B)}\exp(\frac{2\pi i}{\lambda}B\vartheta)\int_{\frac{-D_2}{2}}^{\frac{+D_2}{2}}\exp(\frac{2\pi i\vartheta x}{\lambda})\,dx\,d\vartheta \quad .$$

Here, $\tau_B\equiv\frac{|\vec{B}|\sin\theta_0}{c}$ represents the geometrical delay at the *Antenna 2*, which is separated by a baseline of the length $|\mathbf{B}|$ from the *Antenna 1*, for waves coming from the phase-reference direction θ_0.

Now, if we define the *electric gain* (a complex-value function, in general) of the antenna *j=1,2* as

$$G_{E,j}(\vartheta)\equiv K_j\int_{\frac{-D_j}{2}}^{\frac{+D_j}{2}}\exp(\frac{2\pi i\vartheta x}{\lambda})\,dx=\frac{K_j\lambda}{\pi}\cdot\frac{\sin(\frac{\pi D_j}{\lambda}\vartheta)}{\vartheta} \qquad (1),$$

Generalisation – heterererogeneous arrays

the (complex) cross-correlation/visibility for the (projected) baseline B $V_{1,2}(B)=\langle U_1(t)\cdot\overline{U_2(t)}\rangle$ (the over-line means complex conjugation and the angle brackets time averaging) can be written as

$$V_{1,2}(B)=\langle U_1(t)\cdot\overline{U_2(t)}\rangle=\int_{source} G_{E,1}(\vartheta)\overline{G_{E,2}}(\vartheta)I(\vartheta)\exp(-\frac{2\pi i B}{\lambda}\vartheta)d\vartheta \qquad (2).$$

Here, $I(\vartheta)=\langle E(\vartheta,t)\cdot\overline{E(\vartheta,t)}\rangle$ is the specific intensity of incoming radiation (i.e., directly proportional to the source brightness). The result above has been achieved using the "standard" assumptions for the van Cittert-Zernike (abbreviated as vC-Z in the following) theorem, i.e., (i) The radiation coming from different part of the source is not correlated (has random phases), (ii) The delay τ_D introduced in the correlator delay loop is set to equalize the geometrical (baseline) delay τ_B defined above. If we replace the electric gain G_E by a (differential) antenna area by definition (correct up to some constant real factor for proper units/scaling)

$$A_j(\vartheta)\equiv|G_{E,j}(\vartheta)|^2 \quad ,$$

we can summarize the above result as

$$V_{1,2}(B)=e^{i\Phi_{1,2}}\int_{source}\sqrt{A_1(\vartheta)A_2(\vartheta)}\,I(\vartheta)\exp(-\frac{2\pi i B}{\lambda}\vartheta)\,d\vartheta \qquad (3),$$

Generalisation – heterérogeneous arrays

Calculation of the **structure function** of a simple source

$$F_{uv}(B)=\frac{|V(B)|}{D} \qquad (4),$$

where *V(B)* is the integral in (2) for the projected baseline length *B*.

For the Mars disk we use approximation of homogeneous brightness, which in 1-D reads

$$I(\vartheta)=I_0\chi(-M/2,M/2) \qquad (5),$$

where M is the angular diameter of the Mars disk, and *χ(a,b)* is the so called characteristic function of the interval <*a,b*>, having its value equal to *1* on that interval and *0* outside.

Substituting (1) and (5) into (2), and the result of this substitution finally into (4), we get

$$V(B;D,M)=K^2 I_0\int_{-M/2}^{+M/2}\left(\frac{\lambda}{\pi\vartheta}\right)^2\sin^2\left(\frac{\pi D}{\lambda}\vartheta\right)\exp\left(\frac{-2\pi i B}{\lambda}\vartheta\right)d\vartheta \qquad (6),$$

where the *D* and *M* after semicolon indicate that the visibility function *parametrically* depends on the (effective) antenna diameter and (effective) Mars-disk size. After integrating by parts and some substitution/re-scaling, and inserting the result into (4), we finally arrive to relation

$$F_{uv}(B;D,M)=\frac{K^2 I_0\lambda}{\pi}\left|-\frac{4\sin^2(m/2)\cos(mb)}{m}+(b-1)Si[(b-1)m]+(b+1)Si[(b+1)m]-2bSi(bm)\right|$$

(7).

Here *Si(x)* means the (Fresnel) sine integral function, *b≡B/D* is the (projected) baseline length expressed in units of the antenna diameter, and *m≡πMD/λ* is basically (up to a small numerical factor)

Generalisation – heterergeneous arrays

Calculation of the **structure function** of a simple source

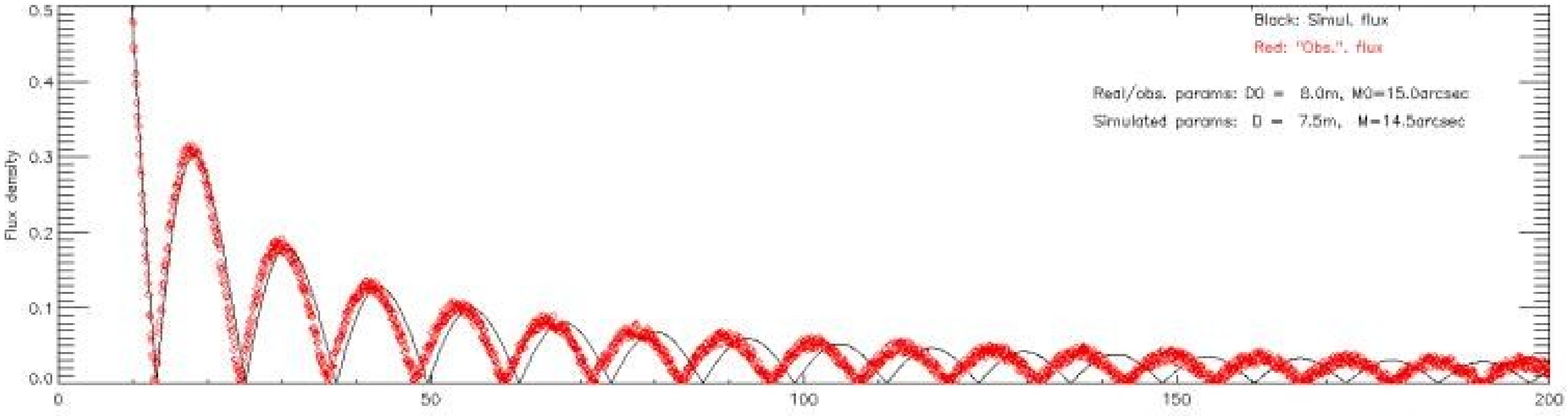

At high (u,v) it depends strongly on the antenna diameter

Aperture synthesis: Mathematical foundations

Van Cittert – Zernike theorem: 2-D geometry

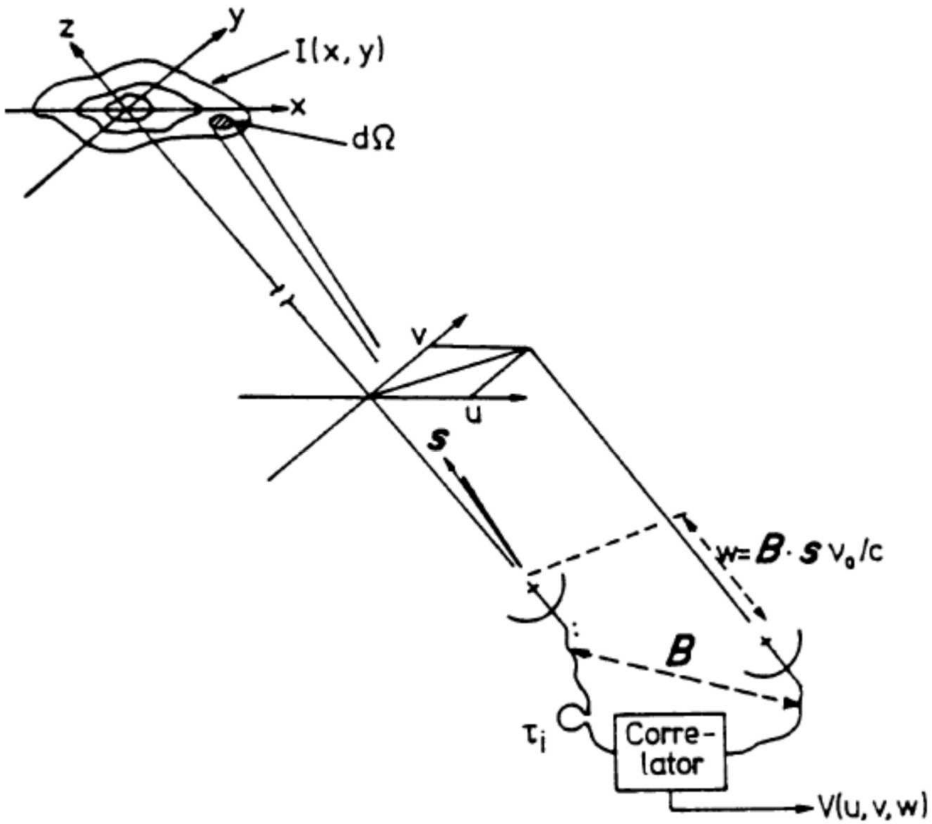

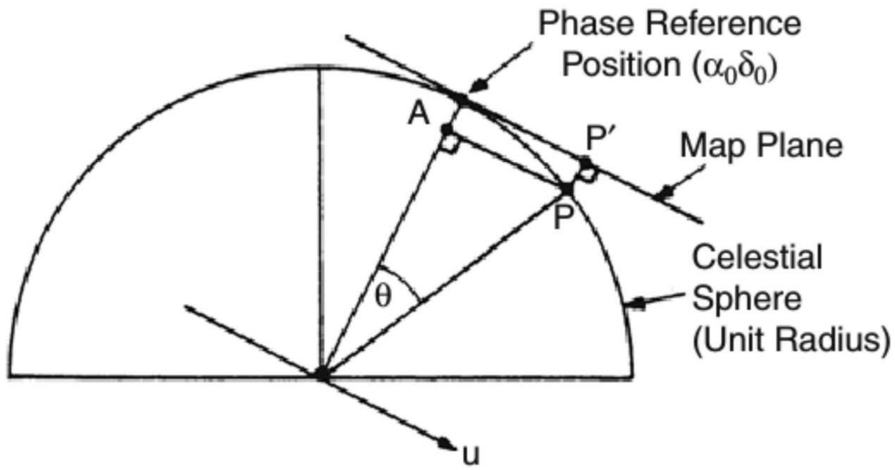

$$\langle P_{12}\rangle = G_1 \overline{G_2} \cdot \iint_{-\infty}^{+\infty} I(\vartheta)\cdot \exp\left(-i\frac{2\pi D\cos\theta_0 \cdot \vartheta}{\lambda}\right) d\vartheta$$

$$R(\boldsymbol{B}) = \iint_{\Omega} A(\boldsymbol{s}) I_\nu(\boldsymbol{s}) \exp\left[\mathrm{i}2\pi\nu\left(\frac{1}{c}\boldsymbol{B}\cdot\boldsymbol{s} - \tau_\mathrm{i}\right)\right] \mathrm{d}\Omega\, \mathrm{d}\nu$$

Aperture synthesis: Mathematical foundations

Van Cittert – Zernike theorem: 2-D geometry

Cross-correlation function

$$R(\boldsymbol{B}) = \iint_{\Omega} A(\boldsymbol{s}) I_{\nu}(\boldsymbol{s}) \exp\left[\mathrm{i} 2\pi\nu \left(\frac{1}{c}\boldsymbol{B}\cdot\boldsymbol{s} - \tau_{\mathrm{i}}\right)\right] \mathrm{d}\Omega\, \mathrm{d}\nu$$

$$\boldsymbol{s} = \boldsymbol{s}_0 + \boldsymbol{\sigma}, \qquad |\boldsymbol{\sigma}| = 1$$

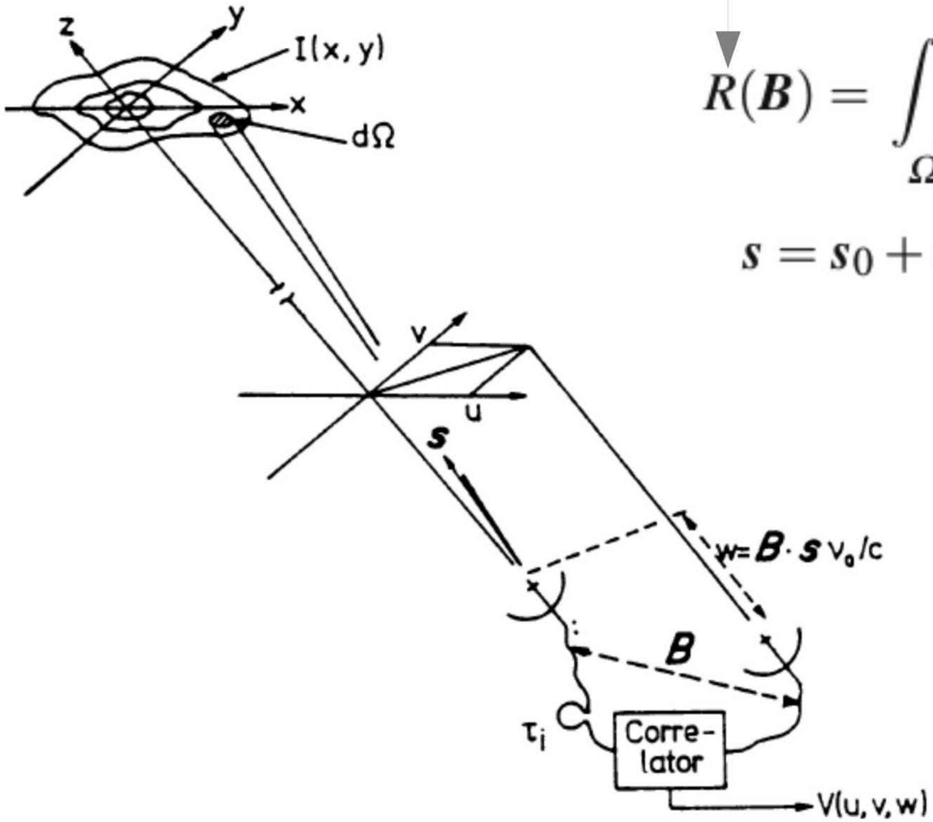

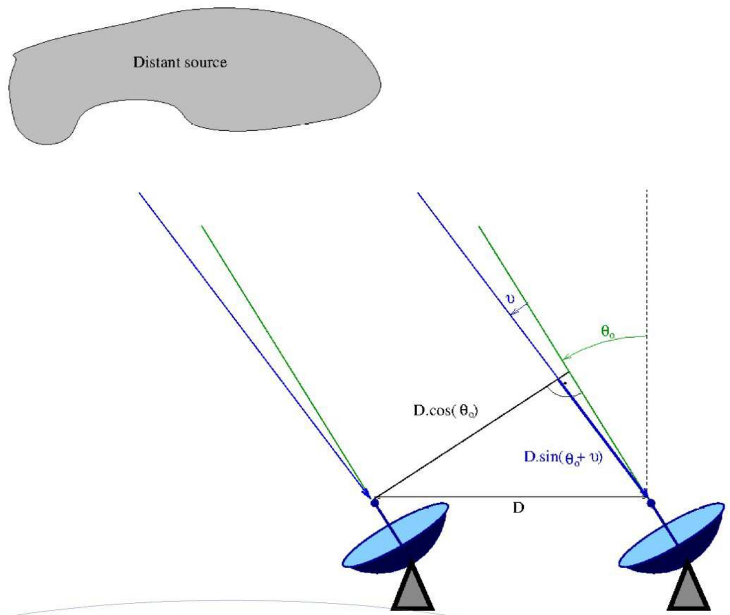

$$R(\boldsymbol{B}) = \exp\left[\mathrm{i}\omega\left(\frac{1}{c}\boldsymbol{B}\cdot\boldsymbol{s}_0 - \tau_{\mathrm{i}}\right)\right] \mathrm{d}\nu \iint_{\sigma} A(\boldsymbol{\sigma}) I(\boldsymbol{\sigma}) \exp\left(\mathrm{i}\,\frac{\omega}{c}\boldsymbol{B}\cdot\boldsymbol{\sigma}\right) \mathrm{d}\boldsymbol{\sigma}\,.$$

Aperture synthesis: Mathematical foundations

Van Cittert – Zernike theorem: 2-D geometry

$$V(\boldsymbol{B}) = \iint_S A(\boldsymbol{\sigma}) I(\boldsymbol{\sigma}) \exp\left(\mathrm{i}\frac{\omega}{c}\boldsymbol{B}\cdot\boldsymbol{\sigma}\right) \mathrm{d}\boldsymbol{\sigma}$$

$$\frac{\omega}{2\pi c}\boldsymbol{B} = (u, v, w)$$

"Visibilities"

$$V(u,v,w) = \int_{-\infty}^{\infty}\int_{-\infty}^{\infty} A(x,y) I(x,y) \times \exp[\mathrm{i}2\pi(ux + vy + w\sqrt{1 - x^2 - y^2})] \frac{\mathrm{d}x\,\mathrm{d}y}{\sqrt{1 - x^2 - y^2}}$$

"compact"-source assumption

$$\sqrt{1 - x^2 - y^2} \cong \mathrm{const} \cong 1$$

$$V(u,v,w)\,\mathrm{e}^{-\mathrm{i}2\pi w} = \int_{-\infty}^{\infty}\int_{-\infty}^{\infty} A(x,y) I(x,y)\,\mathrm{e}^{\mathrm{i}2\pi(ux+vy)}\,\mathrm{d}x\,\mathrm{d}y$$

Aperture synthesis: Mathematical foundations

Van Cittert – Zernike theorem: 2-D geometry

$$V(u,v,w)\,e^{-i2\pi w} = \int_{-\infty}^{\infty}\int_{-\infty}^{\infty} A(x,y)\,I(x,y)\,e^{i2\pi(ux+vy)}\,dx\,dy$$

$$V(u,v,w)\,e^{-i2\pi w} \cong V(u,v,0)$$

$$I'(x,y) = A(x,y)\,I(x,y) = \int_{-\infty}^{\infty} V(u,v,0)\,e^{-i2\pi(ux+vy)}\,du\,dv$$

Primary beam (pbcorr)

The Effect of Bandwidth.

- Real interferometers must accept a range of frequencies. So we now consider the response of our interferometer over frequency.
- Define the frequency response function, $G(\nu)$, as the amplitude and phase variation of the signal over frequency.

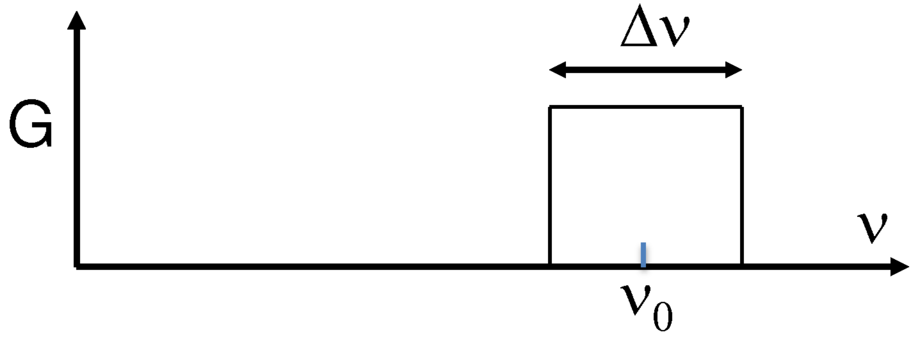

- The function $G(\nu)$ is primarily due to the gain and phase characteristics of the electronics, but can also contain propagation path effects.
- In general, $G(\nu)$ is a complex function.

The Effect of Bandwidth.

- To find the finite-bandwidth response, we integrate our fundamental response over a frequency width $\Delta\nu$, centered at ν_0:

$$V = \int \left(\frac{1}{\Delta\nu} \int_{\upsilon_0-\Delta\upsilon/2}^{\upsilon_0+\Delta\upsilon/2} I(\mathbf{s},\upsilon) G_1(\upsilon) G_2^*(\upsilon) e^{-i2\pi\upsilon\tau_g} d\upsilon \right) d\Omega$$

- If the source intensity does not vary over the bandwidth, and the instrumental gain parameters G_1 and G_2 are square and identical, then

$$V = \iint I_\upsilon(\mathbf{s}) \frac{\sin(\pi\tau_g\Delta\upsilon)}{\pi\tau_g\Delta\upsilon} e^{-2i\pi\nu_0\tau_g} d\Omega = \iint I_\upsilon(\mathbf{s}) \mathrm{sinc}(\tau_g\Delta\upsilon) e^{-2i\pi\nu_0\tau_g} d\Omega$$

where the **fringe attenuation function**, sinc(x), is defined as:

$$\mathrm{sinc}(x) = \frac{\sin(\pi x)}{\pi x}$$

Bandwidth Effect Example

- For a square bandpass, the bandwidth attenuation reaches a null when $\tau_g \Delta\nu$ = 1, or $$\sin\theta = \frac{c}{B\Delta\nu} = \left(\frac{\lambda}{B}\right)\left(\frac{\upsilon_0}{\Delta\upsilon}\right)$$
- For the old VLA, and its 50 MHz bandwidth, and for the 'A' configuration, (B = 35 km), the null was ~1.3 degrees away.
- For the upgraded VLA, $\Delta\nu$ = 2 MHz, and B = 35 km, then the null occurs at about 27 degrees off the meridian.

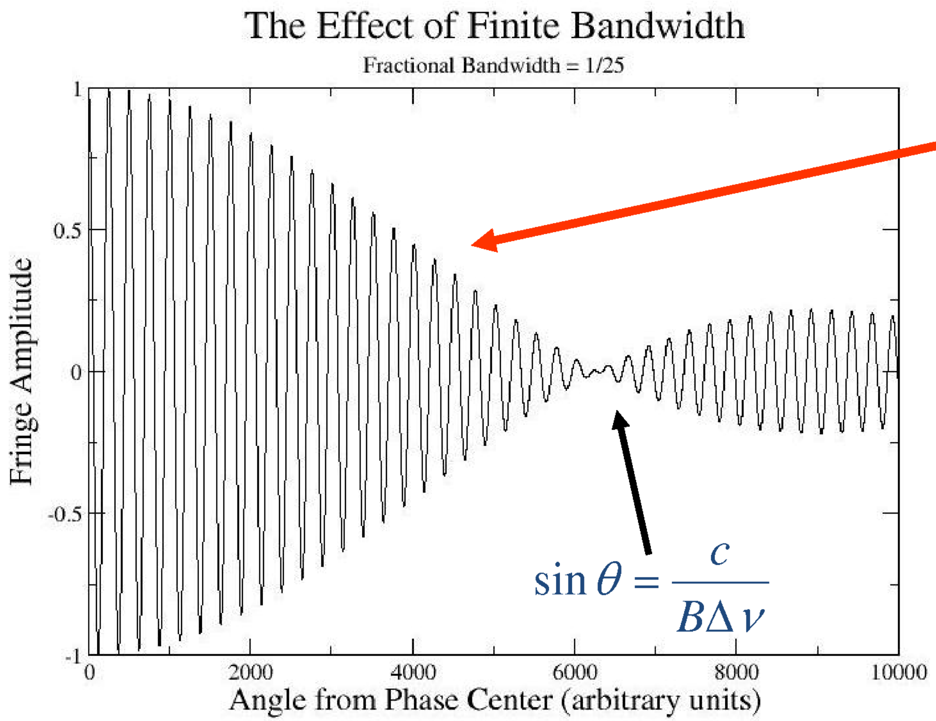

Fringe Attenuation function:

$$\mathrm{sinc}\left(\frac{B}{\lambda}\frac{\Delta\upsilon}{\upsilon}\sin\theta\right) = \mathrm{sinc}\left(\frac{B\Delta\upsilon}{c}\sin\theta\right)$$

Note: The fringe-attenuation function depends only on bandwidth and baseline length – not on frequency.

Observations off the Baseline Meridian

- In our basic scenario -- stationary source, stationary interferometer -- the effect of finite bandwidth will strongly attenuate the visibility from sources far from the meridional plane.
- Since each baseline has its own fringe pattern, the only point on the sky free of attenuation for all baselines is a small angle around the zenith (presuming all baselines are coplanar).
- Suppose we wish to observe an object far from the zenith?
- One solution is to use a very narrow bandwidth – this loses sensitivity, which can only be made up by utilizing many channels – feasible, but computationally expensive.
- Better answer: Shift the fringe-attenuation function to the center of the source of interest.
- How? By adding time delay.

Adding Time Delay

$$\tau_g = \mathbf{b}\cdot\mathbf{s}/c$$

$$\tau_0 = \mathbf{b}\cdot\mathbf{s}_0/c$$

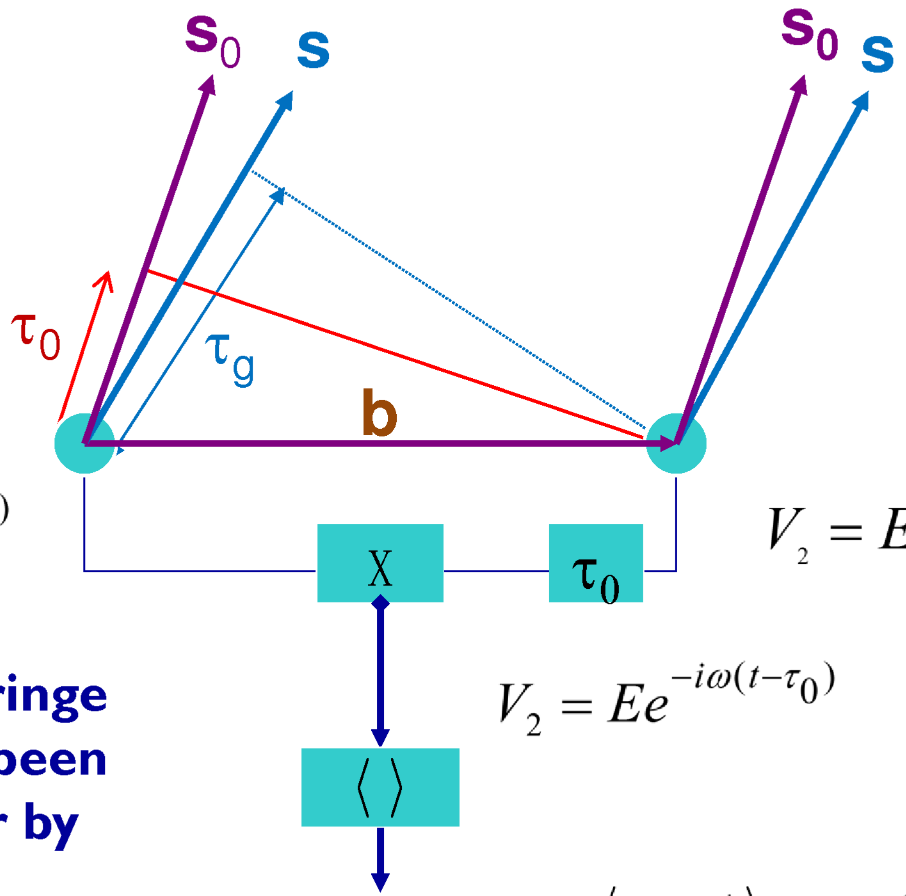

$\mathbf{S}_0$ = reference (delay) direction

$\mathbf{S}$ = general direction

$$V_1 = Ee^{-i\omega(t-\tau_g)}$$

$$V_2 = Ee^{-i\omega t}$$

$$V_2 = Ee^{-i\omega(t-\tau_0)}$$

The entire fringe pattern has been shifted over by angle

sin θ = cτ$_0$/b

$$V = \langle V_1 V_2^* \rangle = E^2 e^{-i[\omega(\tau_0-\tau_g)]}$$

$$= E^2 e^{i2\pi[\nu\mathbf{b}\cdot(\mathbf{s}-\mathbf{s}_0)/c]}$$

NRAO

Downconversion

At radio frequencies, the spectral content within a passband can be shifted – with almost no loss in information, to a lower frequency through multiplication by a 'LO' signal.

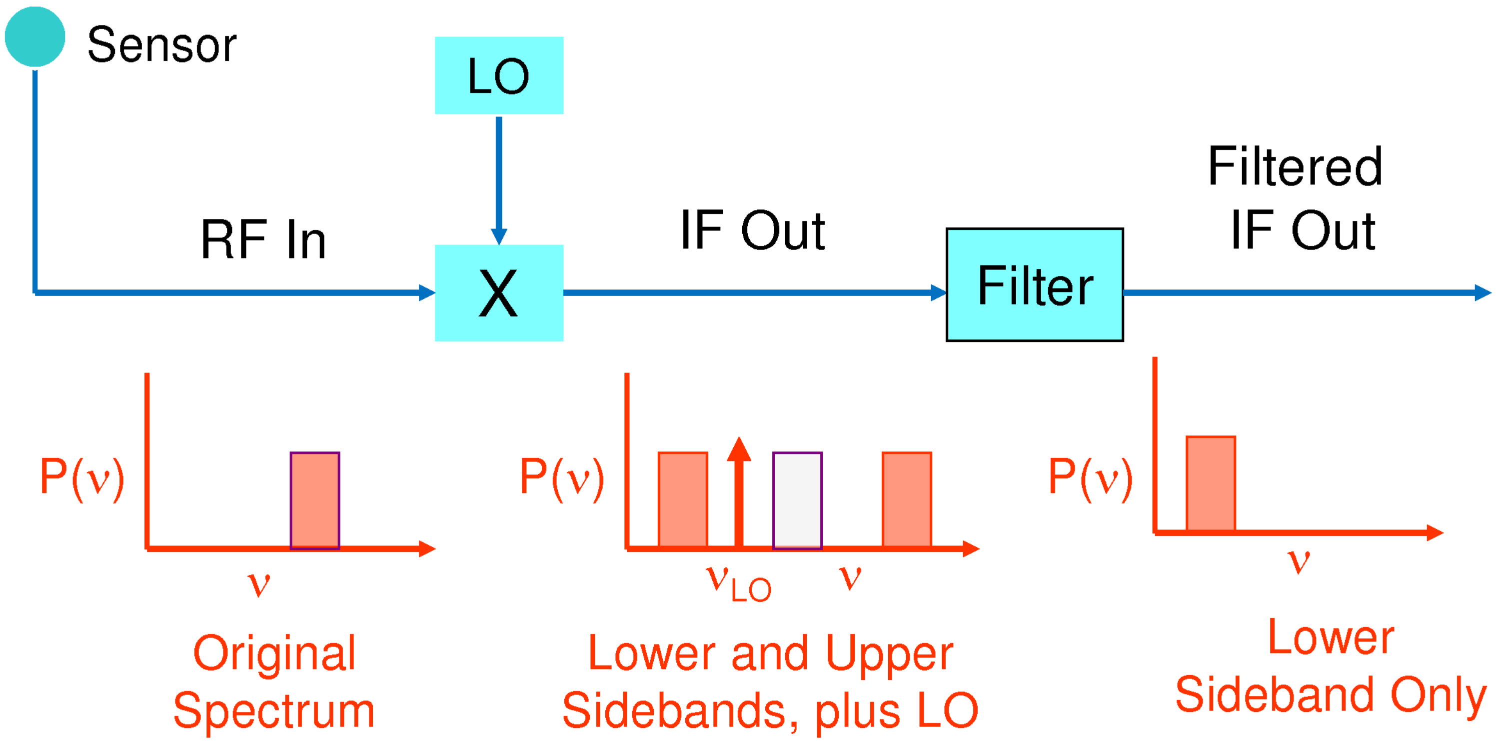

This operation preserves the amplitude and phase relations

Signal Relations, with LO Downconversion

- The RF signals are multiplied by a pure sinusoid, at frequency ν_{LO}
- We can add arbitrary phase ϕ_{LO} on one side.

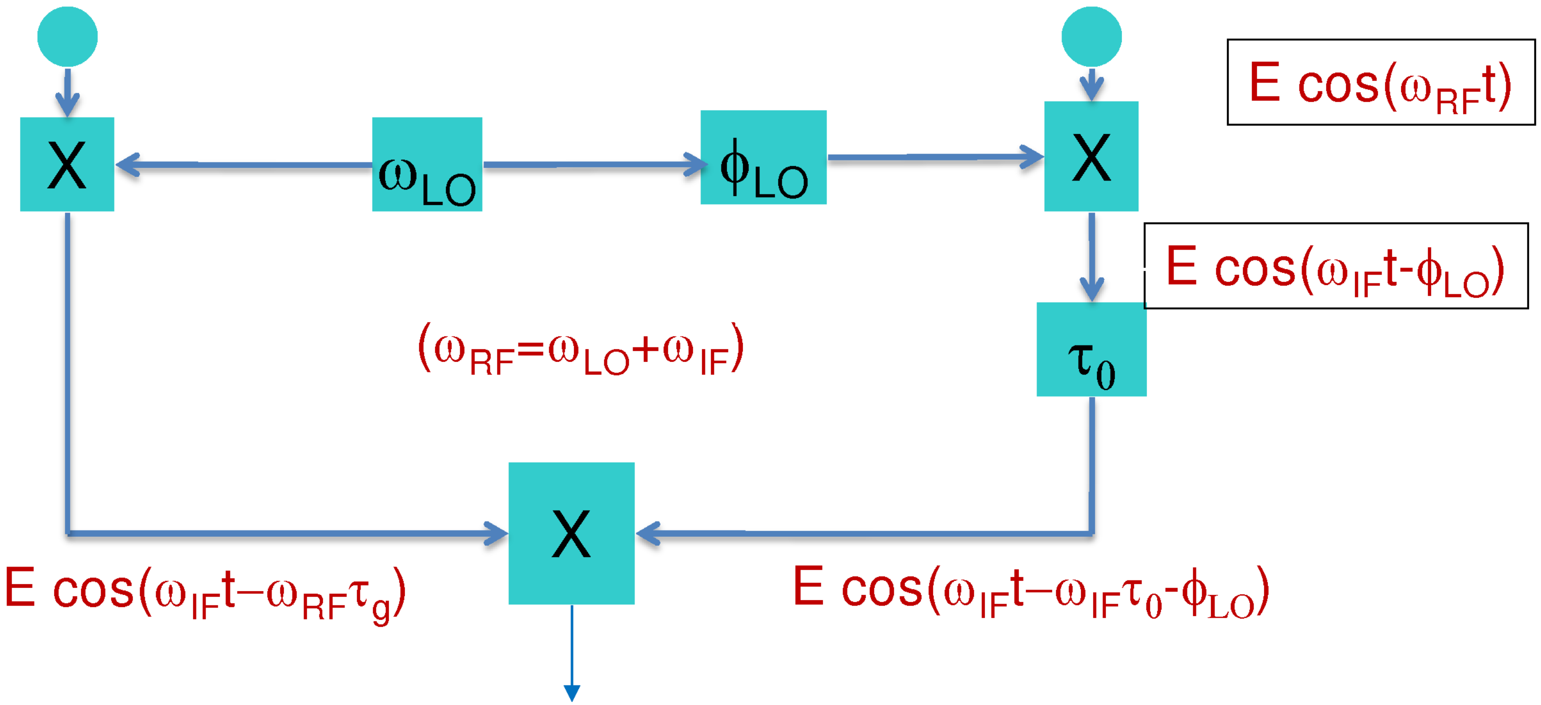

$$V = E^2 e^{-i(\omega_{RF}\tau_g - \omega_{IF}\tau_0 - \phi_{LO})}$$

Recovering the Correct Visibility Phase

- The correct phase (RF interferometer) is: $\omega_{RF}\left(\tau_g - \tau_0\right)$
- The observed phase (with frequency downconversion) is:

$$\omega_{RF}\tau_g - \omega_{IF}\tau_0 - \phi_{LO}$$

- These will be the same when the LO phase is set to:

$$\phi_{LO} = \omega_{LO}\tau_0$$

- This is necessary because the delay, τ_0, has been added in the IF portion of the signal path, rather than at the frequency at which the delay actually occurs.
- The phase adjustment of the LO compensates for the delay having been inserted at the IF , rather than at the RF.

2 antennas

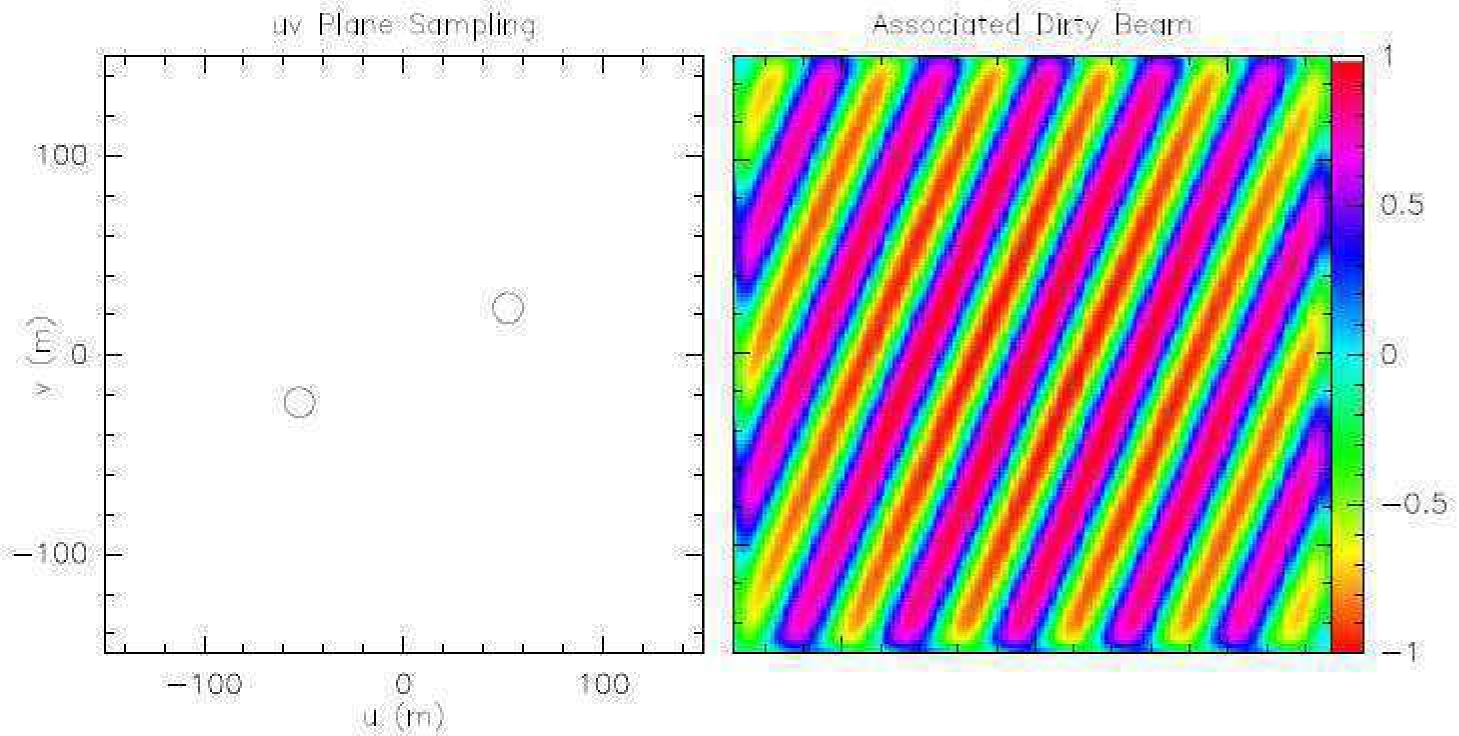

uv Plane Sampling
100
0
−100
v (m)
−100
0
100
u (m)
Associated Dirty Beam
1
0.5
0
−0.5
−1

3 antennas

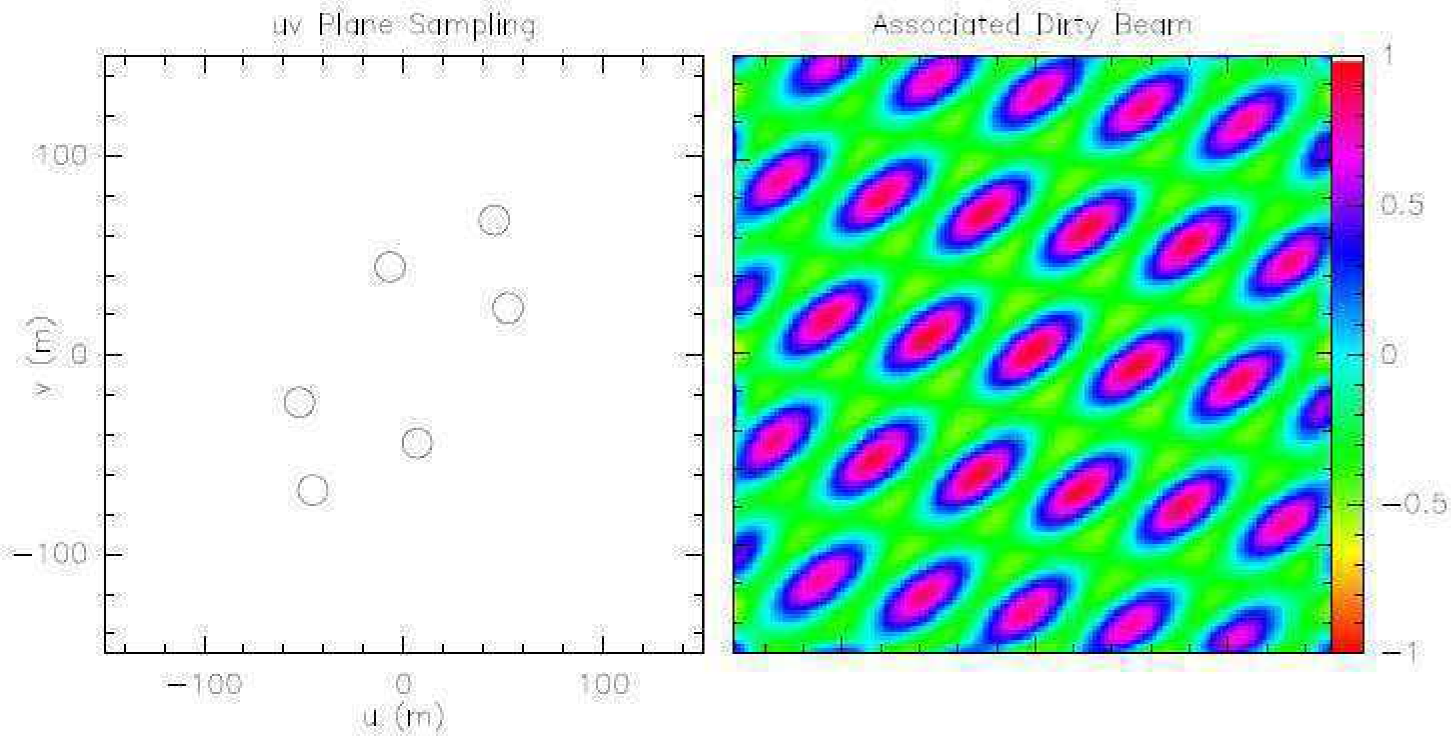

uv Plane Sampling
100
0
−100
v (m)
−100
0
100
u (m)
Associated Dirty Beam
1
0.5
0
−0.5
−1

4 antennas

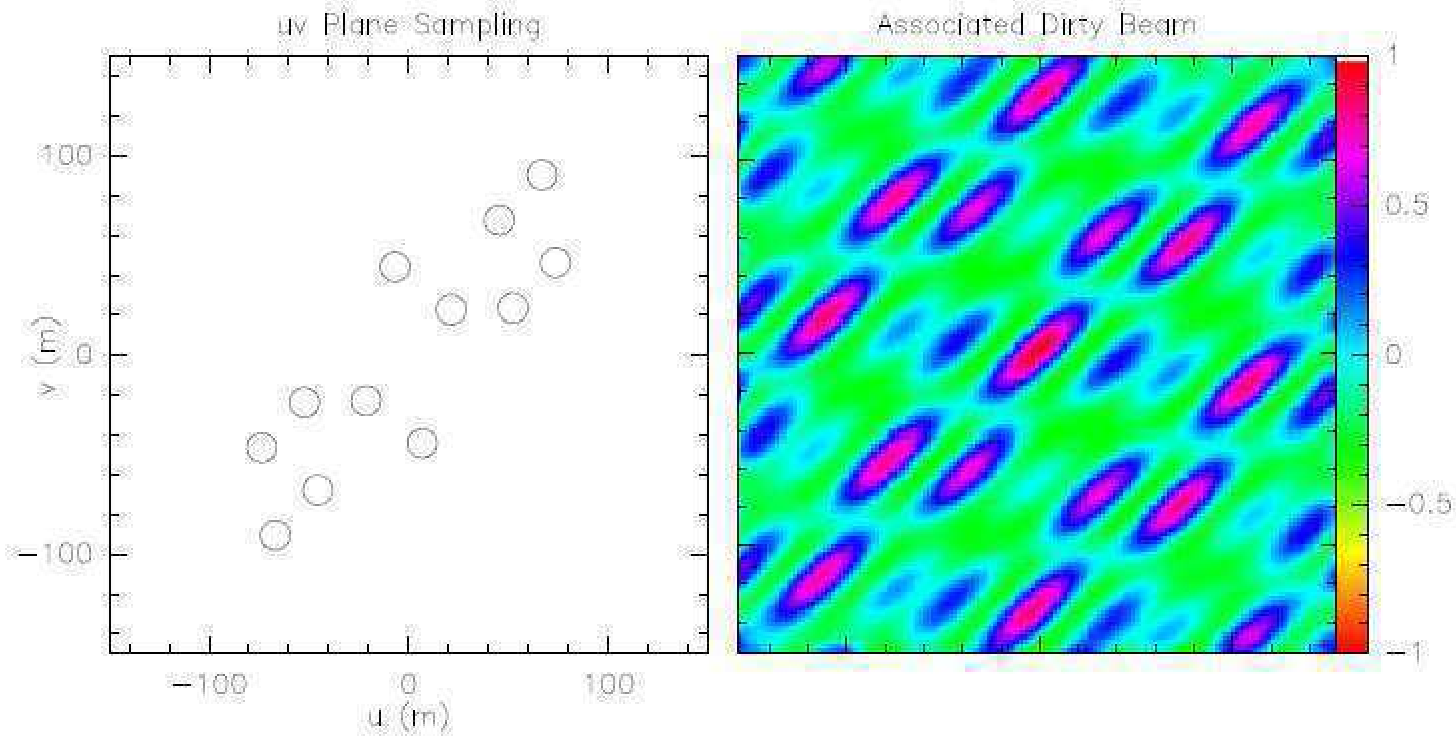

uv Plane Sampling
100
0
−100
v (m)
−100
0
100
u (m)
Associated Dirty Beam
1
0.5
0
−0.5
−1

5 antennas

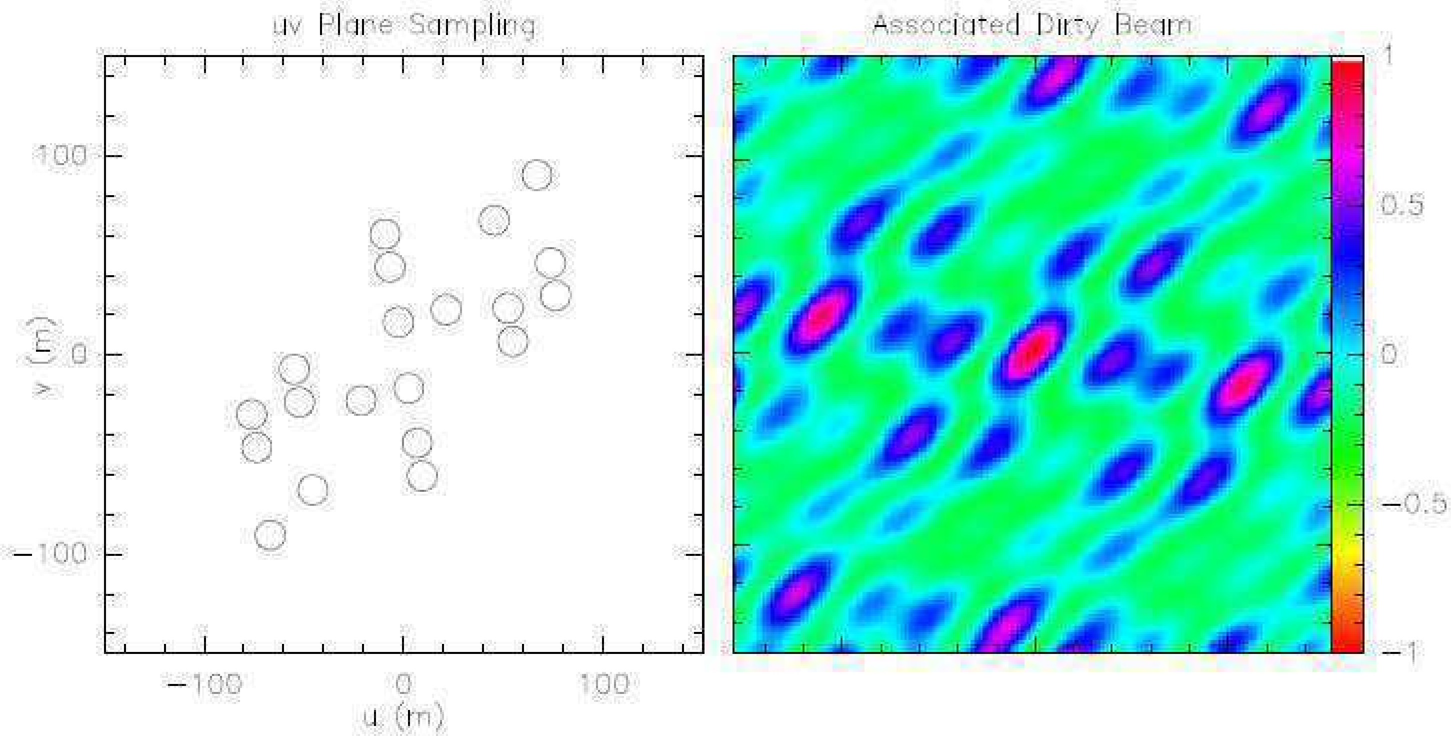
uv Plane Sampling
Associated Dirty Beam
100
0
−100
v (m)
−100
0
100
u (m)
1
0.5
0
−0.5
−1

6 antennas

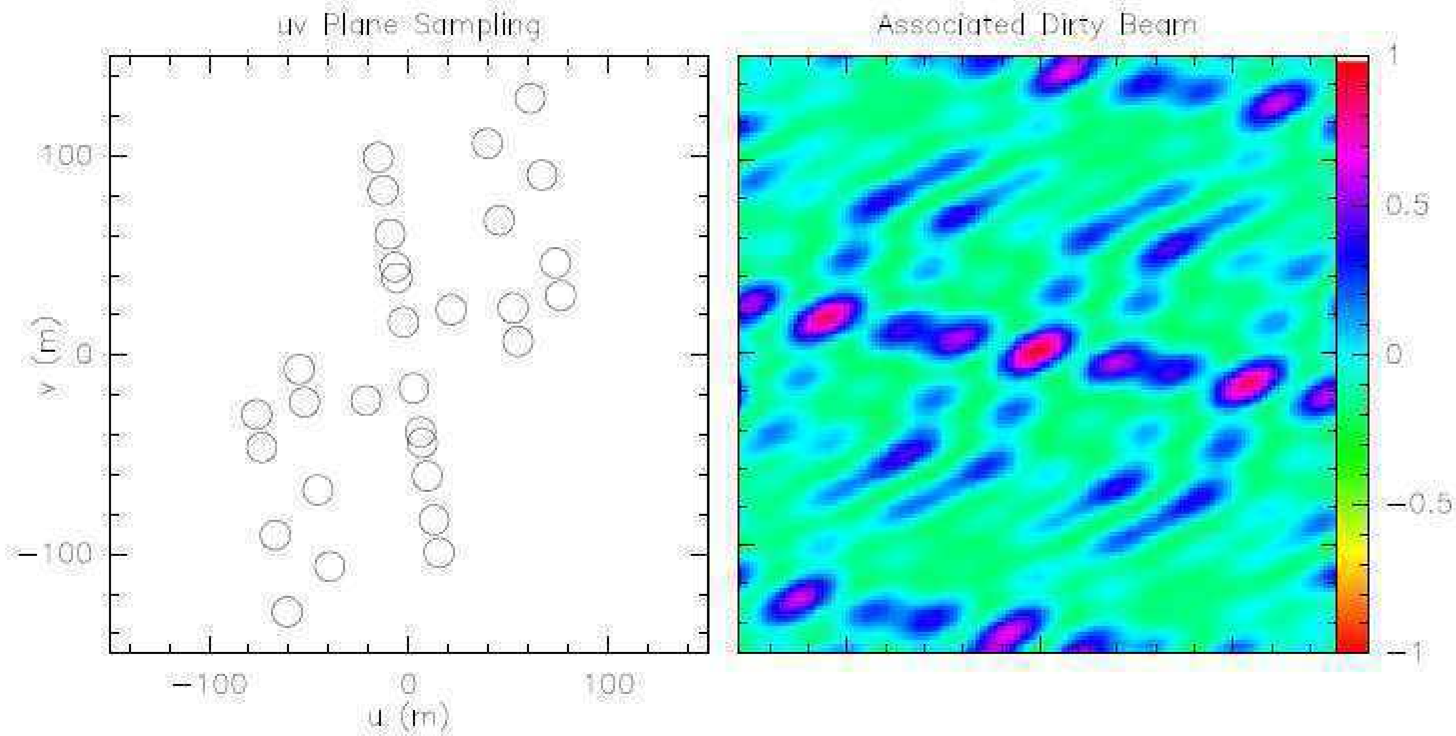
uv Plane Sampling
Associated Dirty Beam
v (m)
u (m)
100
0
−100
1
0.5
0
−0.5
−1

Earth-rotation aperture synthesis

- Geometric delay varies slowly with time due to earth rotation
- Natural fringe rate

$$\tau_g = \frac{\vec{b}\cdot\hat{s}}{c} \qquad\qquad \nu\frac{d\tau_g}{dt} \cong \Omega_{\mathrm{earth}}\frac{b\nu}{c}$$

- τ_g is known from the antenna position, source direction, time −> could be corrected
- u,v depends on the hour angle – as the earth rotates and the source appears to move across the sky, the array samples different u,v at different times

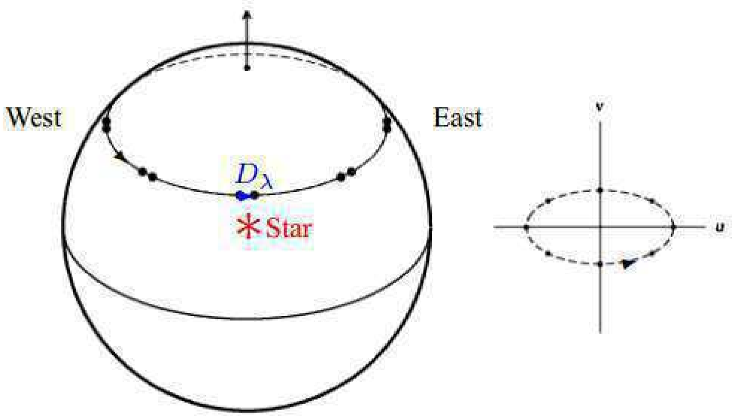

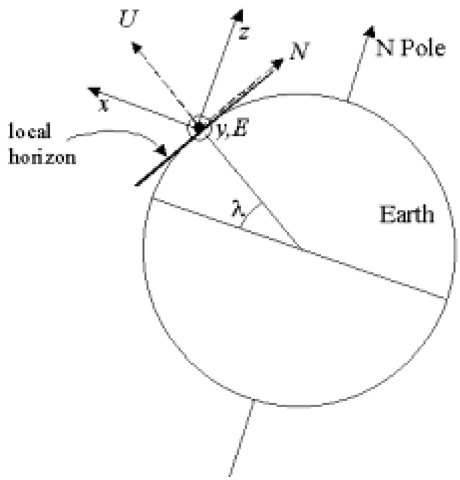

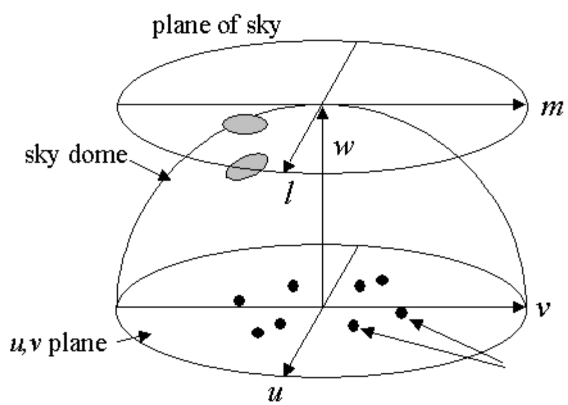

Earth-rotation aperture synthesis

- Incomplete *uv* plane coverage

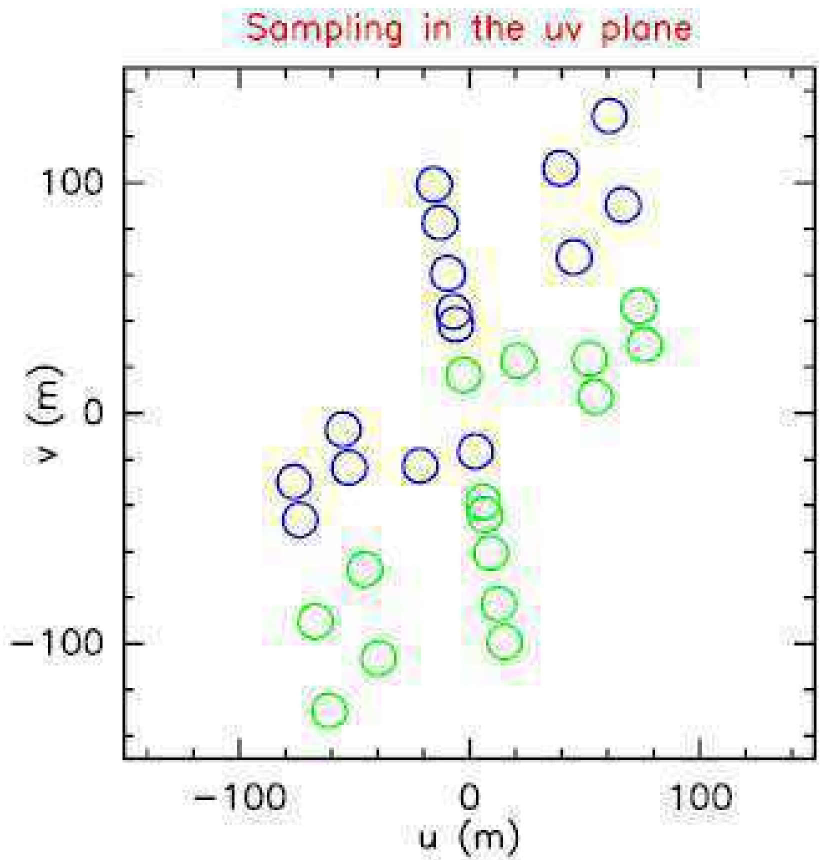

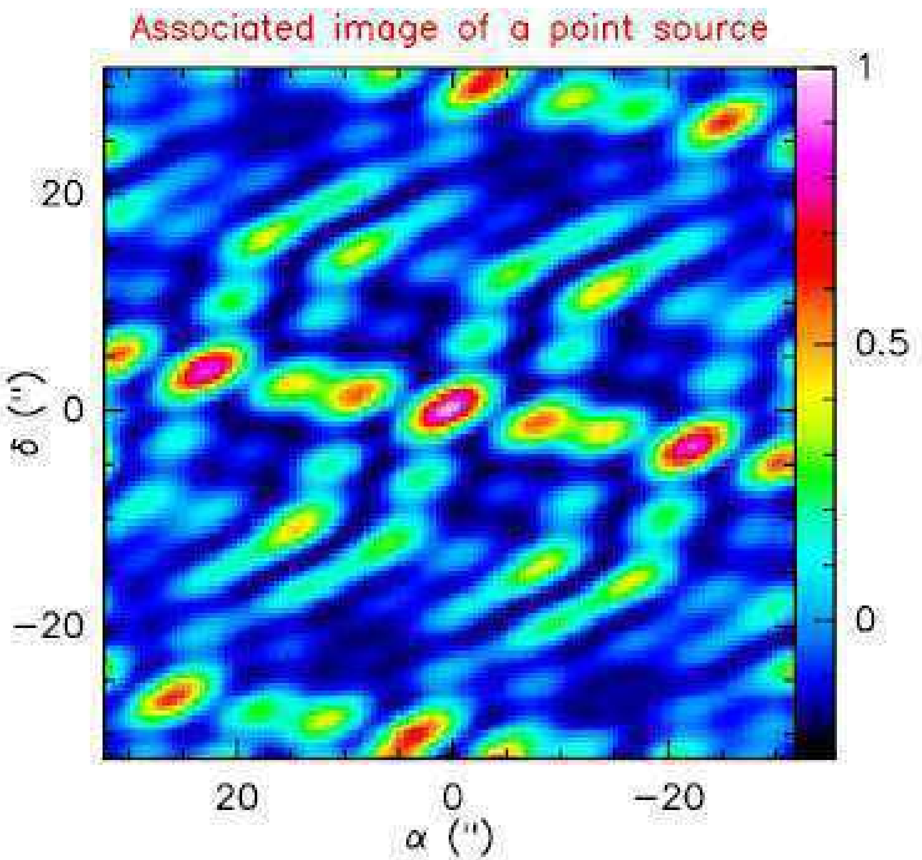

Earth-rotation aperture synthesis

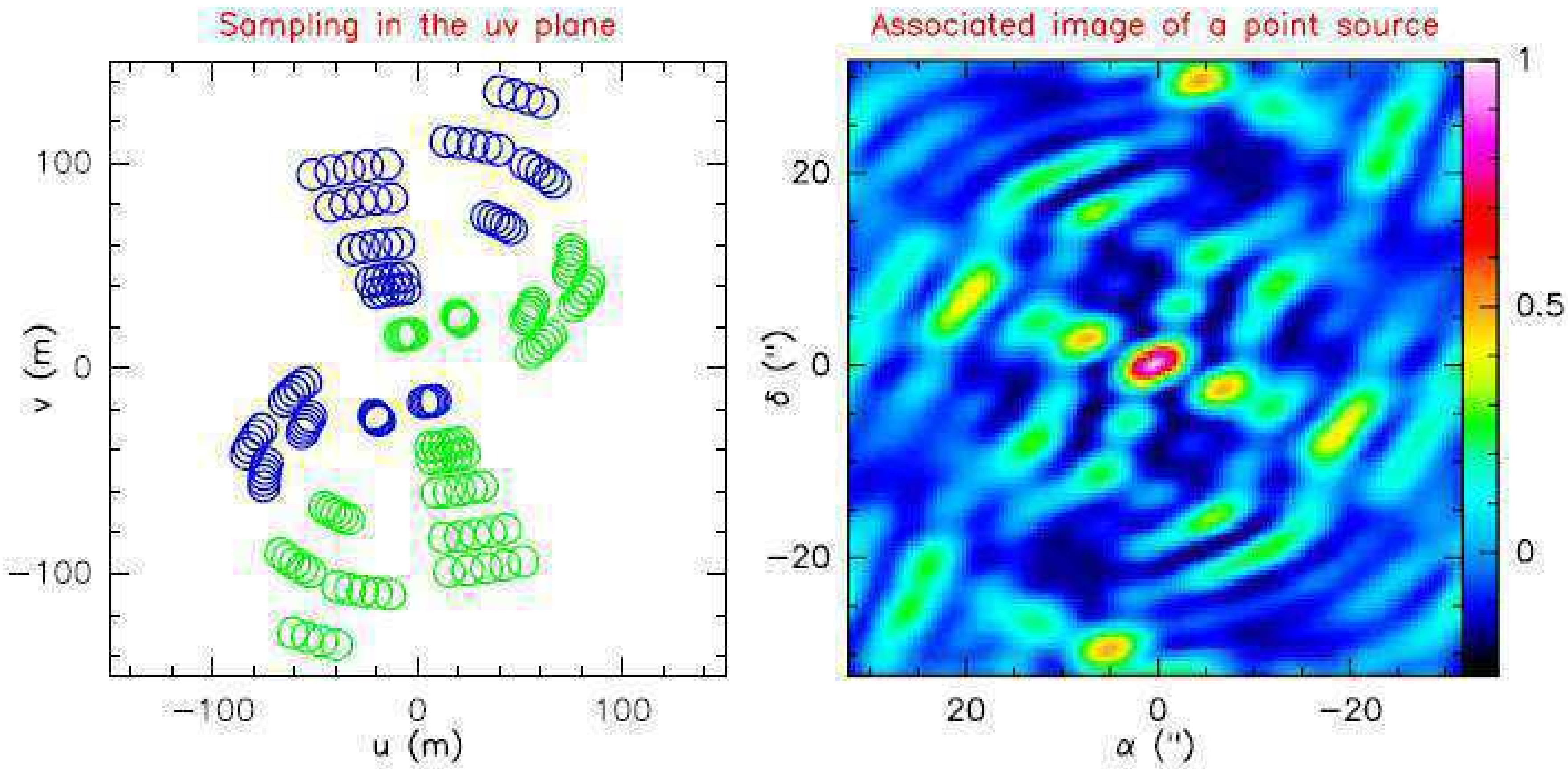

Earth-rotation aperture synthesis

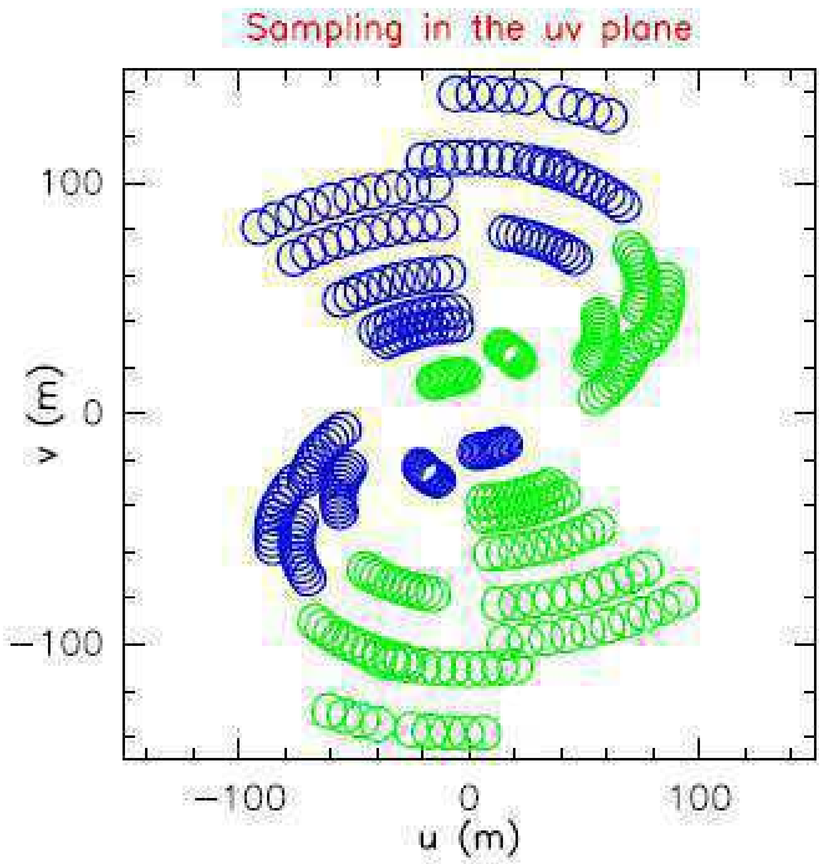

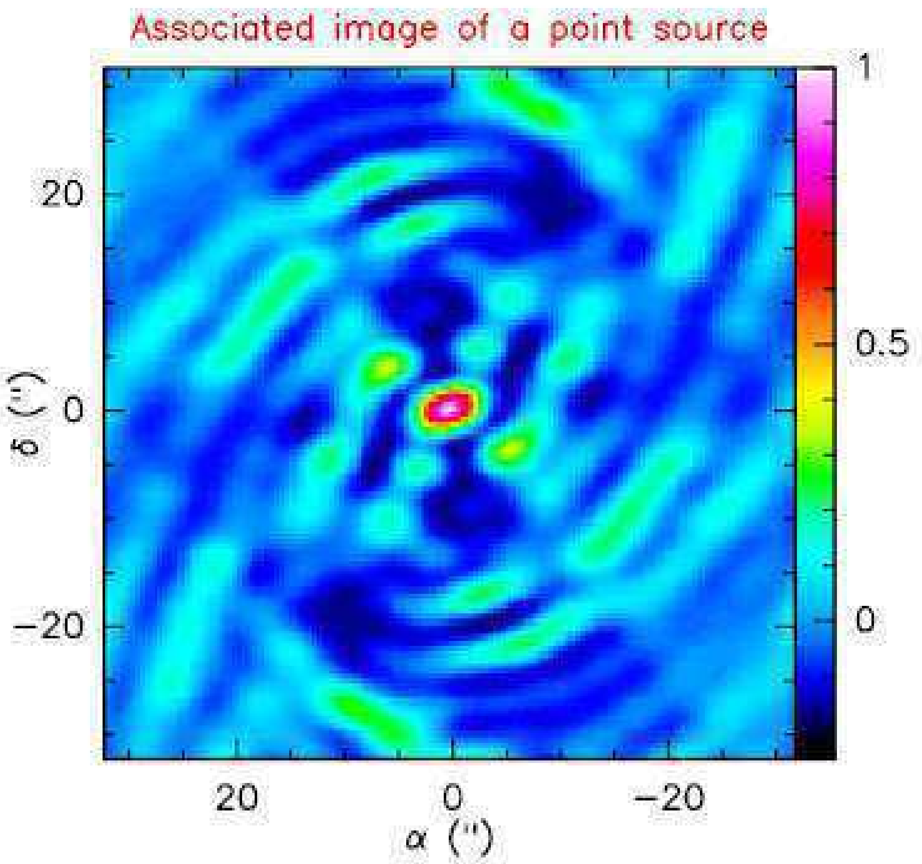

Earth-rotation aperture synthesis

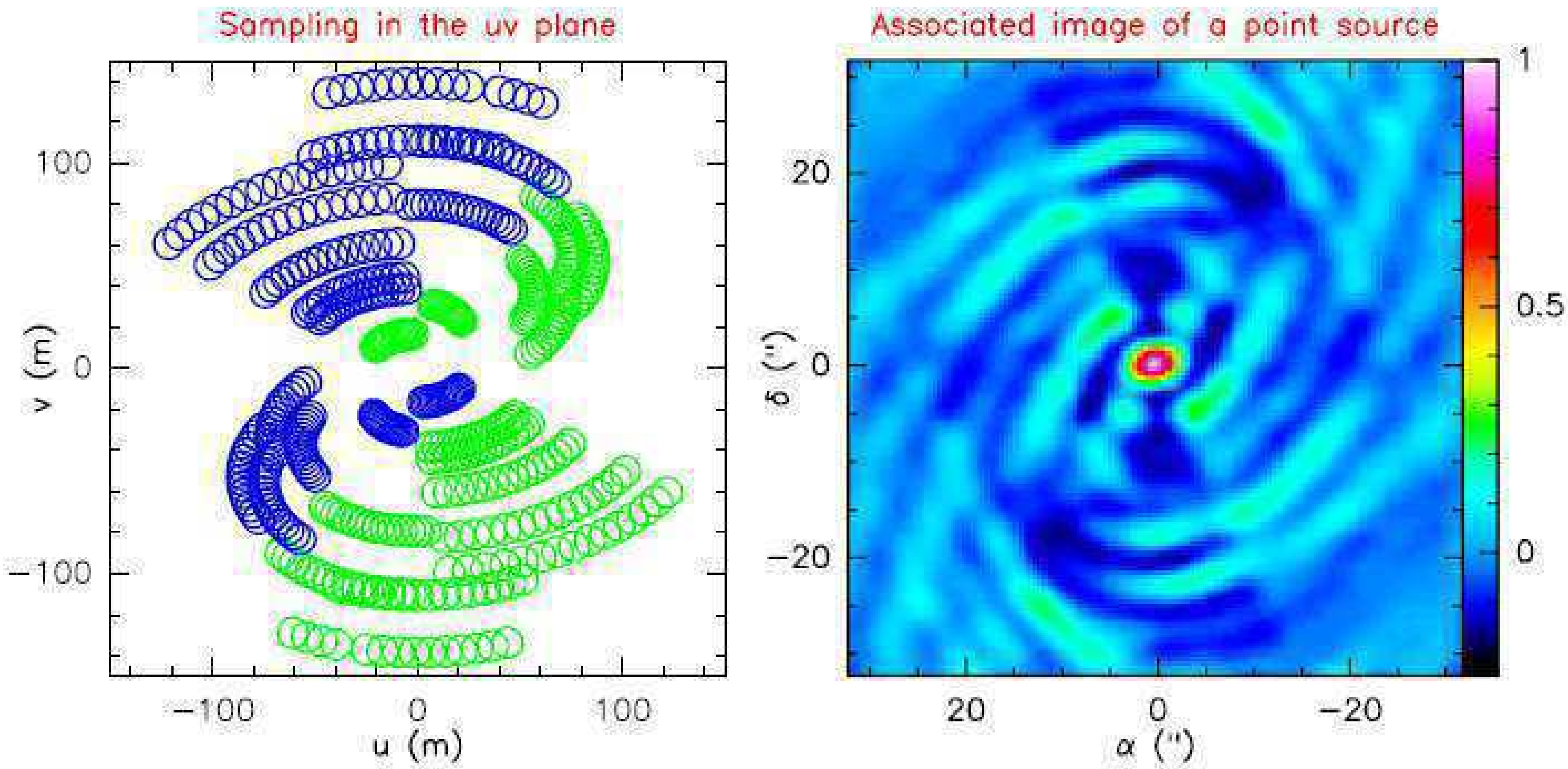

Earth-rotation aperture synthesis

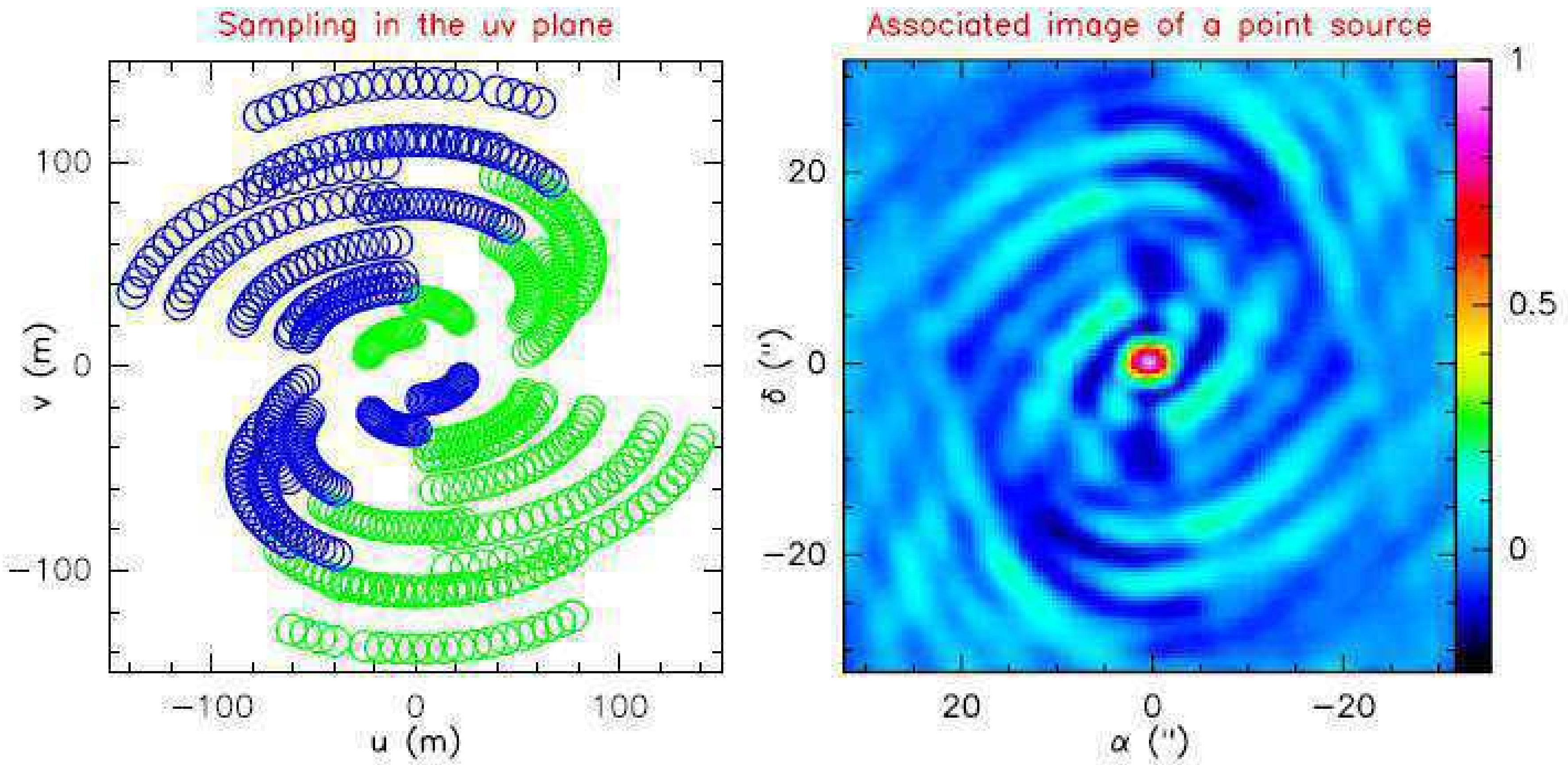

Earth-rotation aperture synthesis

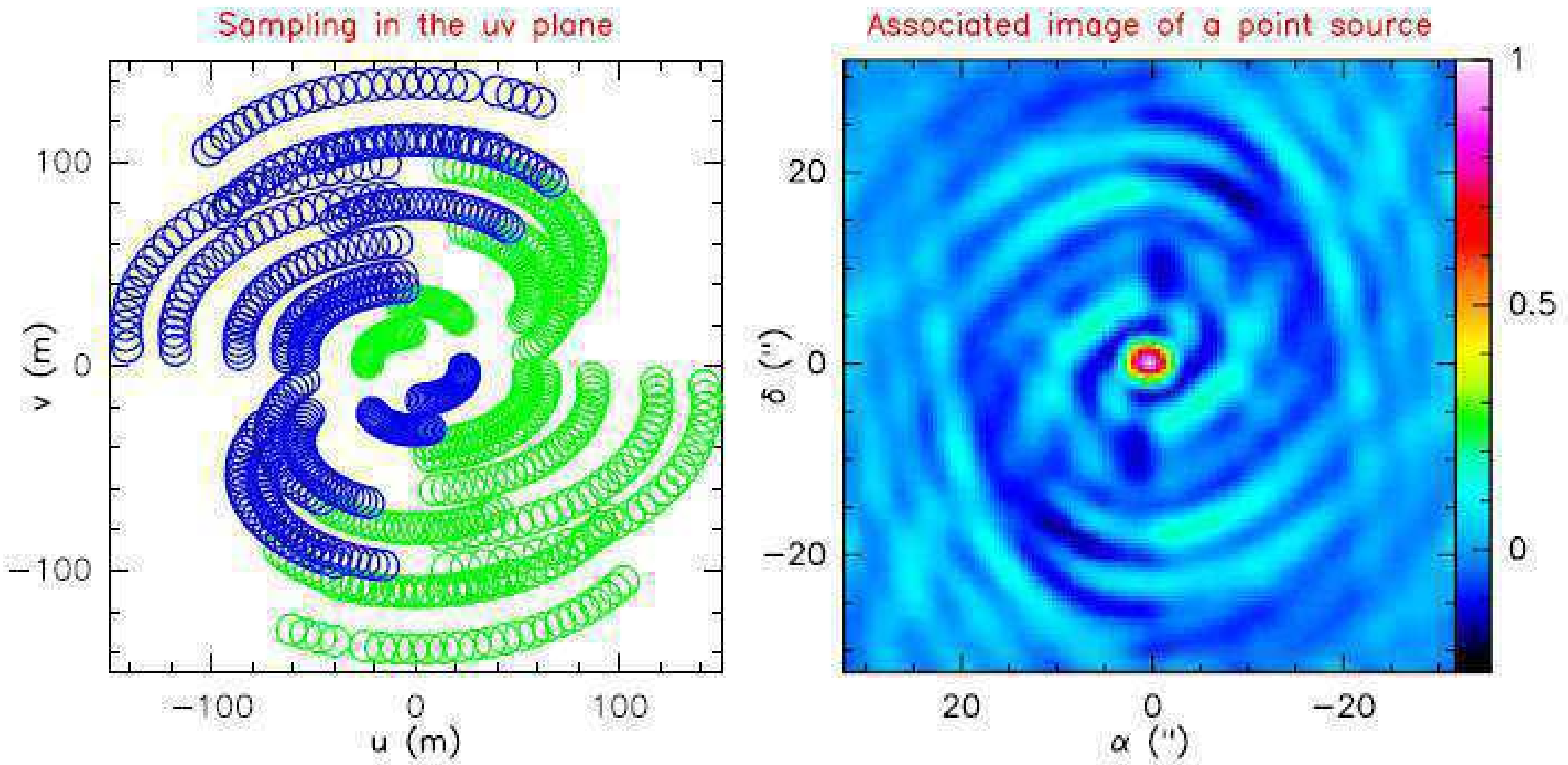

Earth-rotation aperture synthesis

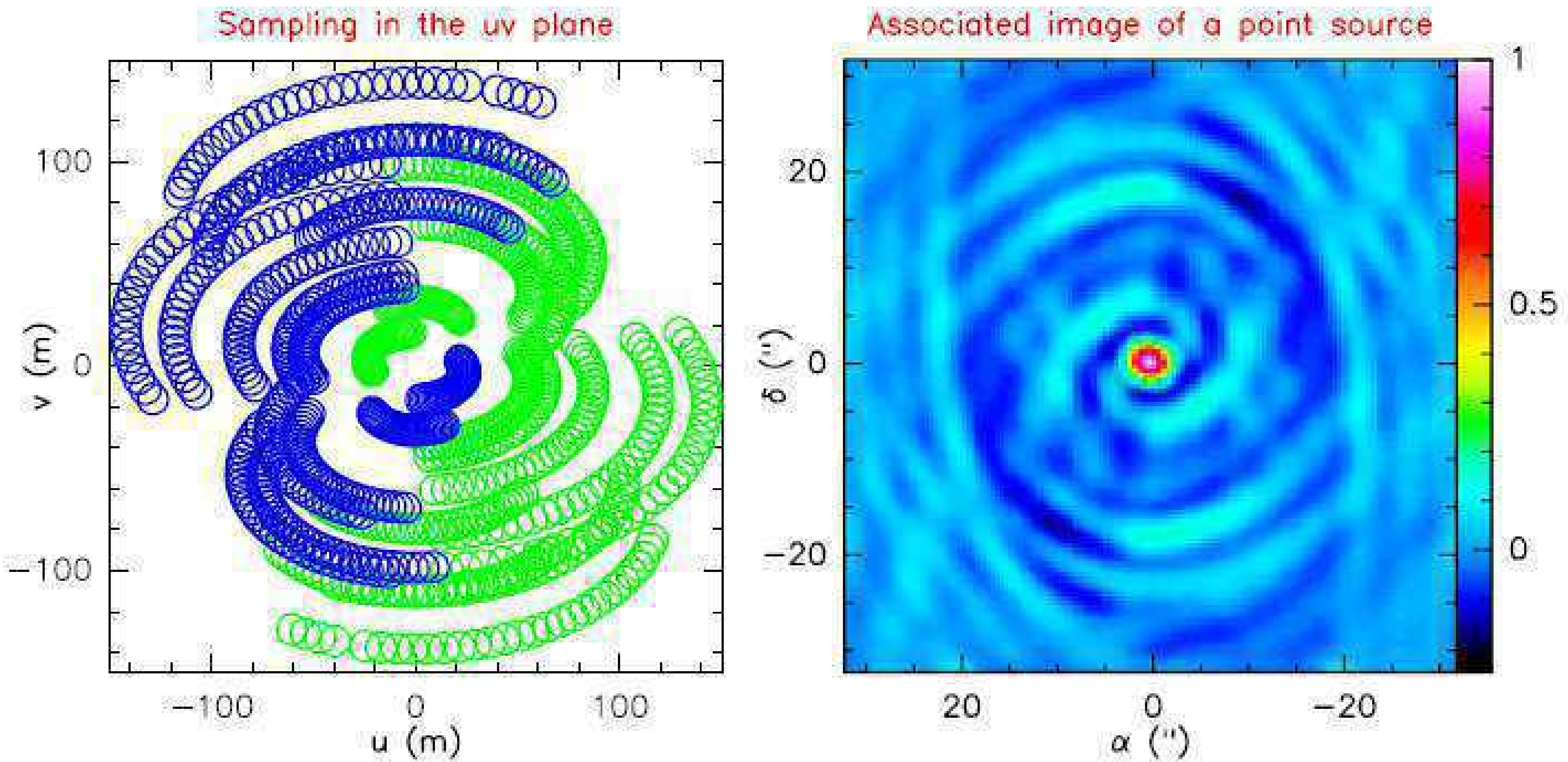

Earth-rotation aperture synthesis

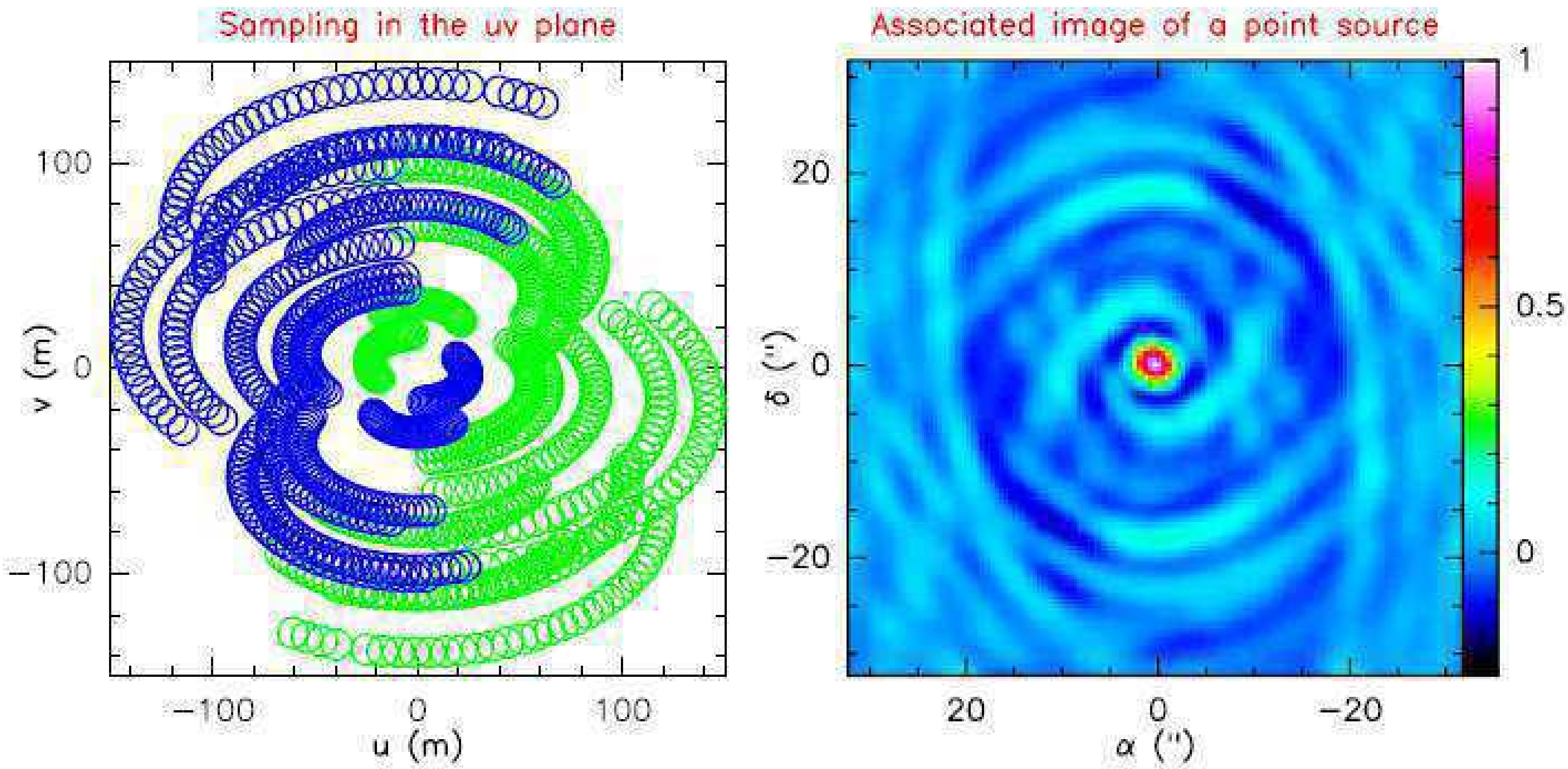

Formal Description

- sample Fourier domain at discrete points

$$B(u, v) = \sum_k (u_k, v_k)$$

- the inverse Fourier transform is

$$T^D(x, y) = FT^{-1}\{B(u, v) \times V(u, v)\}$$

- the convolution theorem tells us

$$T^D(x, y) = b(x, y) \otimes T(x, y)$$

where (the point spread function)

$$b(x, y) = FT^{-1}\{B(u, v)\}$$

Fourier transform of sampled visibilities yields the true sky brightness convolved with the point spread function

(the “dirty image” is the true image convolved with the “dirty beam”)

Dirty Beam and Dirty Image

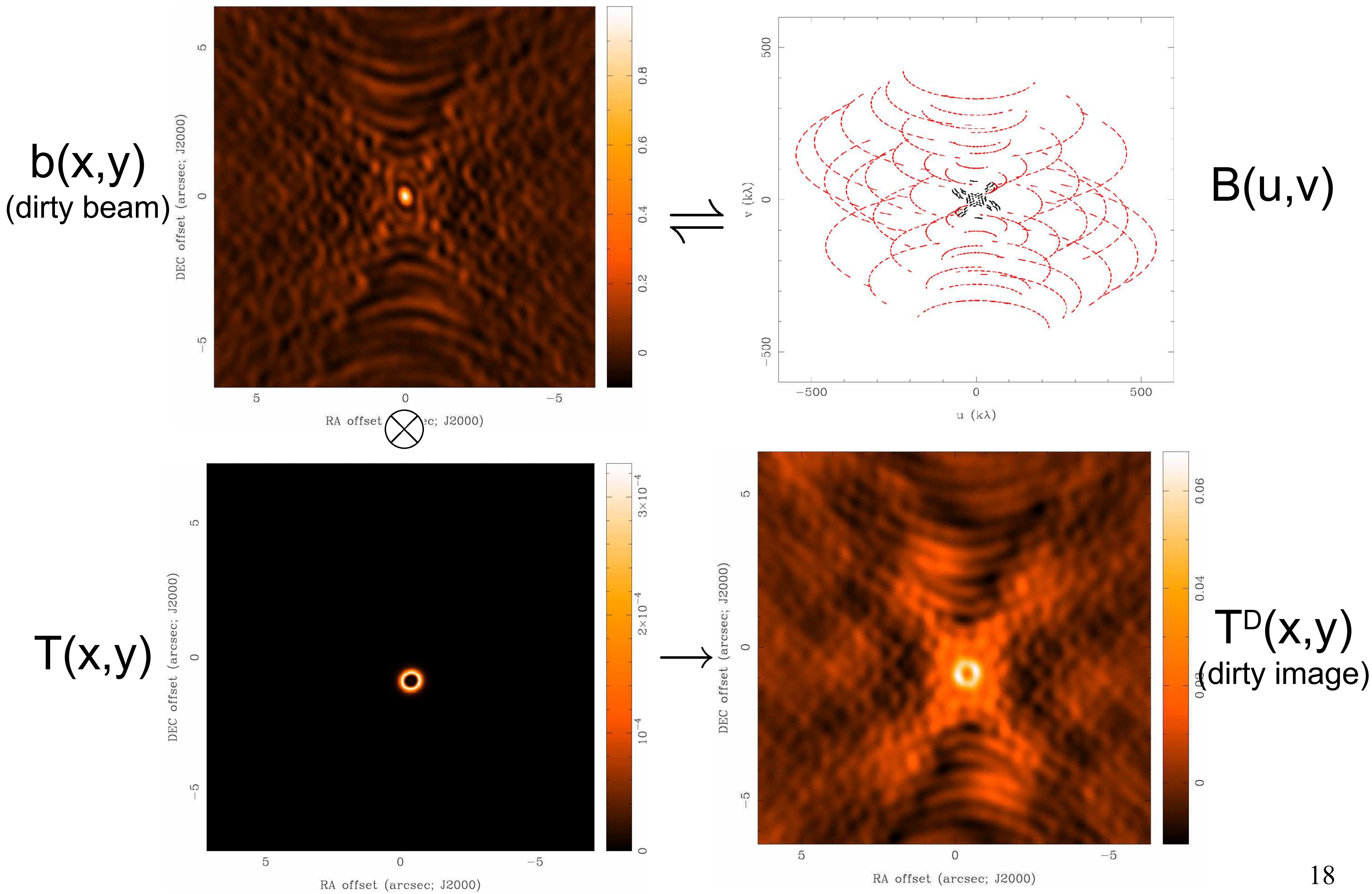

How to analyze interferometer data?

- uv plane analysis
  - best for “simple” sources, e.g. point sources, disks
- image plane analysis
  - Fourier transform V(u,v) samples to image plane, get $T^D(x,y)$
  - but difficult to do science on dirty image
  - deconvolve b(x,y) from $T^D(x,y)$ to determine (model of) T(x,y)

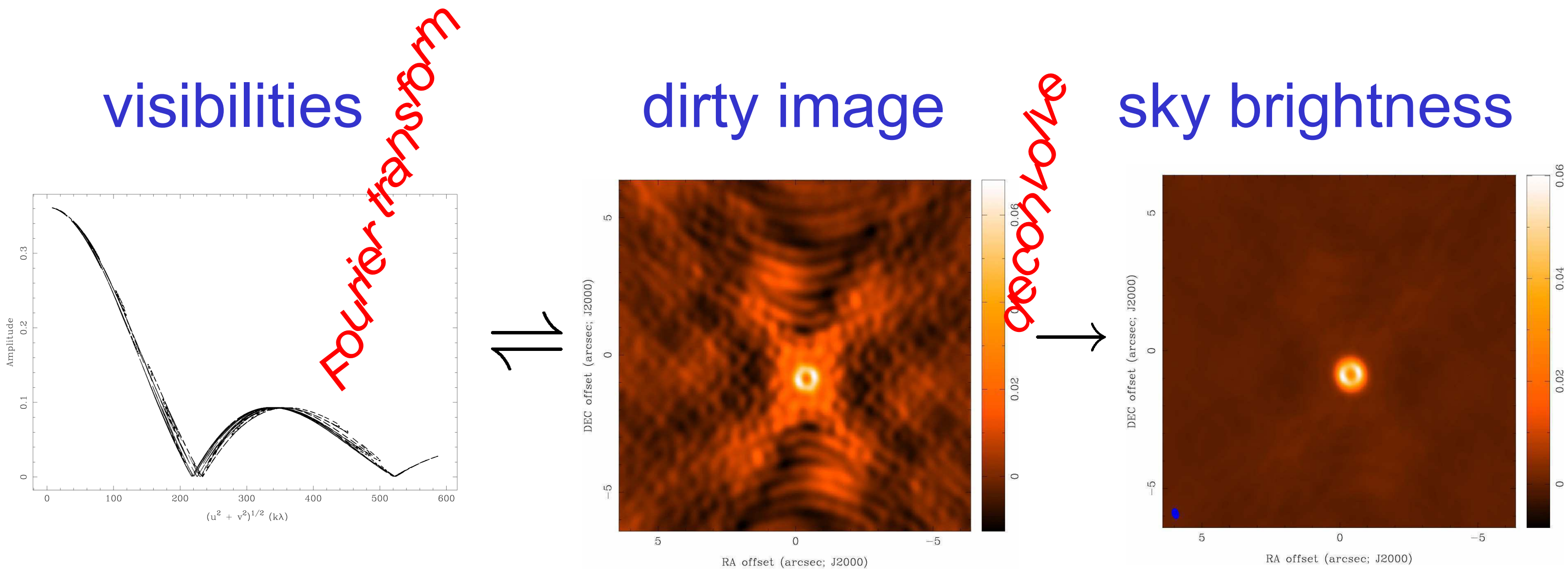

Details of the Dirty Image

- Fourier Transform
  - Fast Fourier Transform (FFT) much faster than simple Fourier summation, O(NlogN) for $2^N \times 2^N$ image
  - FFT requires data on regularly spaced grid
  - aperture synthesis observations not on a regular grid…
- "Gridding" is used to resample V(u,v) for FFT
  - customary to use a convolution technique
    - visibilities are noisy samples of a smooth function
    - nearby visibilities not independent
  - use special ("Spheroidal") functions with nice properties
    - fall off quickly in (u,v) plane (not too much smoothing)
    - fall off quickly in image plane (avoid aliasing)

$$V^G(u,v) = V(u,v)B(u,v) \otimes G(u,v) \rightleftharpoons T^D(x,y)g(x,y)$$

Primary Beam

- A telescope does not have uniform response across the entire sky
  - main lobe approximately Gaussian, fwhm ~1.2λ/D, where D is ant diameter = “primary beam”
  - limited field of view
  - sidelobes, error beam (sometimes important)

- primary beam response modifies sky brightness: T(x,y) → A(x,y)T(x,y)
  - correct with division by A(x,y) in image plane

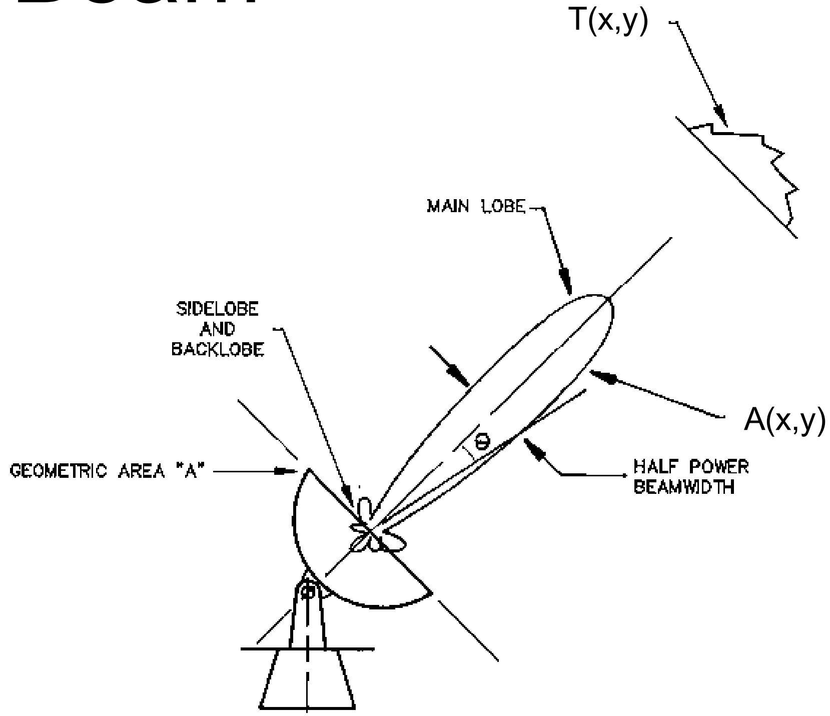

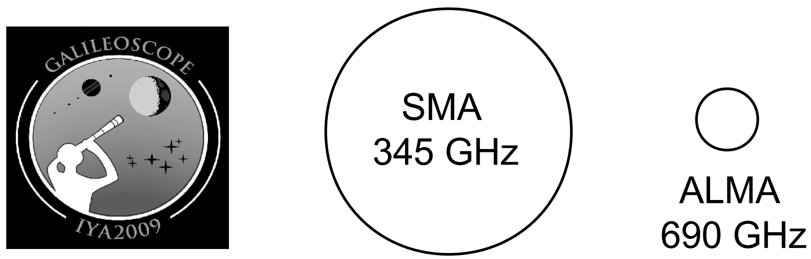

T(x,y) large A(x,y) small A(x,y)

Pixel Size and Image Size

- pixel size
  - should satisfy sampling theorem for the longest baselines, $\Delta x < 1/2\ u_{max}$, $\Delta y < 1/2\ v_{max}$
  - in practice, 3 to 5 pixels across the main lobe of the dirty beam (to aid deconvolution)
  - e.g., SMA: 870 μm, 500 m baselines → 600 kλ→ < 0.1 arcsec

- image size
  - natural resolution in (u,v) plane samples FT{A(x,y)}, implies image size 2x primary beam
  - e.g., SMA: 870 μm, 6 m telescope → 2x 35 arcsec
  - if there are bright sources in the sidelobes of A(x,y), then they will be aliased into the image (need to make a larger image)

Dirty Beam Shape and Weighting

- introduce weighting function W(u,v)

  $$b(x,y) = FT^{-1}\{W(u,v)B(u,v)\}$$

  – W modifies sidelobes of dirty beam
  (W is also gridded for FFT)

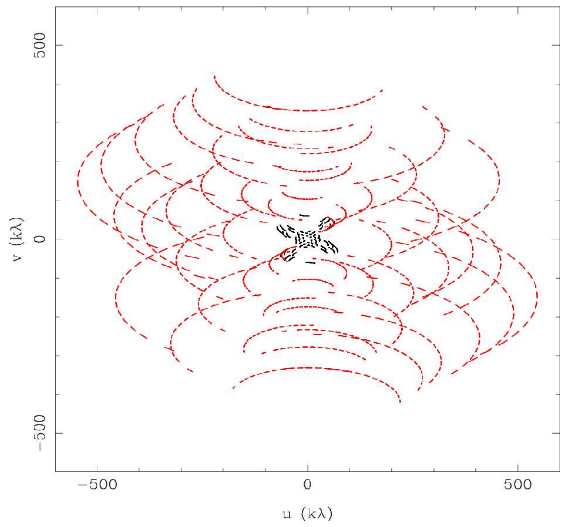

- "Natural" weighting
  – W(u,v) = $1/\sigma^2(u,v)$ at points with data and zero elsewhere, where $\sigma^2(u,v)$ is the noise variance of the (u,v) sample
  – maximizes point source sensitivity (lowest rms in image)
  – generally more weight to short baselines (large spatial scales), degrades resolution

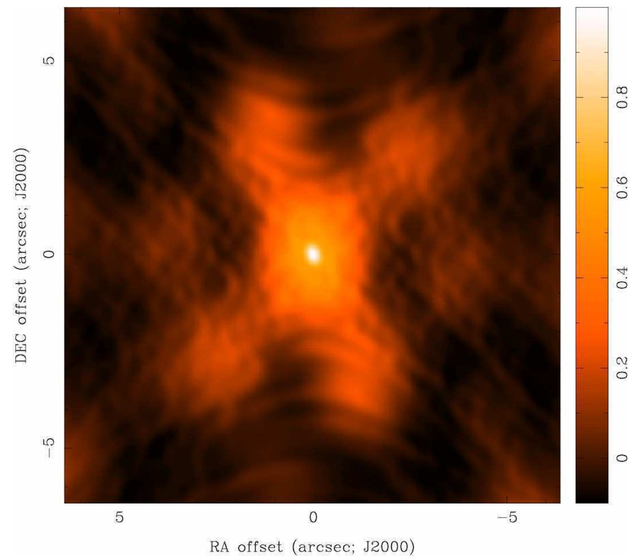

Dirty Beam Shape and Weighting

- "Uniform" weighting
  - W(u,v) is inversely proportional to local density of (u,v) points, so sum of weights in a (u,v) cell is a constant (or zero)
  - fills (u,v) plane more uniformly, so (outer) sidelobes are lower
  - gives more weight to long baselines and therefore higher angular resolution
  - degrades point source sensitivity (higher rms in image)
  - can be trouble with sparse sampling: cells with few data points have same weight as cells with many data points

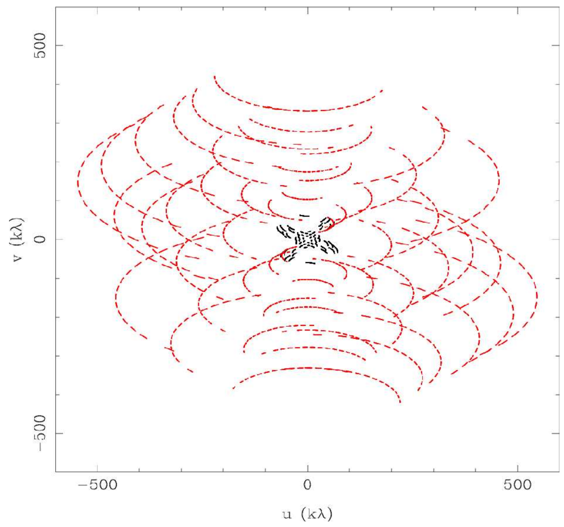

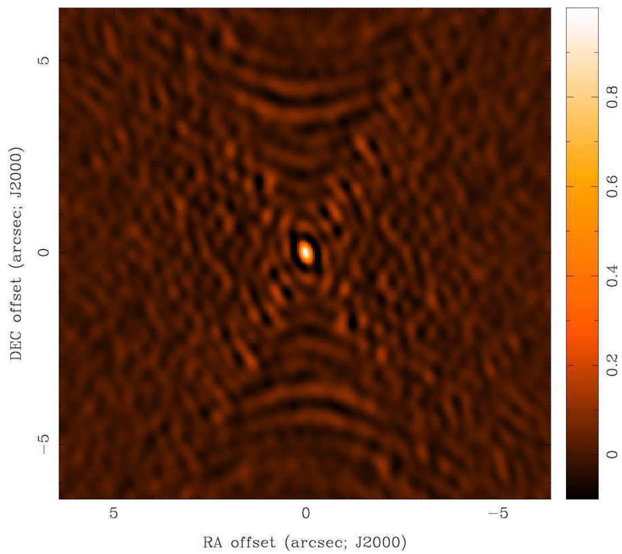

Dirty Beam Shape and Weighting

- "Robust" (Briggs) weighting
  - variant of "uniform" that avoids giving too much weight to cell with low natural weight
  - implementations differ, e.g. S_N is natural weight of a cell, S_t is a threshold

$$W(u,v) = \frac{1}{\sqrt{1+S_N^2/S_{thresh}^2}}$$

  - large threshold → natural weighting
  - small threshold → uniform weighting
  - an adjustable parameter that allows for continuous variation between highest angular resolution and optimal point source sensitivity

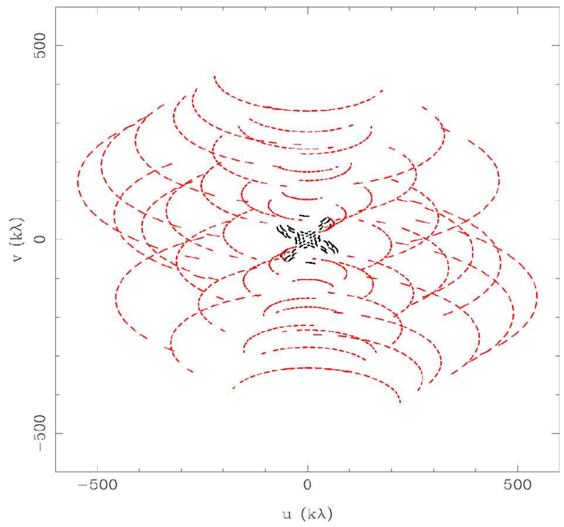

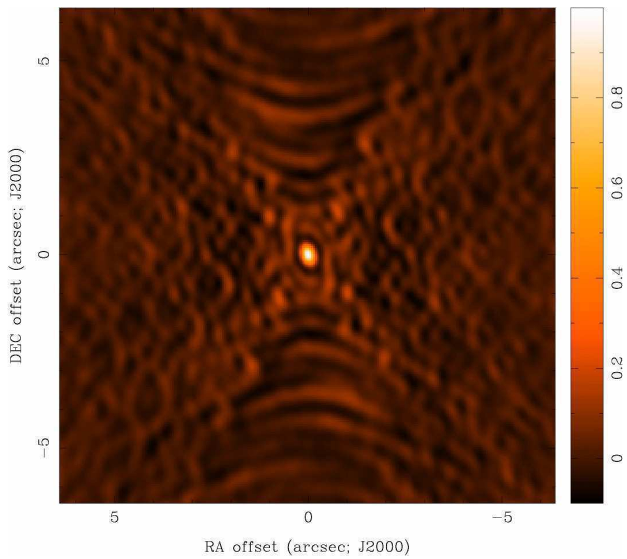

Dirty Beam Shape and Weighting

- "Tapering"
  - apodize the (u,v) sampling by a Gaussian

$$W(u,v) = exp\left\{-\frac{(u^2+v^2)}{t^2}\right\}$$

t = tapering parameter (in kλ; arcsec)

  - like smoothing in the image plane (convolution by a Gaussian)
  - gives more weight to short baselines, degrades angular resolution
  - degrades point source sensitivity but can improve sensitivity to extended structure
  - could use elliptical Gaussian, other function
  - limits to usefulness

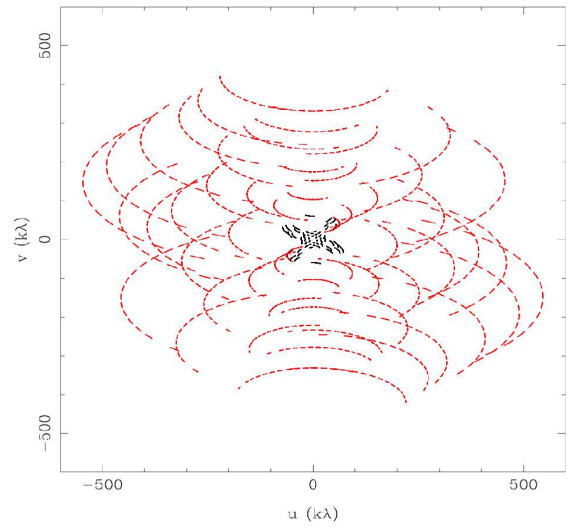

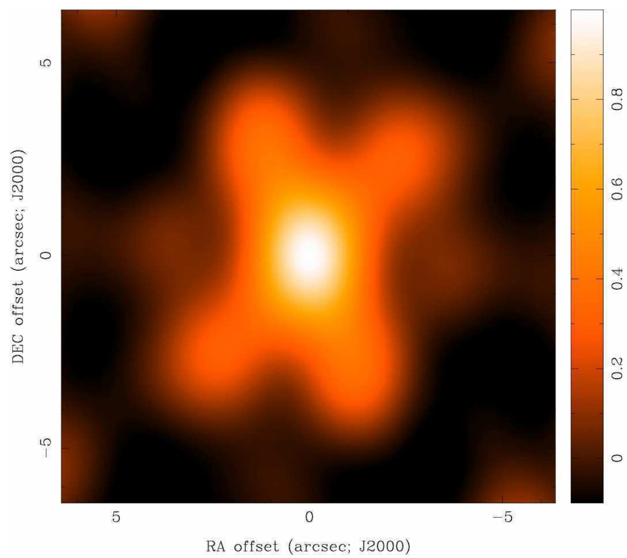

Weighting and Tapering: Noise

Natural
0.77x0.62

σ=1.0

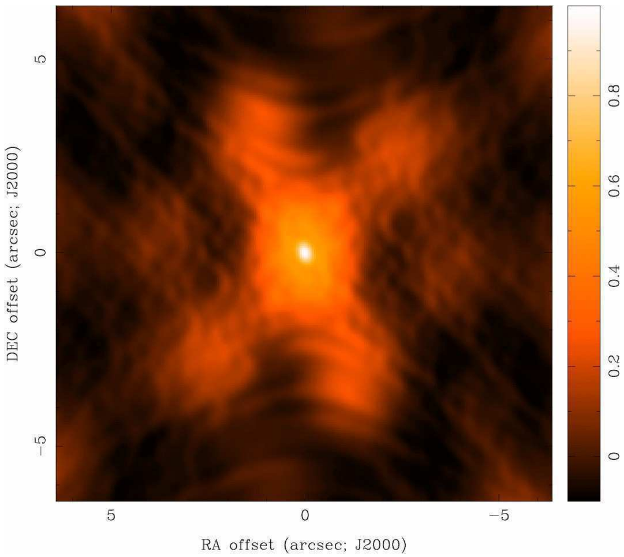

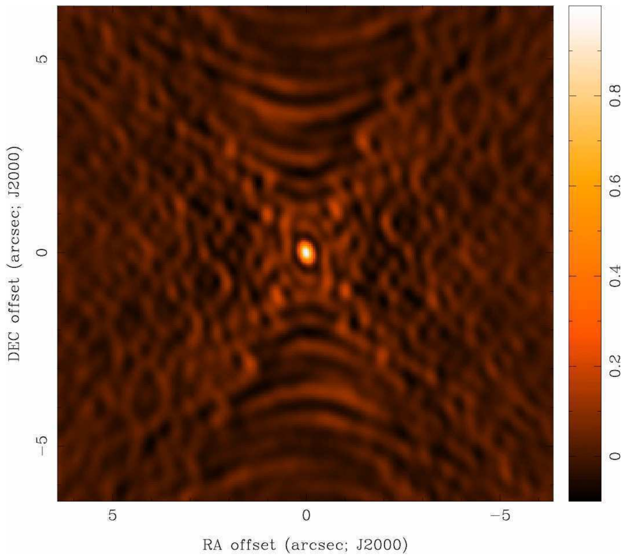

Robust 0
0.41x0.36

σ=1.6

Uniform
0.39x0.31

σ=3.7

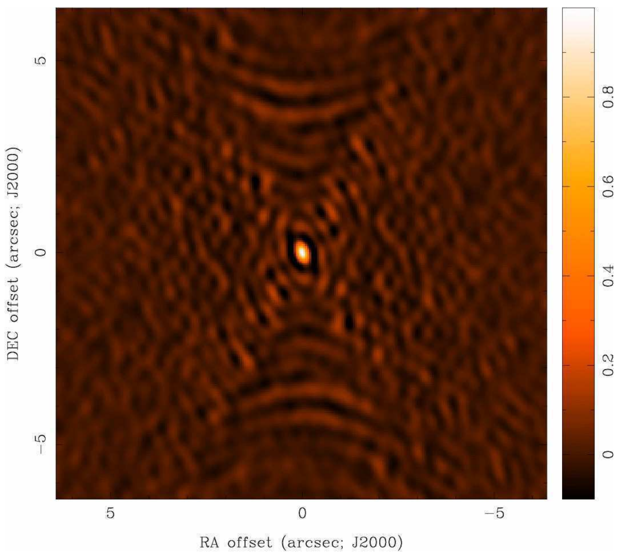

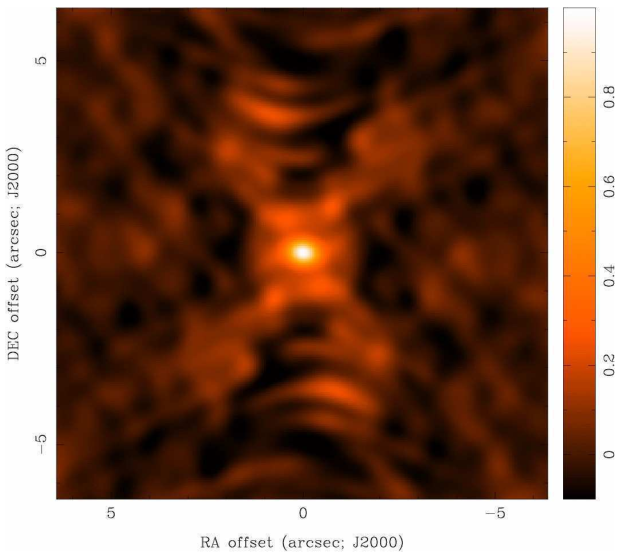

Robust 0
+ Taper
0.77x0.62

σ=1.7

Weighting and Tapering: Summary

- imaging parameters provide a lot of freedom
- appropriate choice depends on science goals

	Robust/Uniform	Natural	Taper
Resolution	higher	medium	lower
Sidelobes	lower	higher	depends
Point Source Sensitivity	lower	maximum	lower
Extended Source Sensitivity	lower	medium	higher

Deconvolution

- difficult to do science on dirty image
- deconvolve b(x,y) from $T^D(x,y)$ to recover T(x,y)
- information is missing, so be careful!
  (there's noise, too)

dirty image

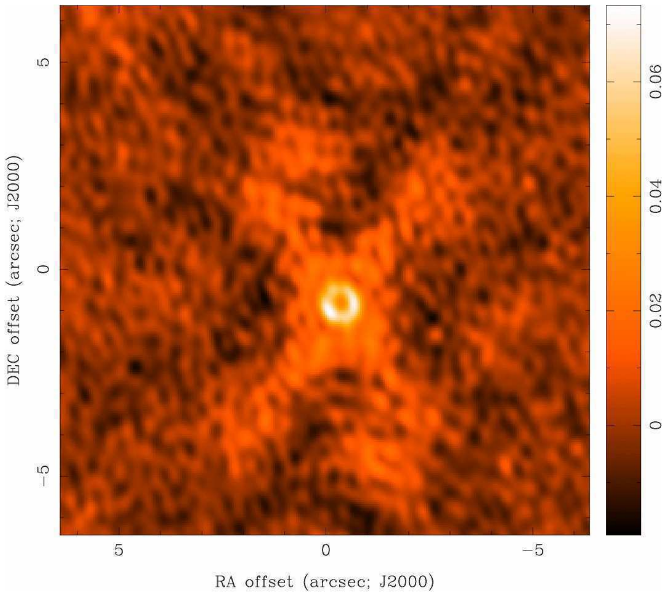

"CLEAN" image

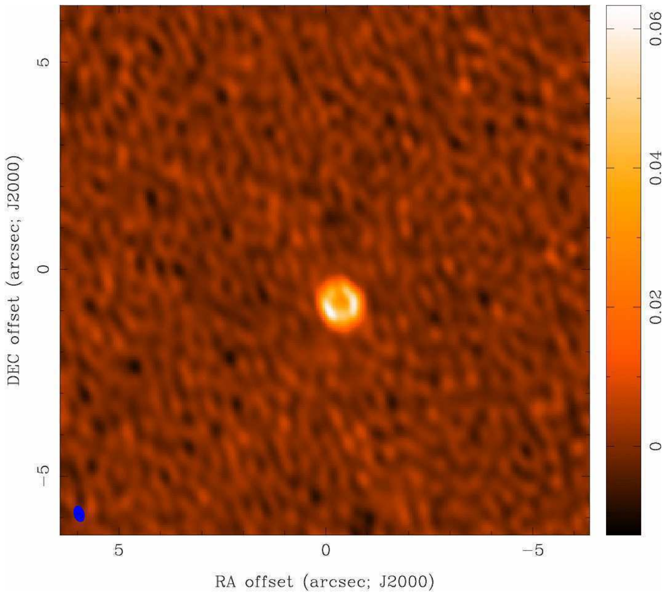

Deconvolution Philosophy

- to keep you awake at night
  - ∃ an infinite number of T(x,y) compatible with sampled V(u,v), i.e. "invisible" distributions R(x,y) where $b(x,y) \otimes R(x,y) = 0$
    - no data beyond u_{max} ,v_{max} → unresolved structure
    - no data within u_{min} ,v_{min} → limit on largest size scale
    - holes between u_{min} ,v_{min} and u_{max} ,v_{max} → sidelobes
  - noise → undetected/corrupted structure in T(x,y)
  - no unique prescription for extracting optimum estimate of true sky brightness from visibility data
- deconvolution
  - uses non-linear techniques effectively interpolate/extrapolate samples of V(u,v) into unsampled regions of the (u,v) plane
  - aims to find a **sensible** model of T(x,y) compatible with data
  - requires *a priori* assumptions about T(x,y)

Deconvolution Algorithms

- most common algorithms in radio astronomy
  - CLEAN (Högbom 1974)
    - *a priori* assumption: T(x,y) is a collection of point sources
    - variants for computational efficiency, extended structure
  - Maximum Entropy (Gull and Skilling 1983)
    - *a priori* assumption: T(x,y) is smooth and positive
    - vast literature about the deep meaning of entropy (Bayesian)
  - hybrid approaches of these can be effective

- deconvolution requires knowledge of beam shape and image noise properties (usually OK for aperture synthesis)
  - atmospheric seeing can modify effective beam shape
  - deconvolution process can modify image noise properties

Basic CLEAN Algorithm

1. Initialize
   - a *residual* map to the dirty map
   - a *Clean component* list to empty

– Identify strongest feature in *residual* map as a point source

– Add a fraction g (the loop gain) of this point source to the clean component list

– Subtract the fraction g times b(x,y) from *residual* map

– If stopping criteria not reached, goto step 2 (an iteration)

– Convolve *Clean component* (cc) list by an estimate of the main lobe of the dirty beam (the “Clean beam”) and add *residual* map to make the final “restored” image

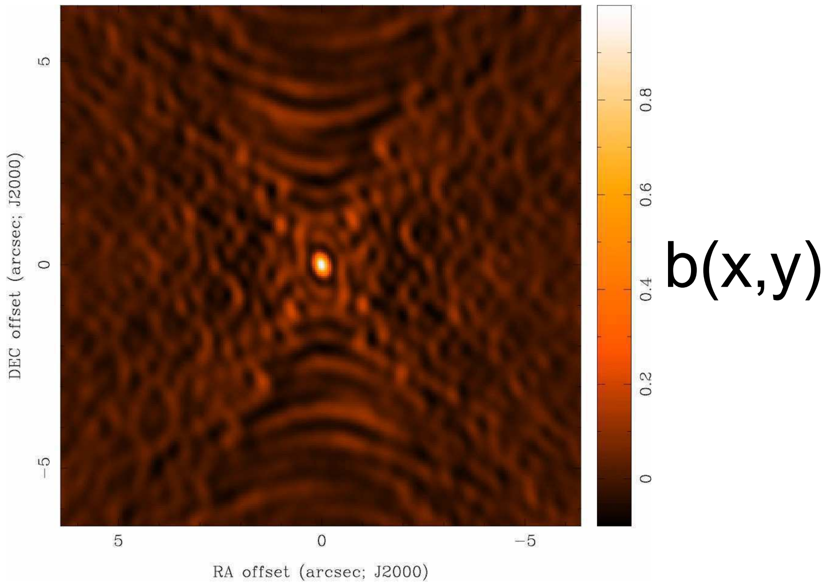

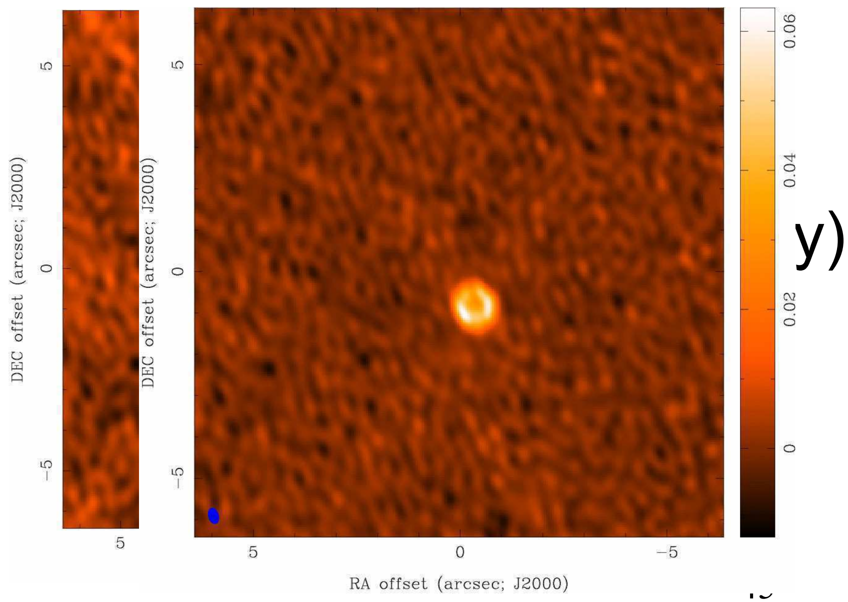

Basic CLEAN Algorithm (cont)

- stopping criteria
  - r*esidual* map max < multiple of rms (when noise limited)
  - r*esidual* map max < fraction of dirty map max (dynamic range limited)
  - max number of clean components reached (no justification)
- loop gain
  - good results for g ~ 0.1 to 0.3
  - lower values can work better for smoother emission, g ~ 0.05
- easy to include *a priori* information about where to search for clean components ("clean boxes")
  - very useful but potentially dangerous!

- Schwarz (1978): CLEAN is equivalent to a least squares fit of sinusoids, in the absense of noise

CLEAN

$T^D(x,y)$

CLEAN model

restored image

residual map

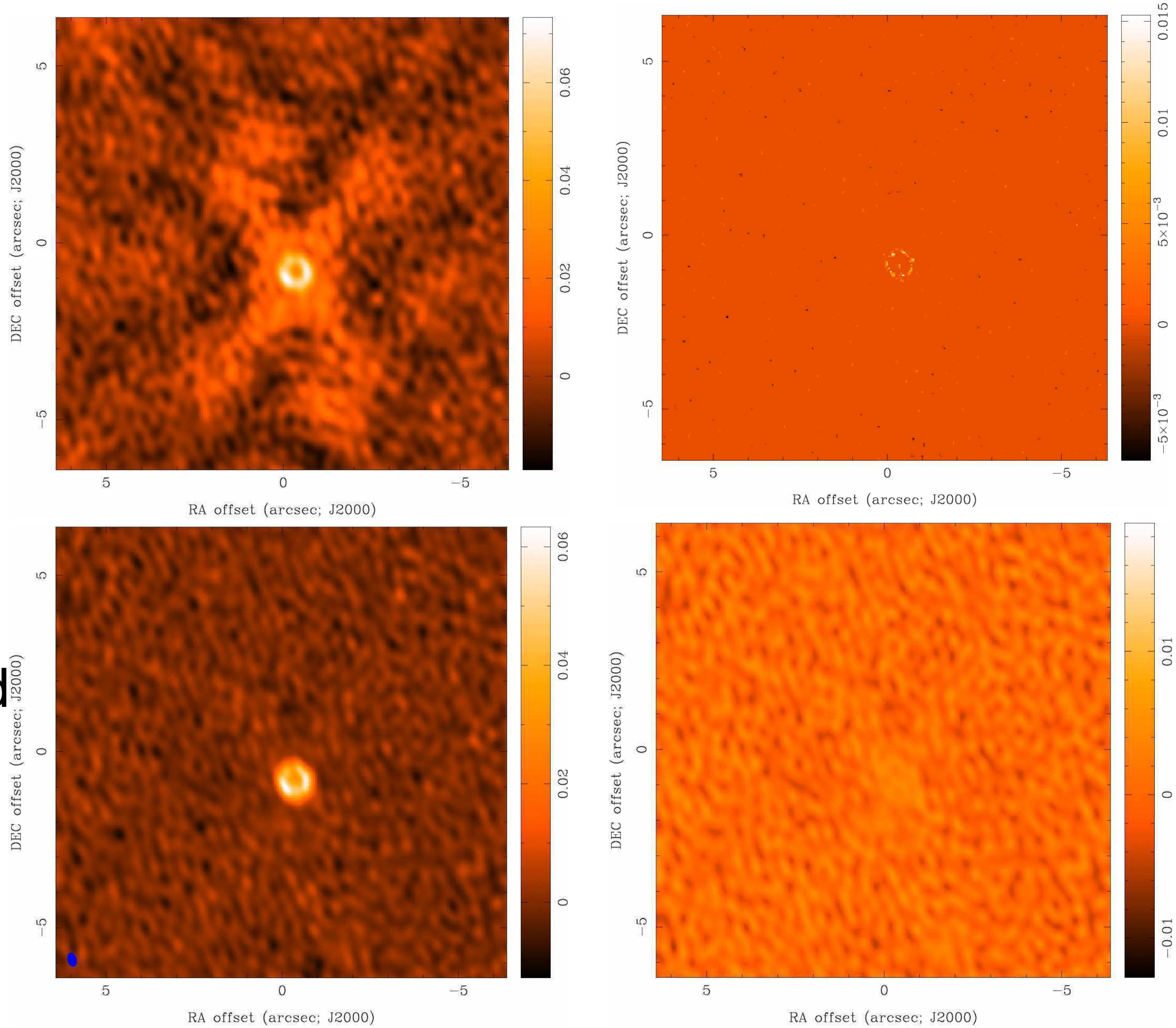

CLEAN with Box

$T^D(x,y)$

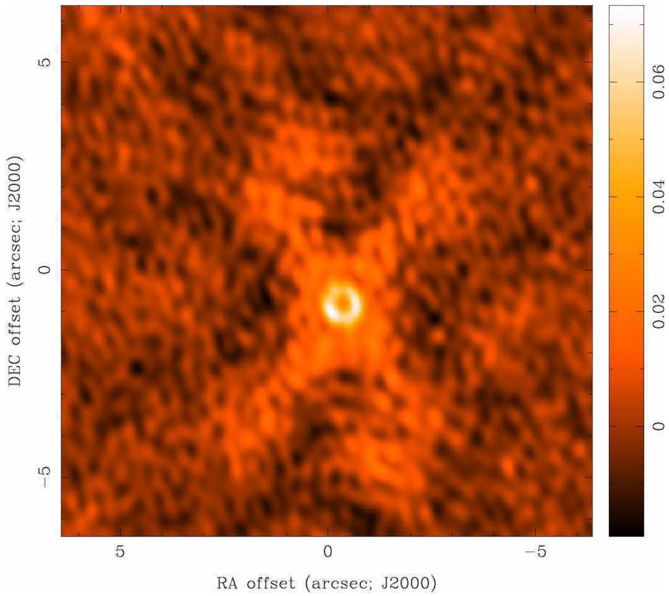

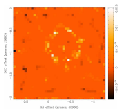

CLEAN
model

restored
image

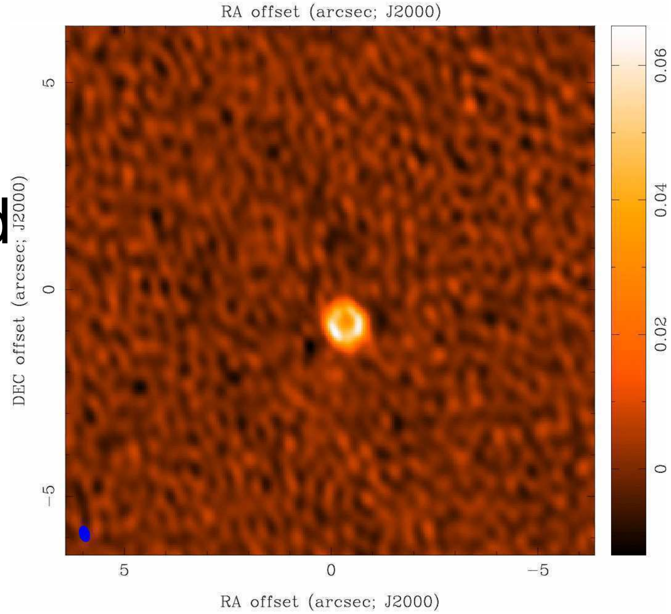

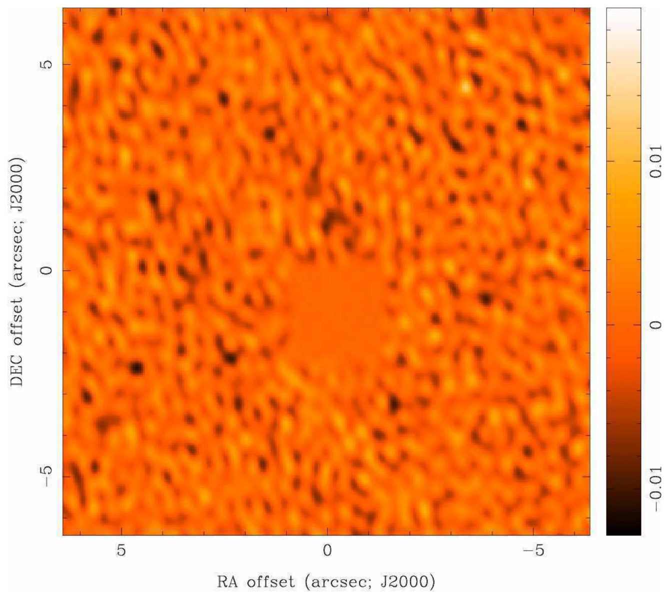

residual
map

CLEAN with Poor Choice of Box

$T^D(x,y)$

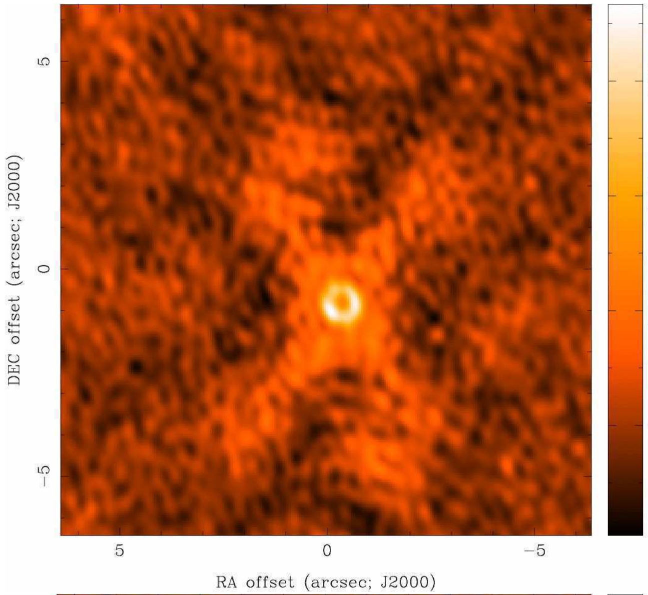

CLEAN model

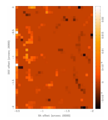

restored image

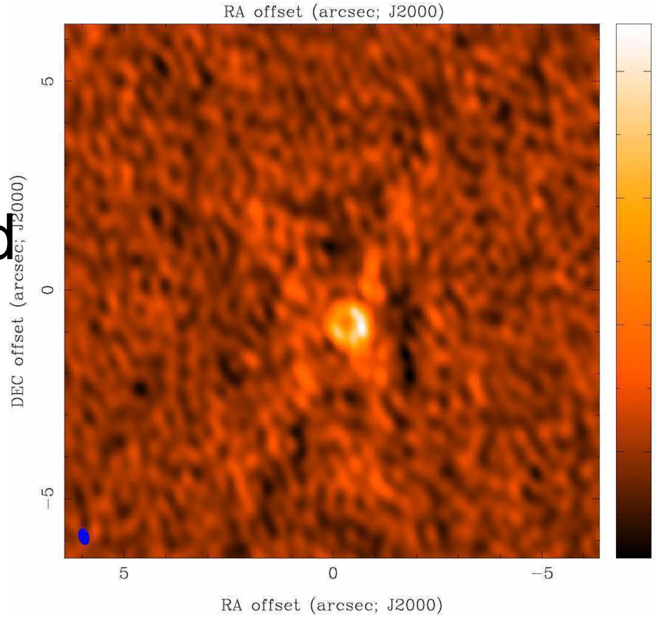

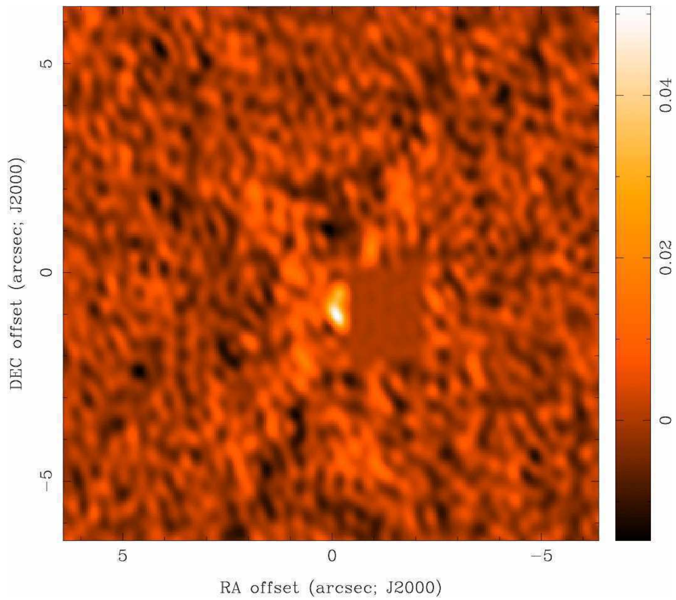

residual map

CLEAN Variants

- Clark CLEAN
  - aims at faster speed for large images
  - Högbom-like "minor" cycle w/ truncated dirty beam, subset of largest residuals
  - in "major" cycle, cc's are FFT'd and subtracted from the FFT of the residual image from the previous "major" cycle
- Cotton-Schwab CLEAN (MX)
  - in "major" cycle, cc's are FFT'd and subtracted from ungridded visibilities
  - more accurate but slower (gridding steps repeated)
- Steer, Dewdny, Ito (SDI) CLEAN
  - aims to supress CLEAN "stripes" in smooth, extended emission
  - in "minor" cycles, any point in the residual map greater than a fraction (<1) of the maximum is taken as a cc
- Multi-Resolution CLEAN
  - aims to account for coupling between pixels by extended structure
  - independently CLEAN a smooth map and a difference map, fewer cc's

“Restored” Images

- CLEAN beam size:
  - natural choice is to fit the central peak of the dirty beam with elliptical Gaussian
  - unit of deconvolved map is Jy per CLEAN beam area
    (= intensity, can convert to brightness temperature)
  - minimize unit problems when adding dirty map residuals
  - modest super resolution often OK, but be careful

- photometry should be done with caution
  - CLEAN does not conserve flux (extrapolates)
  - extended structure missed, attenuated, distorted
  - phase errors (e.g. seeing) can spread signal around

Noise in Images

- point source sensitivity: straightforward
  - telescope area, bandwidth, integration time, weighting
  - in image, modify noise by primary beam response
- extended source sensitivity: problematic
  - not quite right to divide noise by $\sqrt{n}$ beams covered by source: smoothing = tapering, omitting data → lower limit
  - Interferometers always missing flux at some spatial scale
- be careful with low signal-to-noise images
  - if position known, 3σ OK for point source detection
  - if position unknown, then 5σ required (flux biased by $\sim 1\sigma$)
  - if $< 6\sigma$, cannot measure the source size (require $\sim 3\sigma$ difference between "long" and "short" baselines)
  - spectral lines may have unknown position, velocity, width

Maximum Entropy Algorithm

- Maximize a measure of smoothness (the entropy)

$$H = -\sum_k T_k \log\left(\frac{T_k}{M_k}\right)$$

subject to the constraints

$$\chi^2 = \sum_k \frac{|V(u_k,v_k) - \mathrm{FT}\{T\}|^2}{\sigma_k^2}$$

$$F = \sum_k T_k$$

- M is the “default image”
- fast (NlogN) non-linear optimization solver due to Cornwell and Evans (1983)
- optional: convolve with Gaussian beam and add residual map to make image

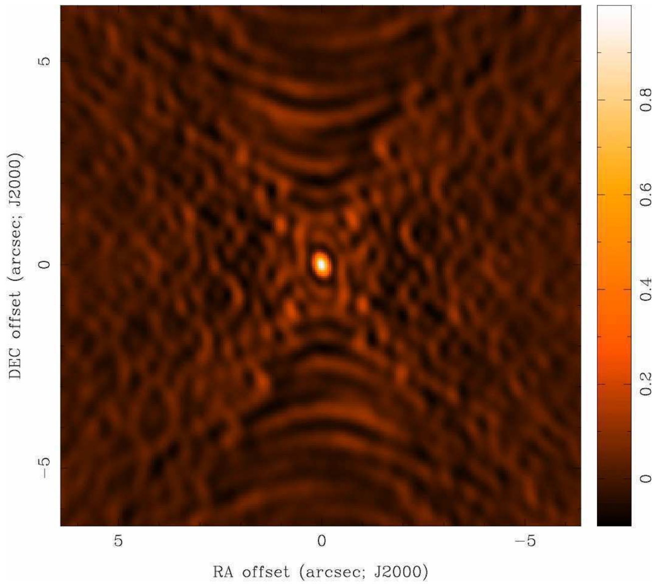

b(x,y)

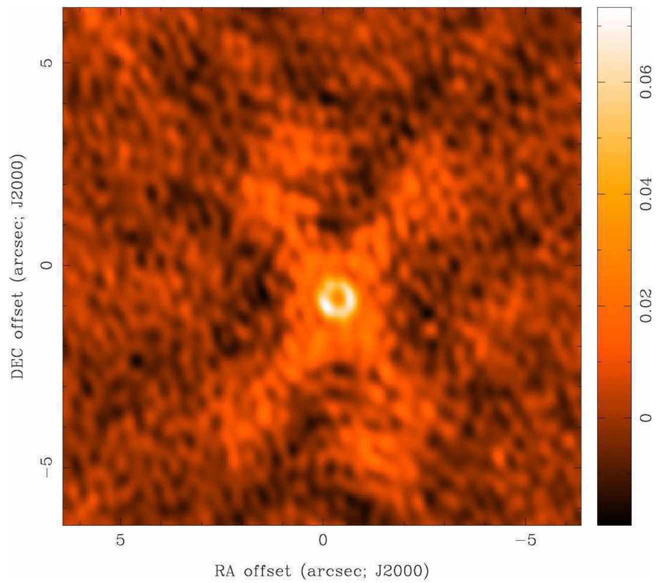

$T^D(x,y)$

Maximum Entropy Algorithm (cont)

- easy to include *a priori* information with default image
  - flat default best only if nothing known (or nothing observed!)
- straightforward to generalize χ^2 to combine different observations/telescopes and obtain optimal image
- many measures of "entropy" available
  - replace log with cosh → "emptiness" (does not enforce positivity)

- less robust and harder to drive than CLEAN
- works well on smooth, extended emission
- trouble with point source sidelobes
- no noise estimate possible from image

Maximum Entropy

$T^D(x,y)$

MAXEN model

restored image

residual map

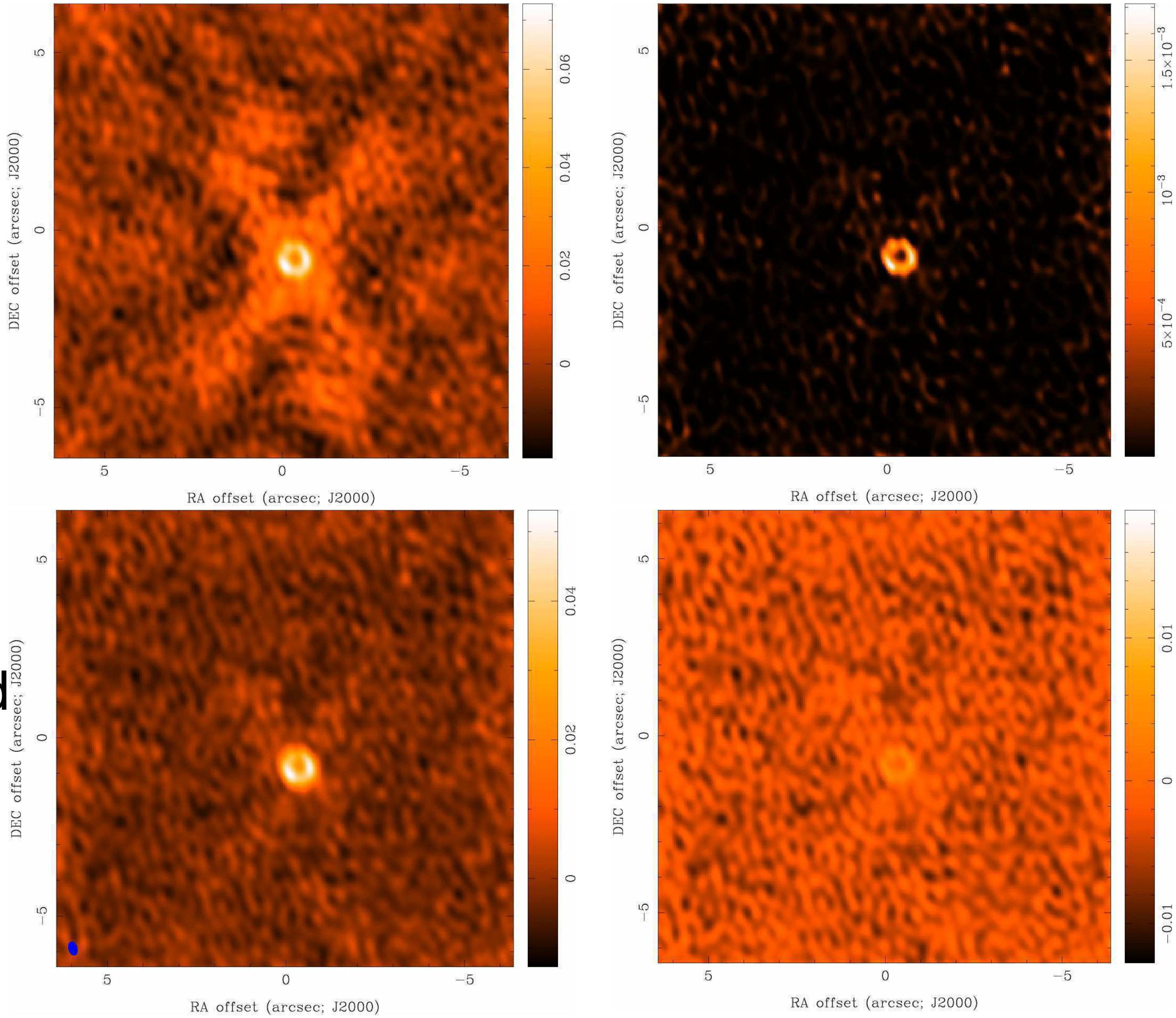

Imaging Results

Natural Weight Beam

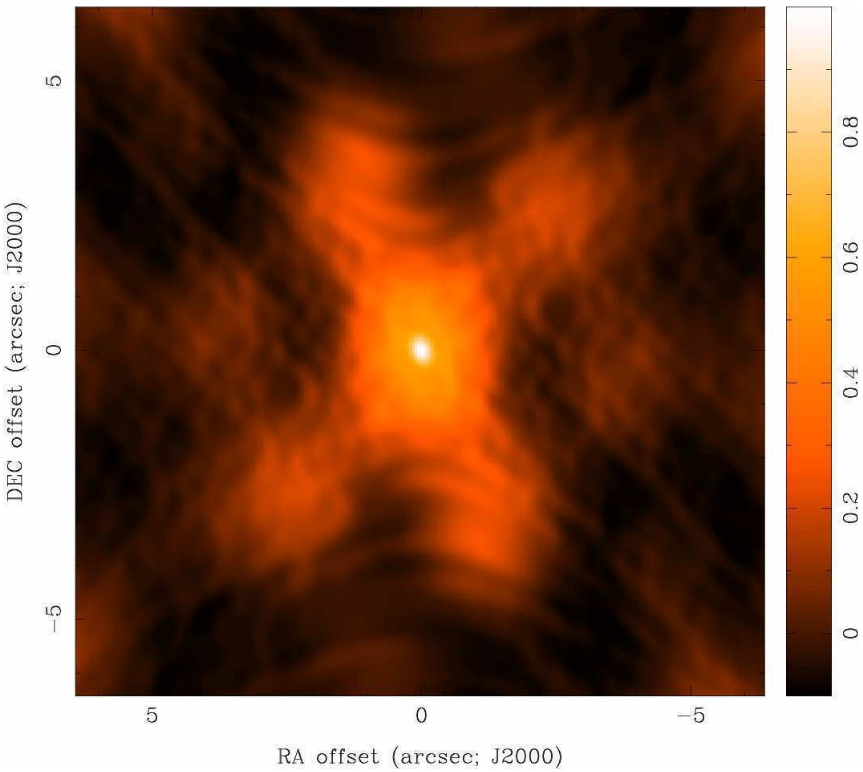

CLEAN image

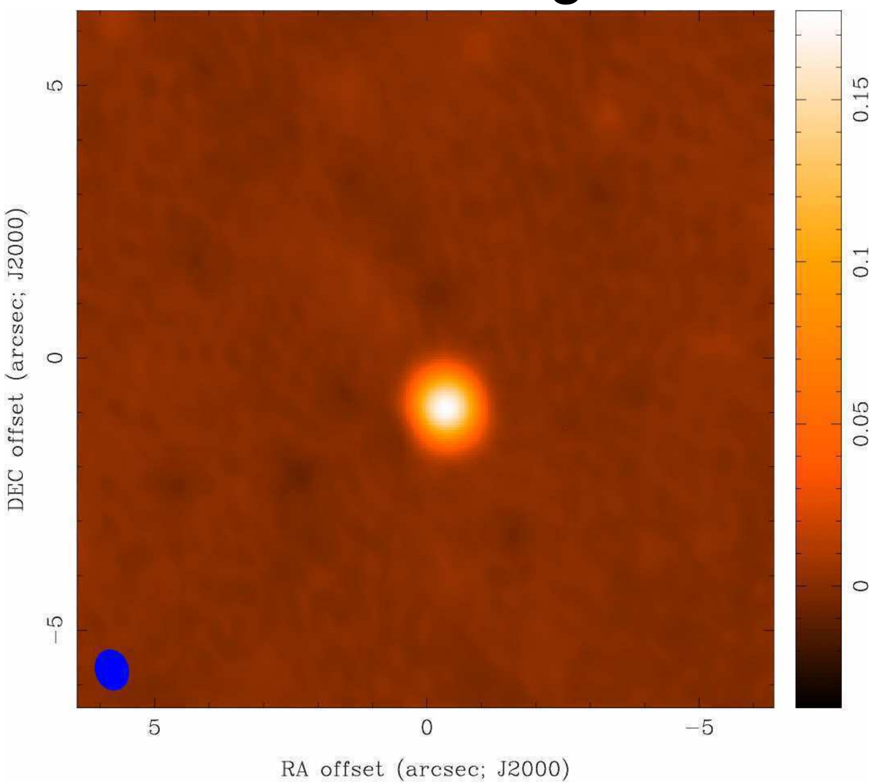

Imaging Results

Uniform Weight Beam

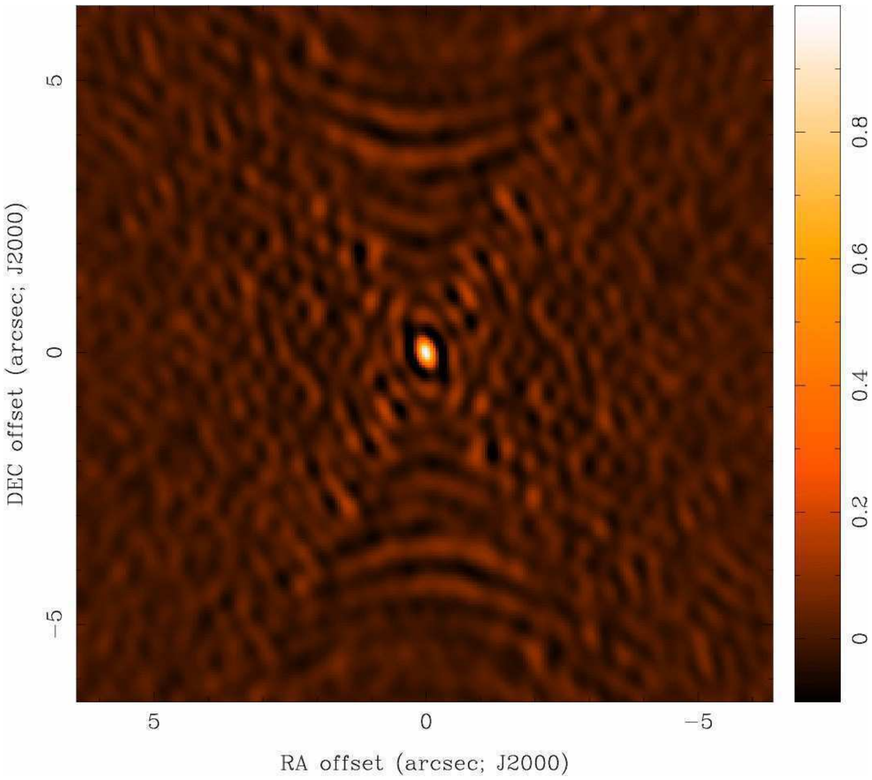

CLEAN image

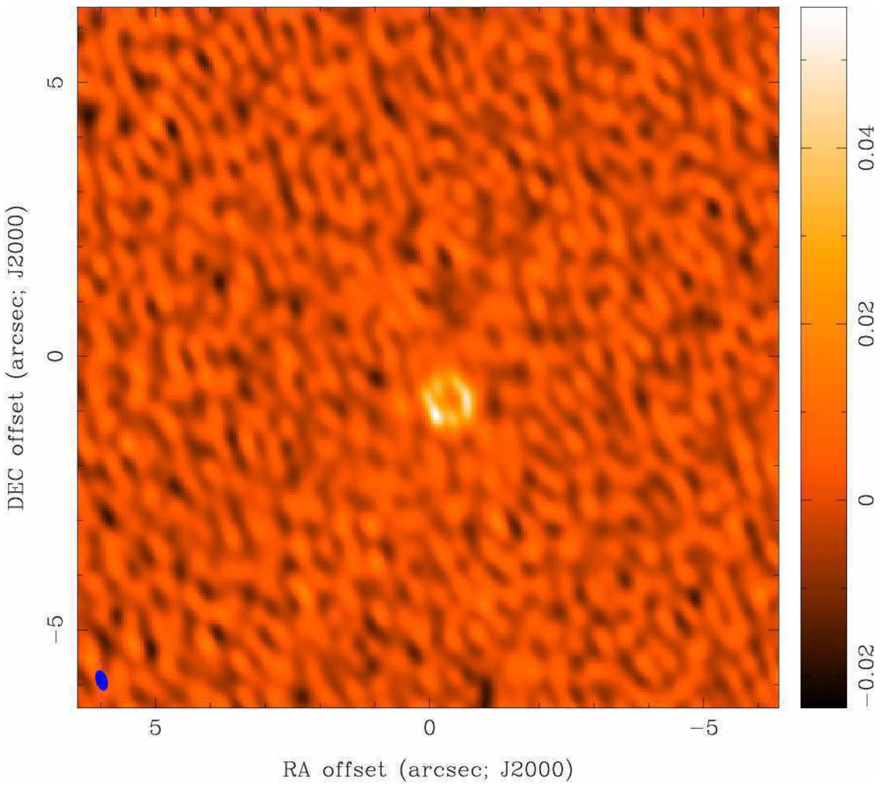

Imaging Results

Robust=0 Beam

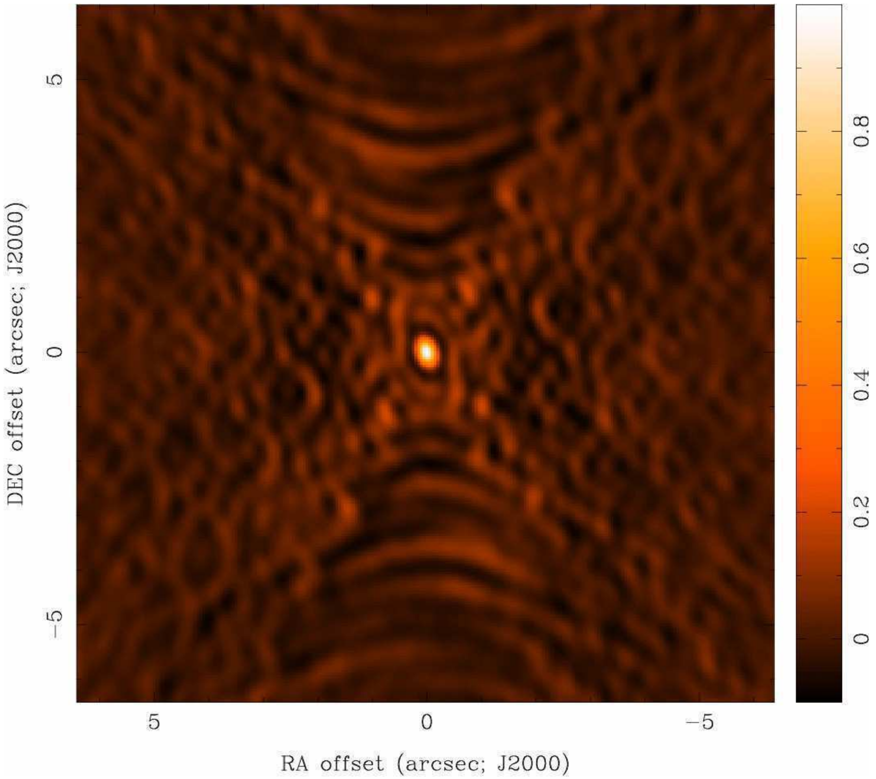

CLEAN image

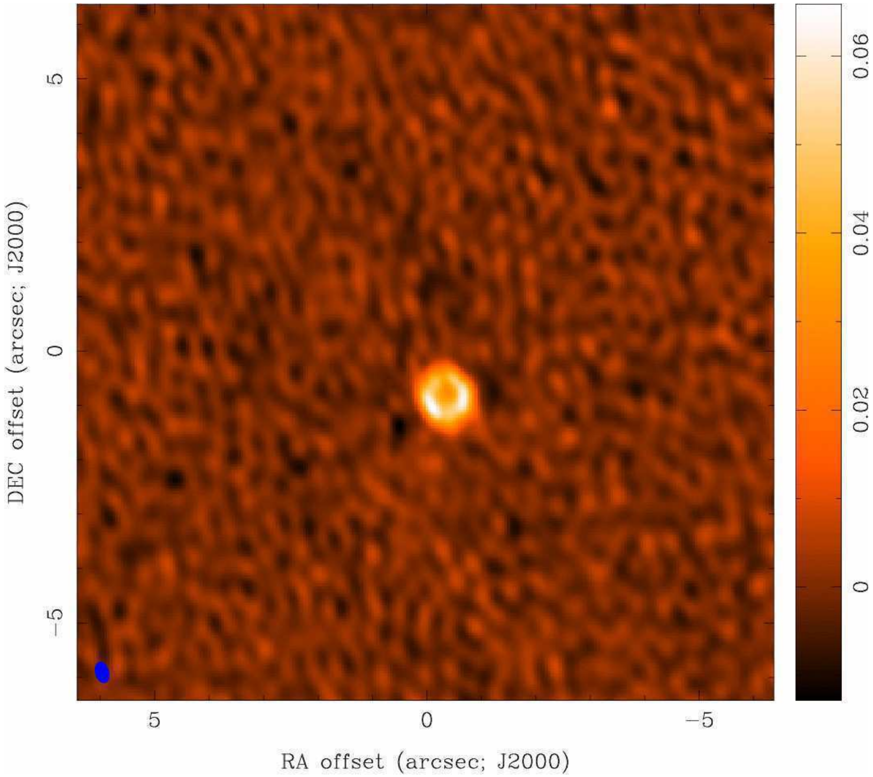

Imaging Results

Robust=0 Beam

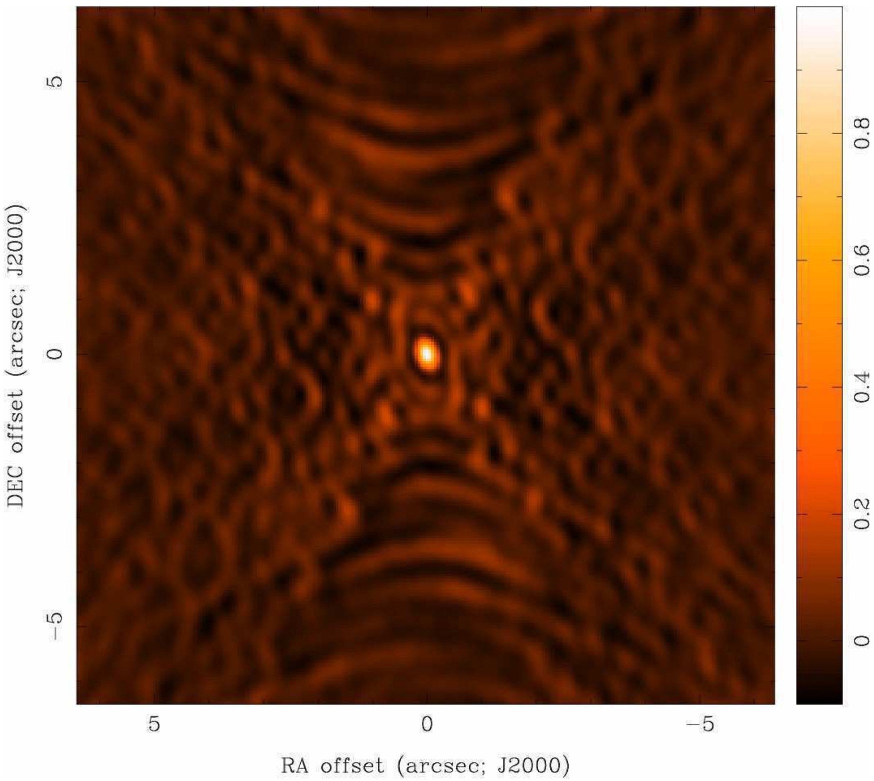

MAXEN image

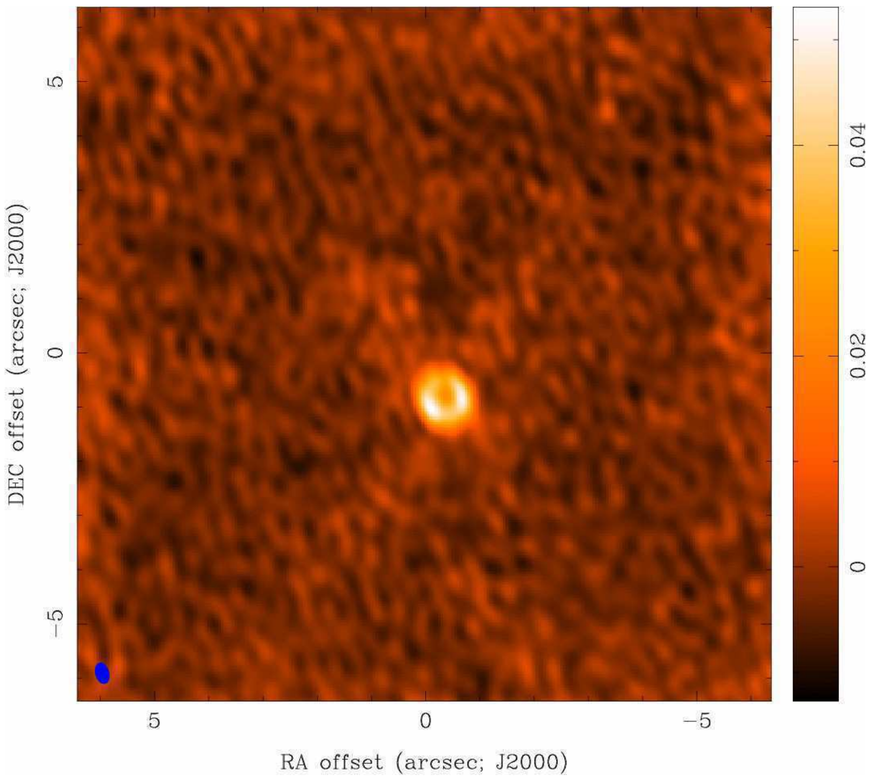

Tune Resolution/Sensitivity to suit Science

- e.g. Andrews, Wilner et al. 2009, ApJ, 700, 1502
  - SMA 870 μm images of "transitional" protoplanetary disks with resolved inner holes, note images of WSB 60

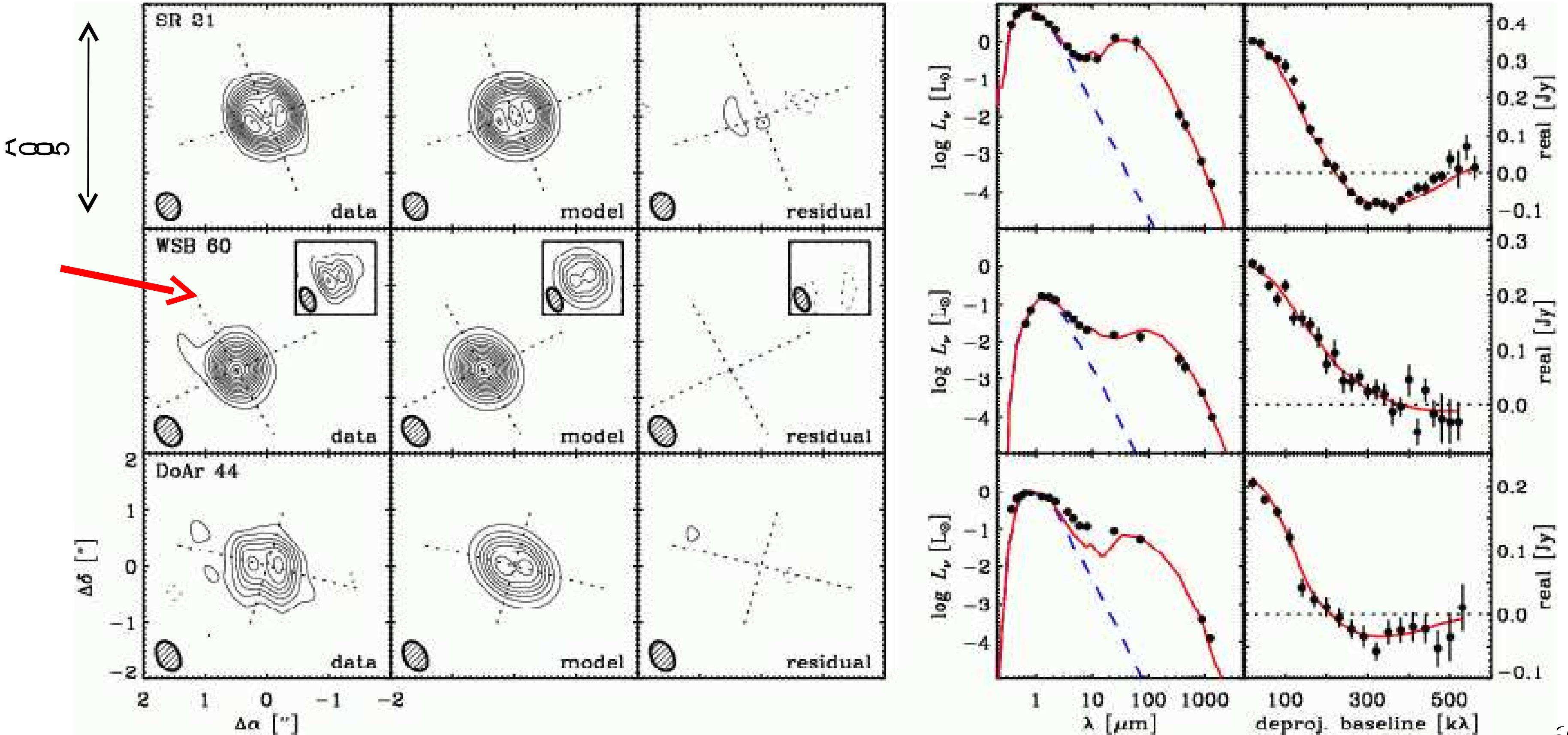

Missing Short Spacings

Do the visibilities in the example discriminate between these models of the sky brightness distribution, T(x,y)?

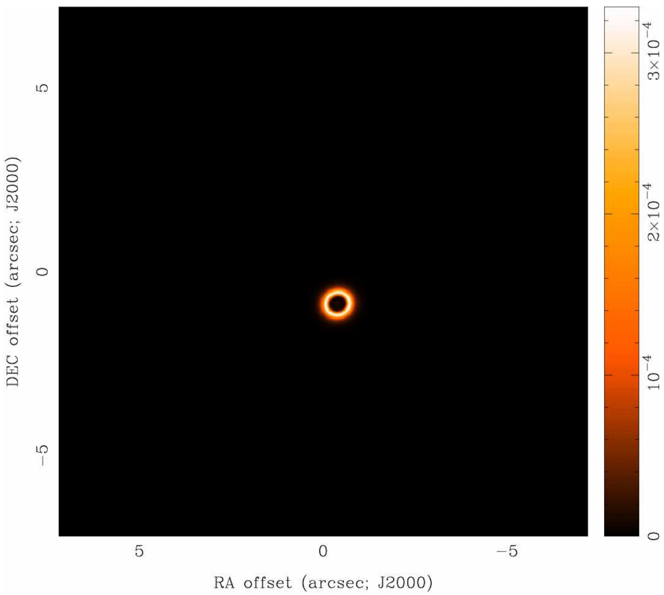

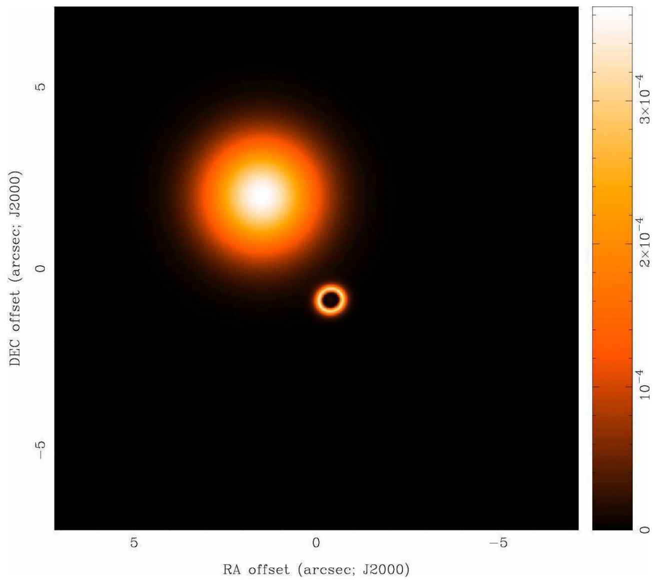

Yes… but only on baselines shorter than ~100 kλ.

Missing Short Spacings: Demonstration

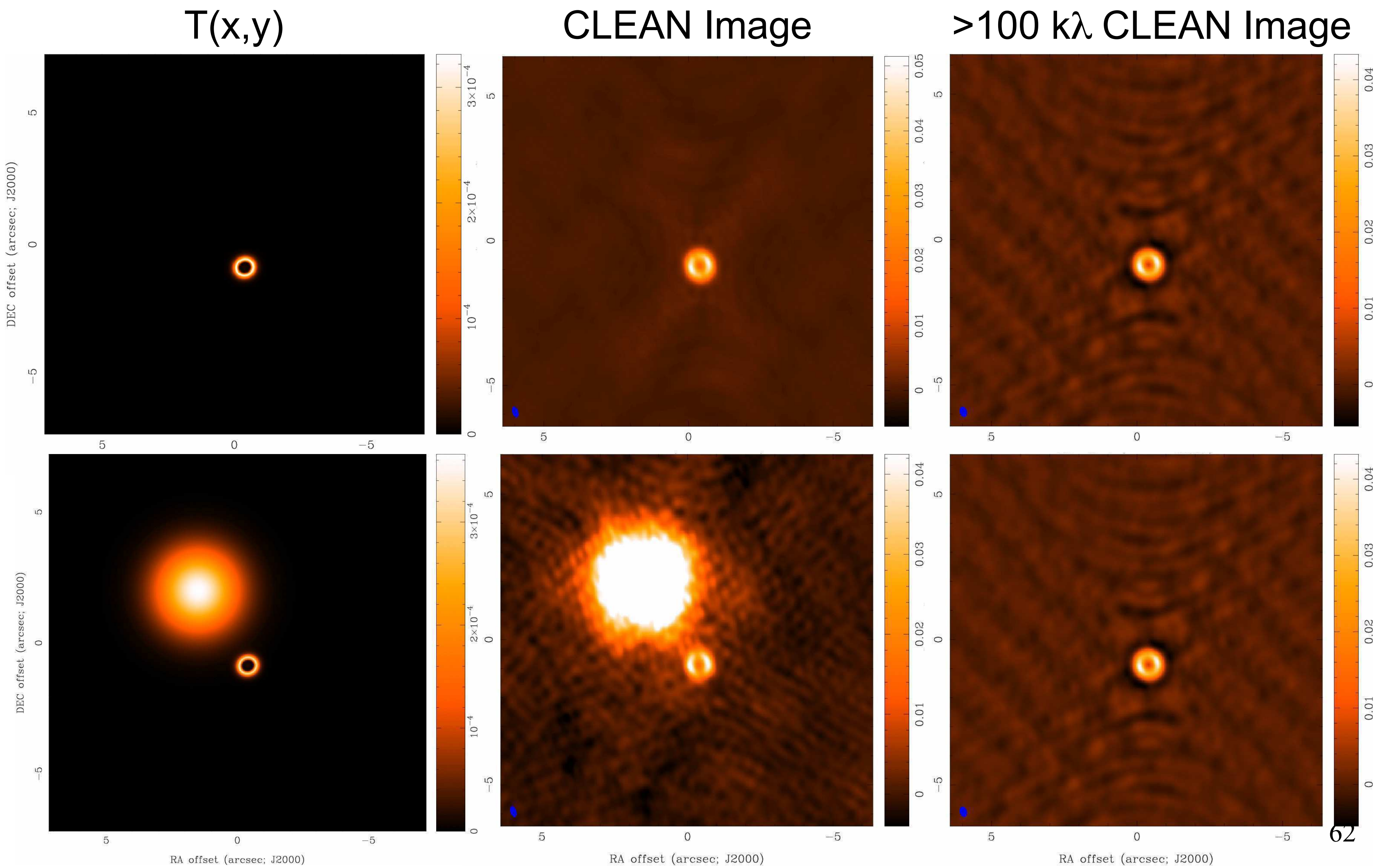

Low Spatial Frequencies (I)

- Large Single Telescope
  - make an image by scanning across the sky
  - all Fourier components from 0 to D sampled, where D is the telescope diameter (weighting depends on illumination)

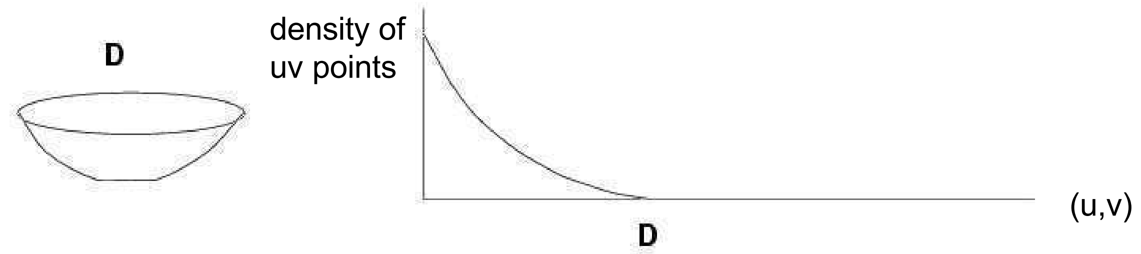

  - Fourier transform single dish map = T(x,y) $\otimes$ A(x,y), then divide by a(x,y) = FT{A(x,y)}, to estimate V(u,v)

$$\hat{V}(u,v) = \frac{[V(u,v)a(u,v)]}{\hat{a}(u,v)}$$

  - choose D large enough to overlap interferometer samples of V(u,v) and avoid using data where a(x,y) becomes small

Low Spatial Frequencies (II)

- separate array of smaller telescopes
  - use smaller telescopes observe short baselines not accessible to larger telescopes
  - shortest baselines from larger telescopes total power maps

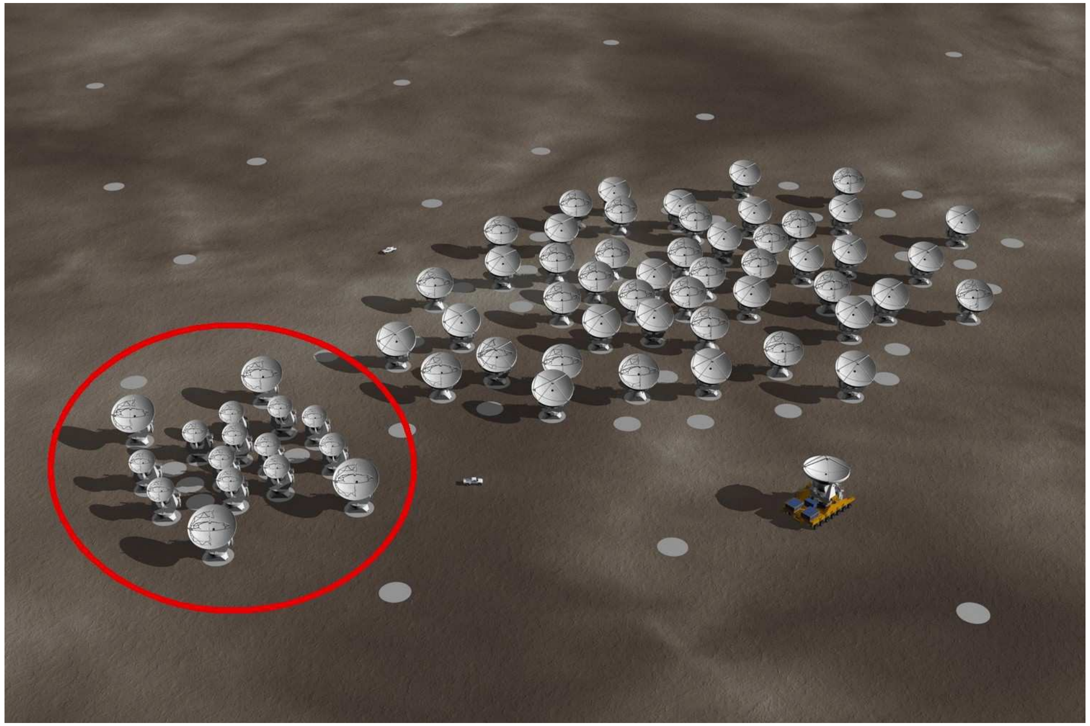

ALMA with ACA

50 x 12 m: 12 m to 14 km

+12 x 7 m: fills 7 to 12 m
+ 4 x 12 m: fills 0 to 7 m

Low Spatial Frequencies (III)

- mosaic with a homogeneous array
  - recover a range of spatial frequencies around the nominal baseline b using knowledge of A(x,y) (Ekers and Rots 1979) (and get shortest baselines from total power maps)

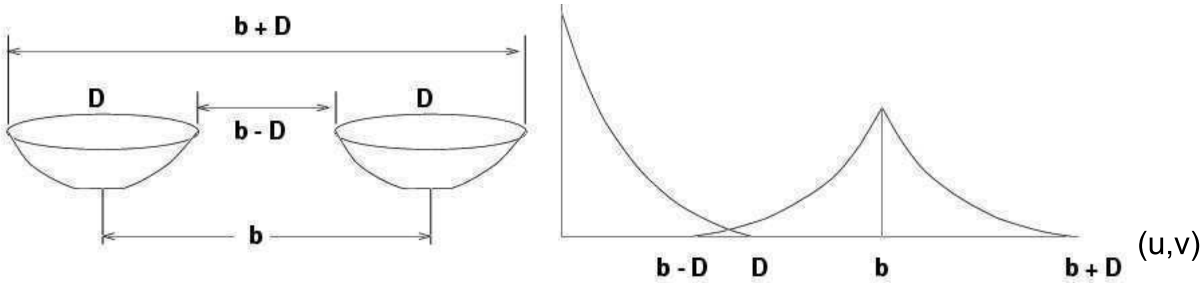

  - V(u,v) is linear combination of baselines from b-D to b+D
  - depends on pointing direction (x_0,y_0) as well as (u,v)

$$V(u,v;x_o,y_o) = \int\int T(x,y)A(x-x_o,y-y_o)e^{2\pi i(ux+vy)}dxdy$$

  - Fourier transform with respect to pointing direction (x_0,y_0)

$$V(u-u_o,v-v_o) = \frac{\int\int V(u,v;x_o,y_o)e^{2\pi i(u_o x_o+v_o y_o)}dx_o dy_o}{a(u_o,v_o)}$$

How does ALMA work?

Radio interferometry / aperture synthesis

ACA = Atacama Compact Array – twelve 7-m antennas

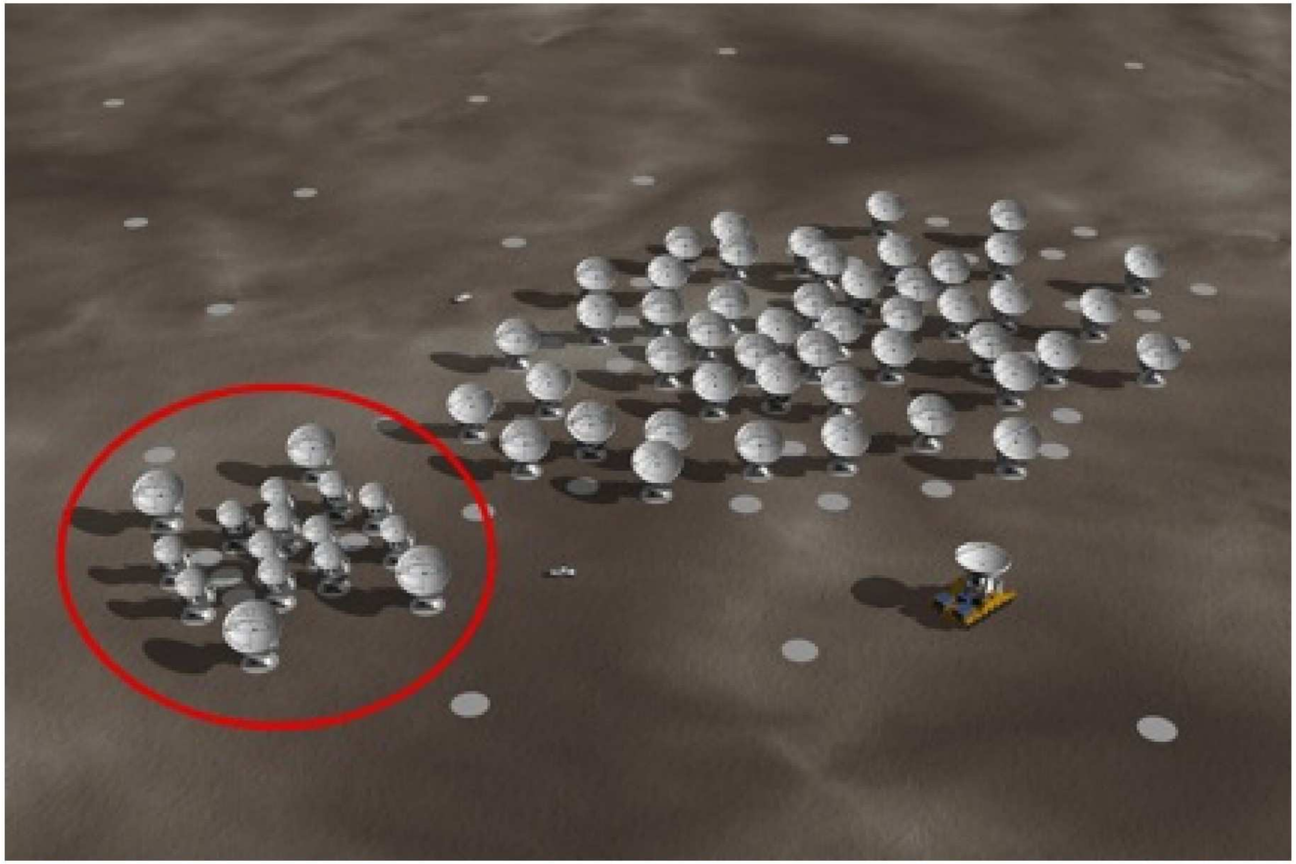

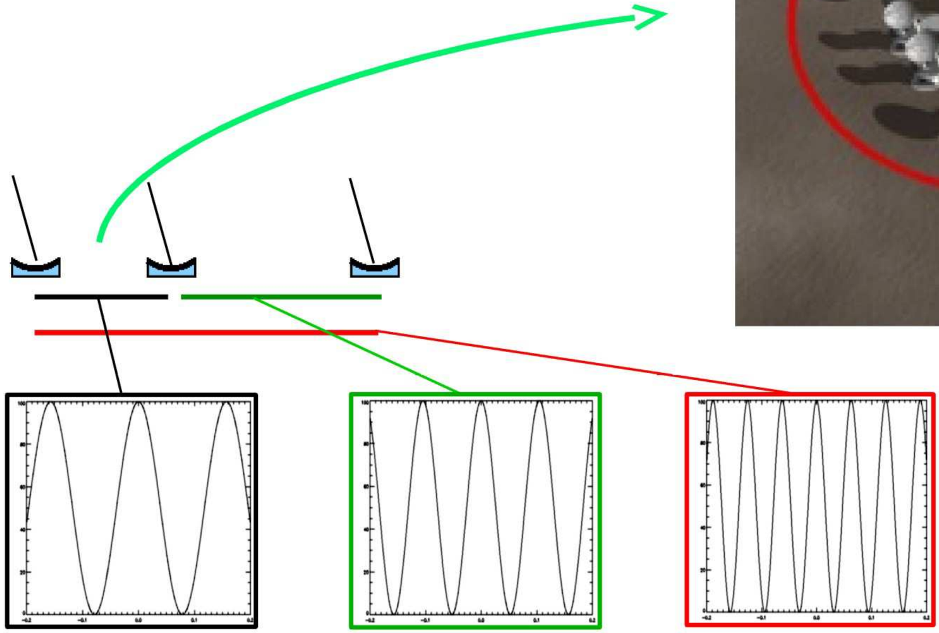

How does ALMA work?

Radio interferometry / aperture synthesis

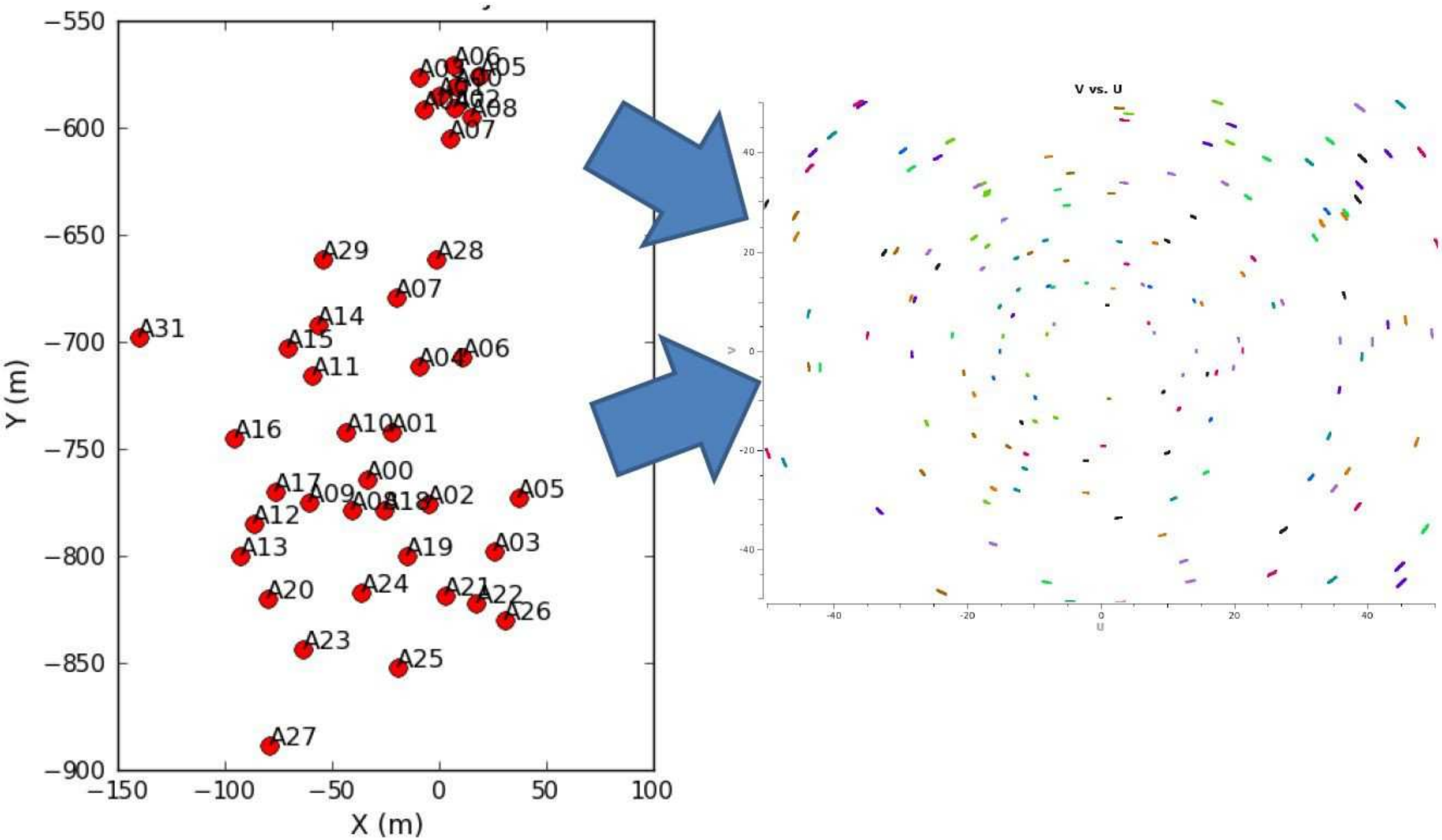

How does ALMA work?

Radio interferometry / aperture synthesis

Extended sources with fine structures: Combined approach

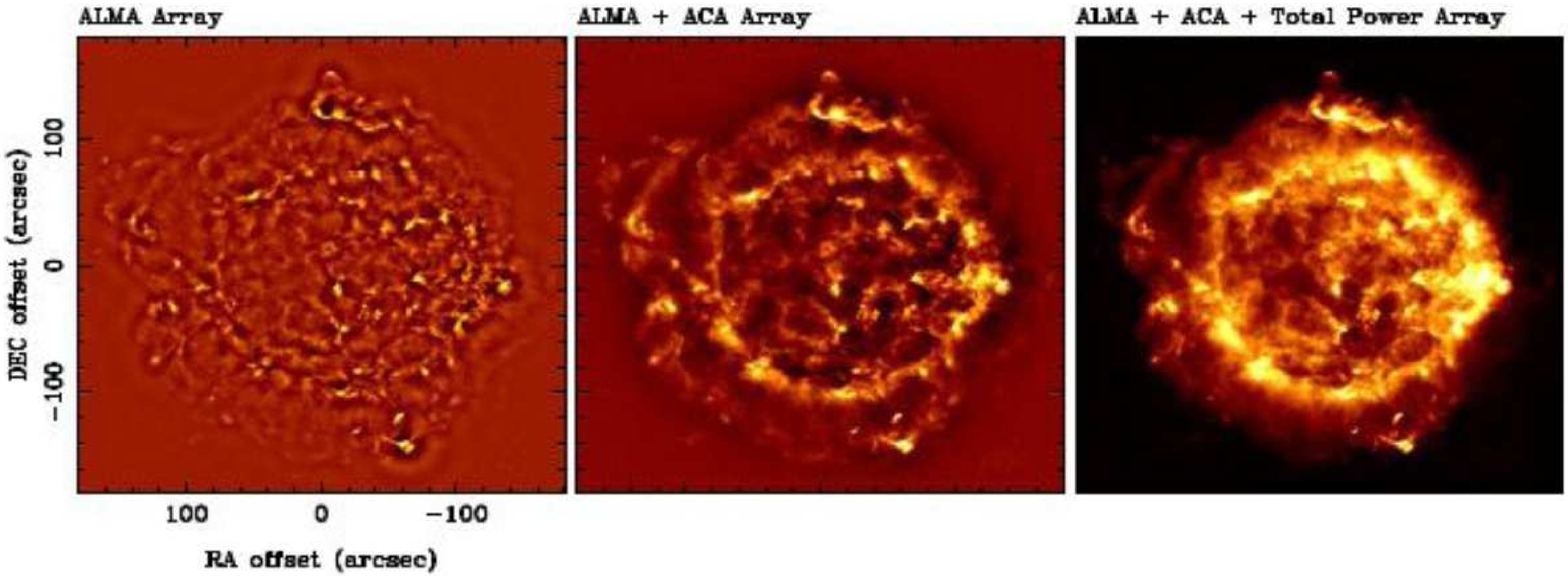

simple simulation of ALMA observation by Y.Kurono

Calibration of interferometric data

$$\langle P_{AB} \rangle = G_A G_B \iint_{-\infty}^{\infty} I(l,m) \cdot \exp(-2\pi i\,(ul + vm)\; dl\; dm + P_{sys}$$

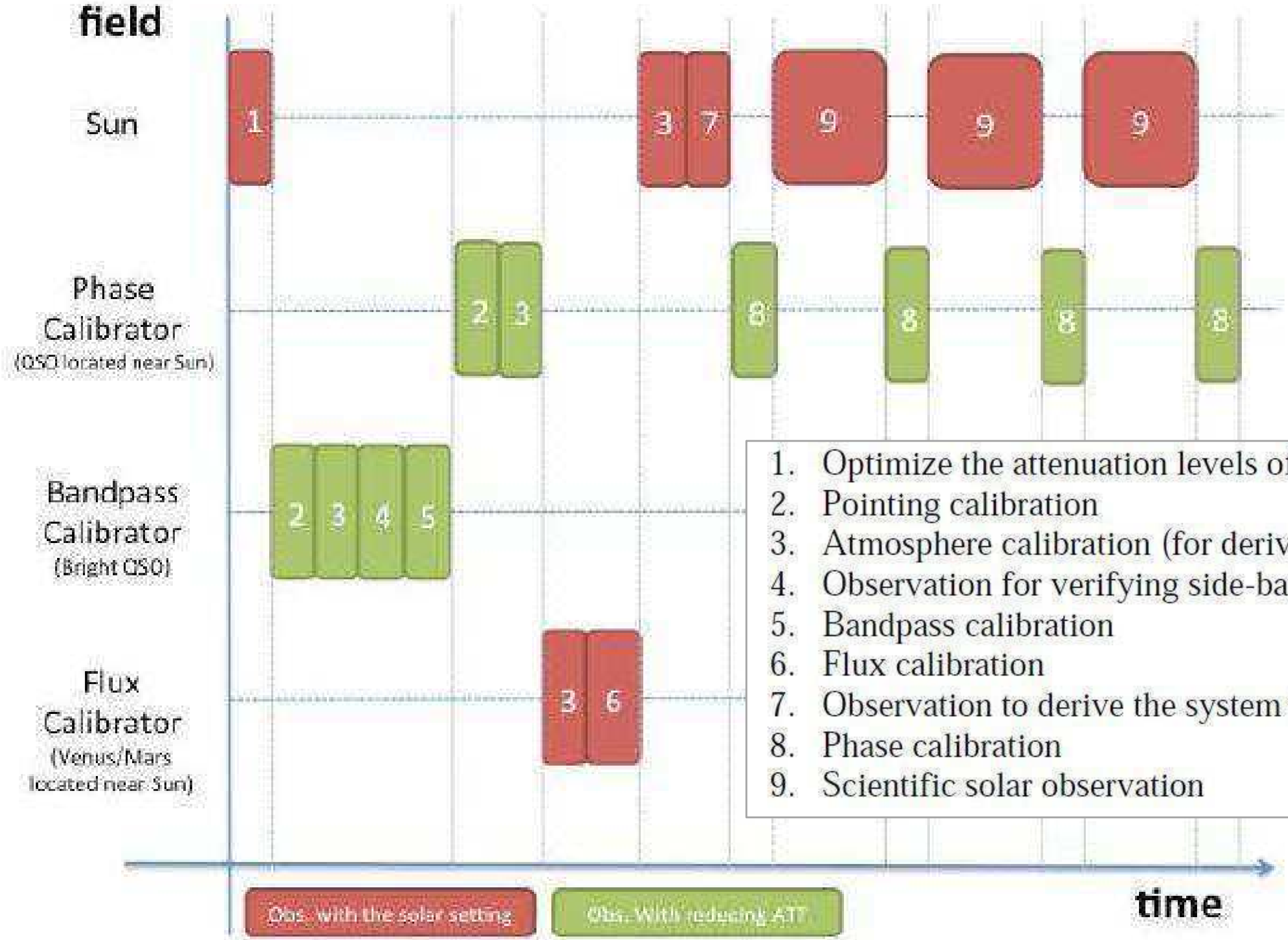

1. Optimize the attenuation levels of the receiver
2. Pointing calibration
3. Atmosphere calibration (for deriving the system temperature on the sky)
4. Observation for verifying side-band separation
5. Bandpass calibration
6. Flux calibration
7. Observation to derive the system temperature on the target region
8. Phase calibration
9. Scientific solar observation

Examples of modern systems AS

Příklady moderních AS systémů

Příklady moderních AS systémů

SSRT

MUSER

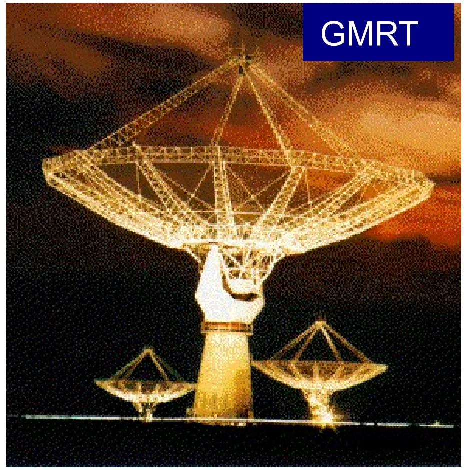

LOFAR

ALMA

SKA

Moderní AS systémy – některé dedikované pro sluneční výzkum

- SSRT Badary [RU]
- MUSER [CN]
- **E-OVSA [US]**

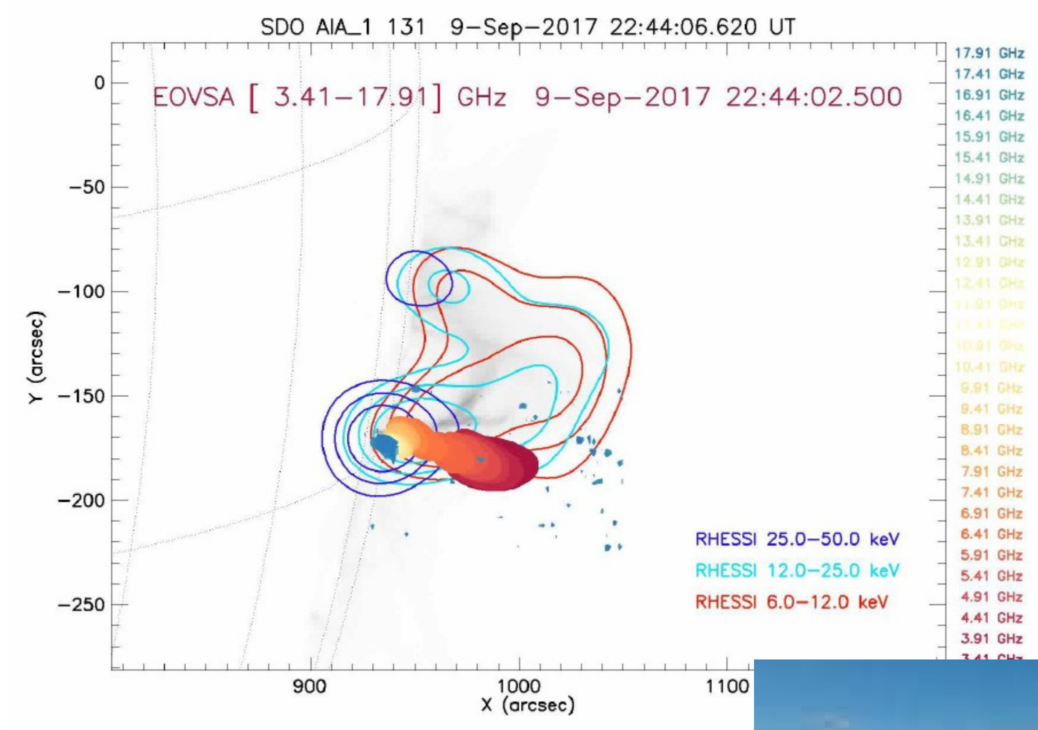

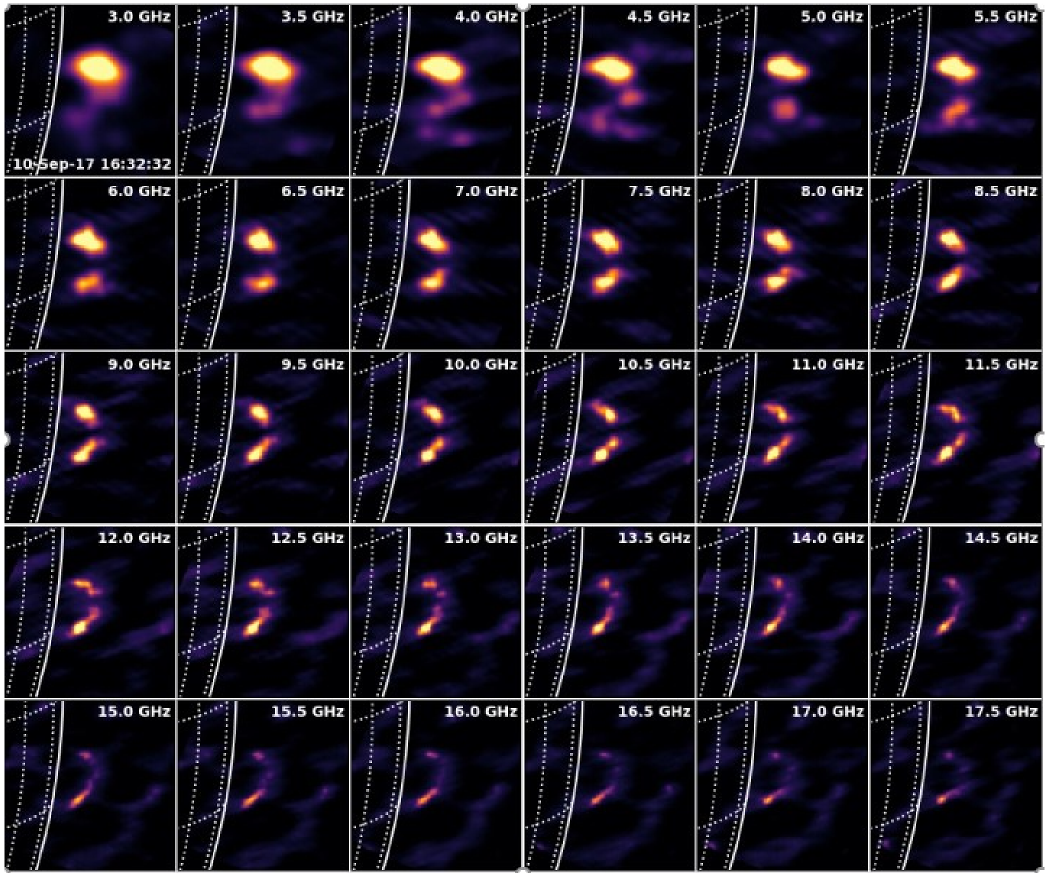

D. Garry, G. Nitta: E-OVSA
CESRA 2019 presentations

Observatory ALMA

ALMA: učebnicový příklad moderního systému AS

- ALMA = **A**tacama **L**arge **M**illimeter/submillimeter **A**rray. Největší projekt současné pozemní pozorovací astronomie vybudovaný v chilské poušti Atacama, ~5100 m n.m.
- Postavený a provozovaný v partnerství **ESO**, NRAO and NAOJ
- Systém padesáti 12m precizních antén + dvanáct 7m (ACA) sfázovaných do interferometru,+ čtyři 12m single-dish (TP)

Co je ALMA?


to Central America/ Caribbean
Venezuela
Guyana
Suriname
French Guiana
Colombia
Ecuador
Peru
Brazil
Bolivia
Paraguay
Argentina
Chile
Uruguay
Falkland Is.
South Georgia & S Sandwich Is.
©1996 Brandon Plewe


South latitude
Ollague
Bolivia
22°
Pacific Ocean
Calama Airport
Pampa la Bola
Chajnantor region
(5000m)
23°
San Pedro de Atacama
(2450m)
Chile
Port
Antofagasta Airport
24°
Paranal (2400 m)
Argentina
25°
100km
Taltal
West longitude
70°
69°
68°
67°

Co je ALMA?

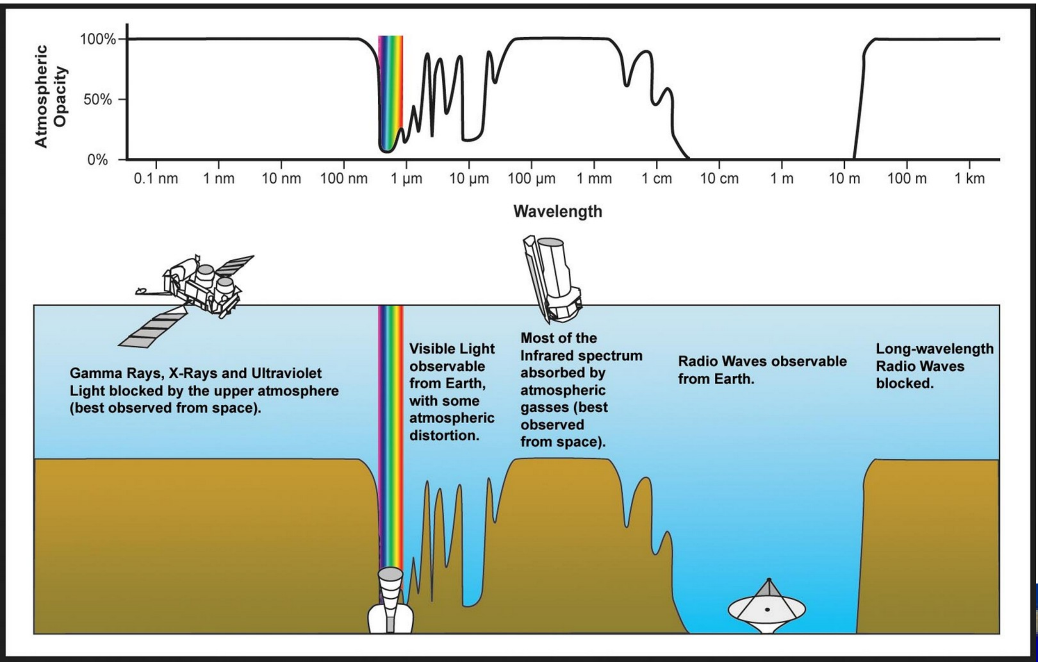
Atmospheric Opacity
100%
50%
0%
0.1 nm
1 nm
10 nm
100 nm
1 μm
10 μm
100 μm
1 mm
1 cm
10 cm
1 m
10 m
100 m
1 km
Wavelength
Gamma Rays, X-Rays and Ultraviolet Light blocked by the upper atmosphere (best observed from space).
Visible Light observable from Earth, with some atmospheric distortion.
Most of the Infrared spectrum absorbed by atmospheric gasses (best observed from space).
Radio Waves observable from Earth.
Long-wavelength Radio Waves blocked.


CALAMA
LAGUNA VERDE
SAN PEDRO DE ATACAMA
CHAJNANTOR ALMA
SALAR DE ATACAMA
ANTOFAGASTA
ACIFIC OCEAN
LOS ANDES


15 km
28 km
ALMA Operations Site
AOS
Operations Support Facilities
OSF
Toconao

How does ALMA work?

Variable array configurations
– baselines up to 16km

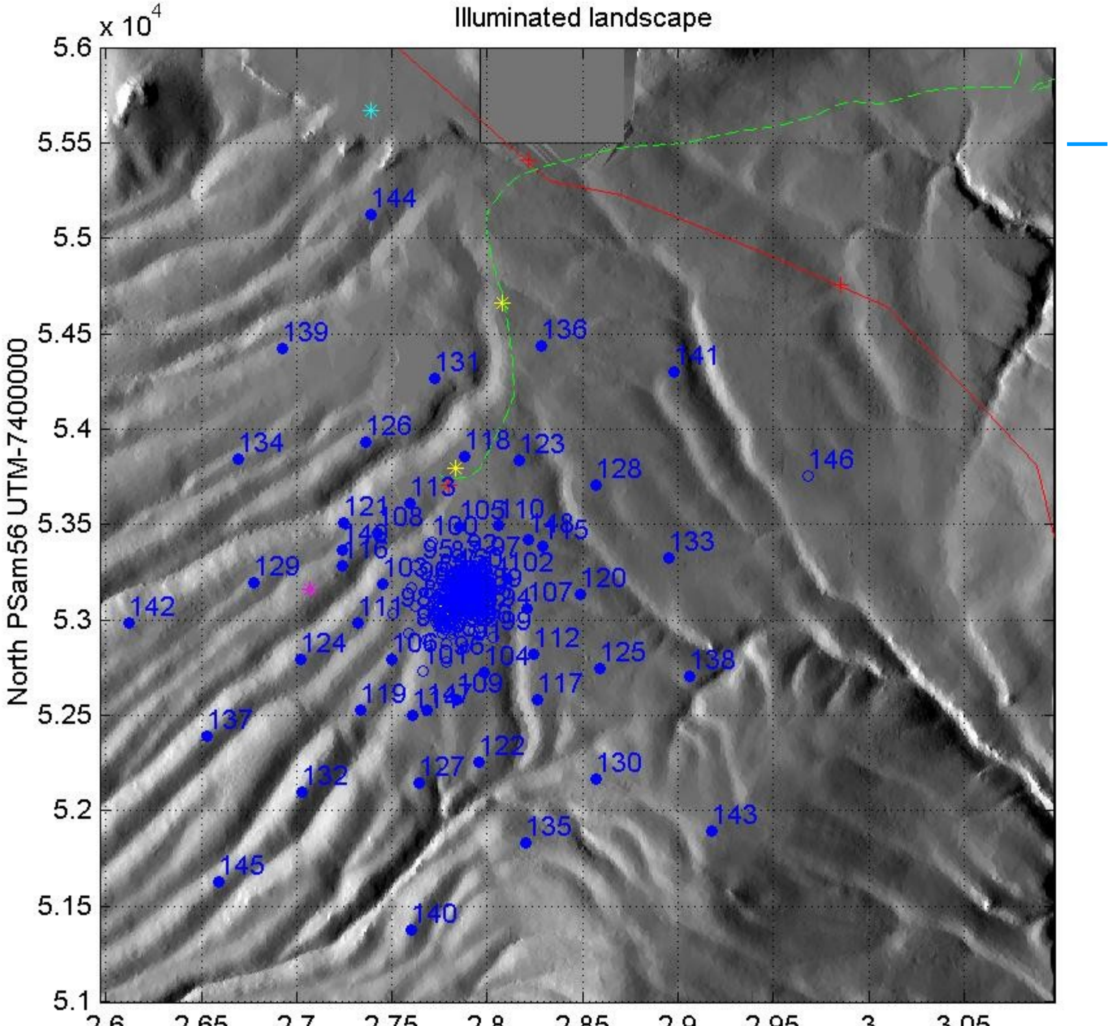

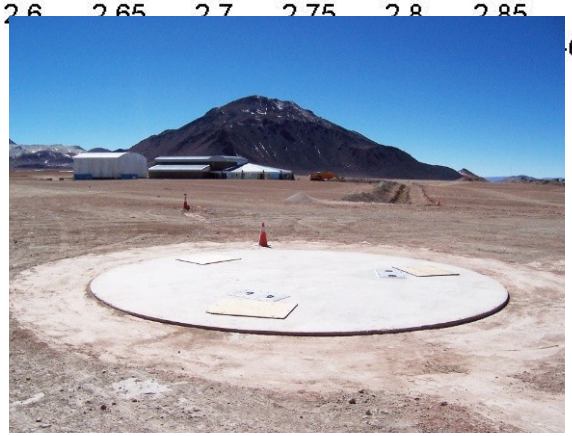

How does ALMA work?

ACA = Atacama Compact Array – twelve 7-m antennas

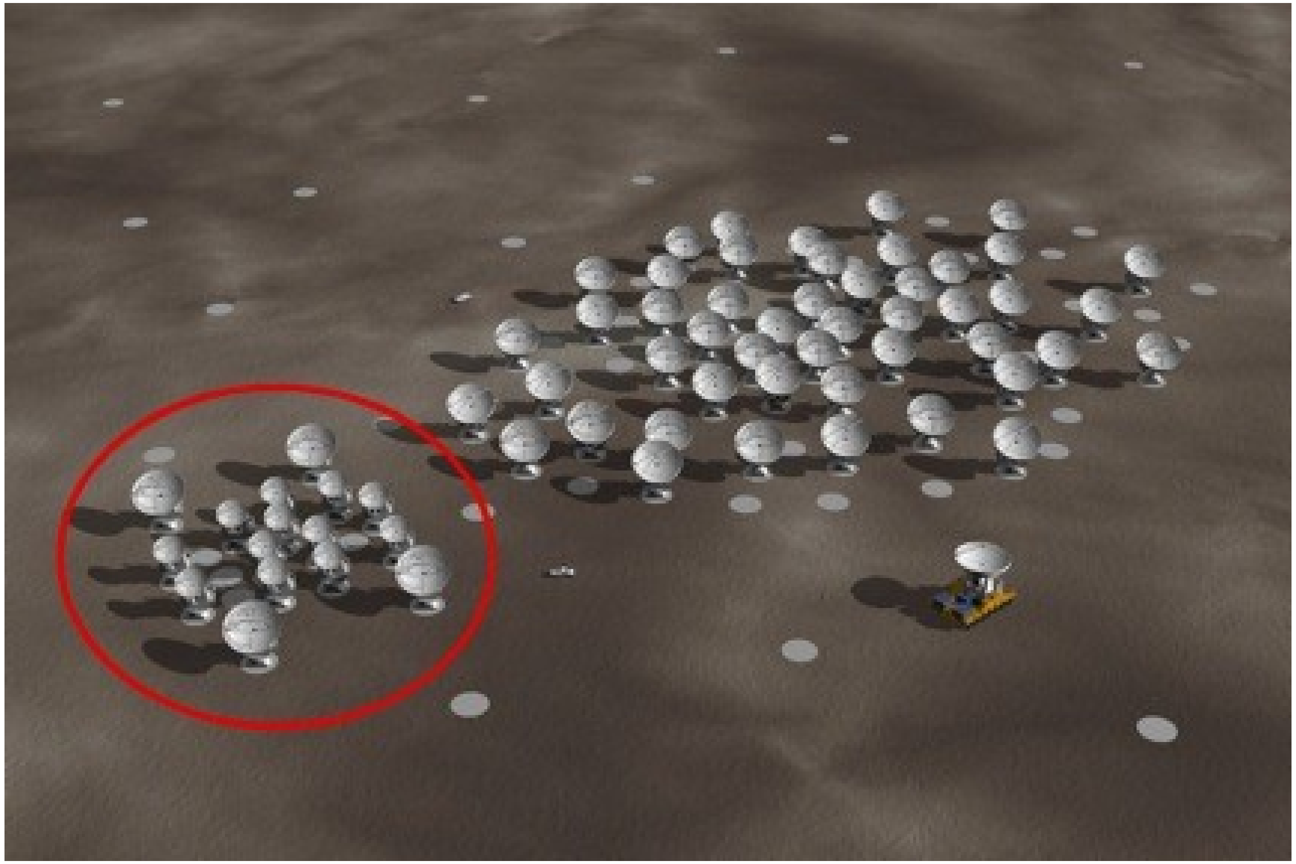

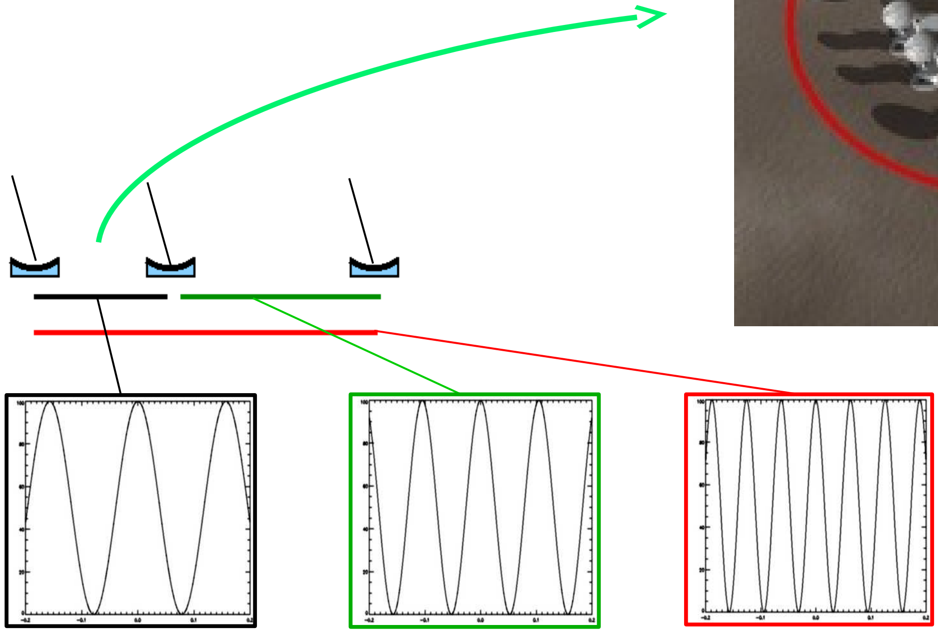

How does ALMA work?

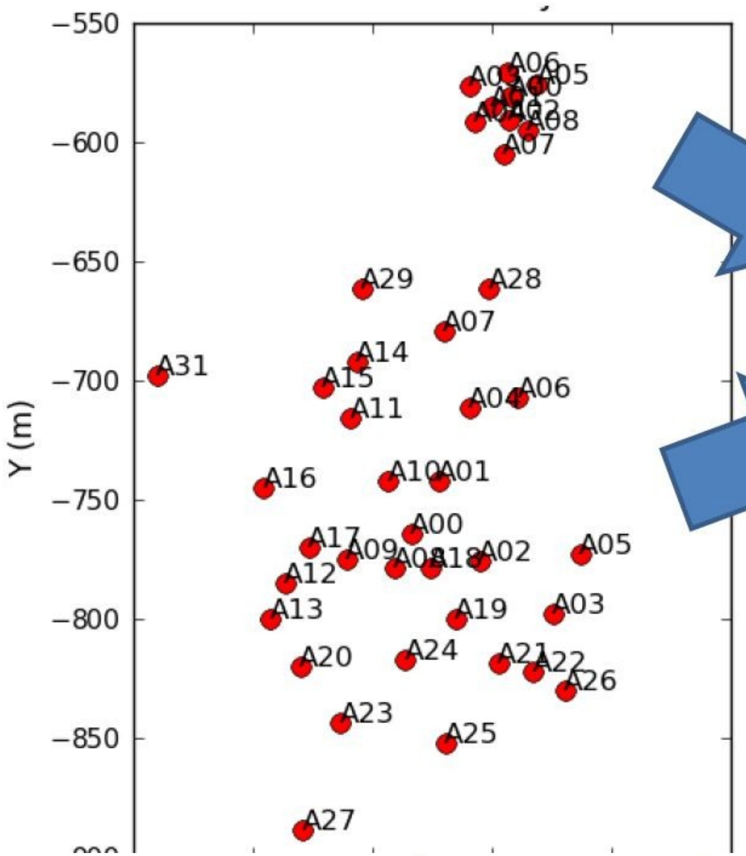

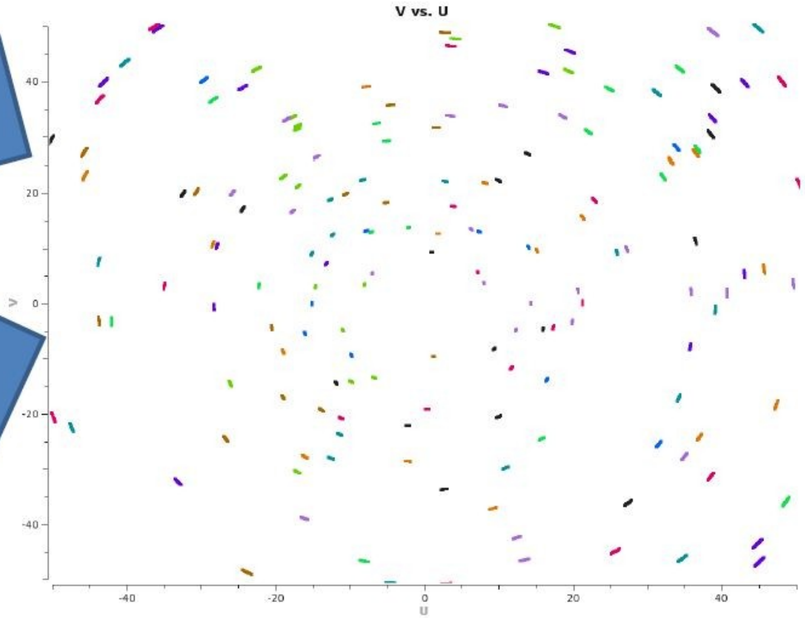

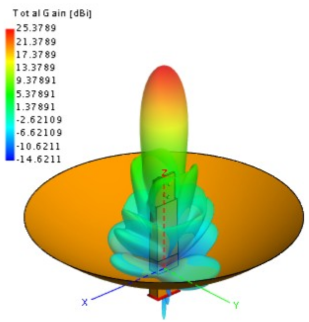

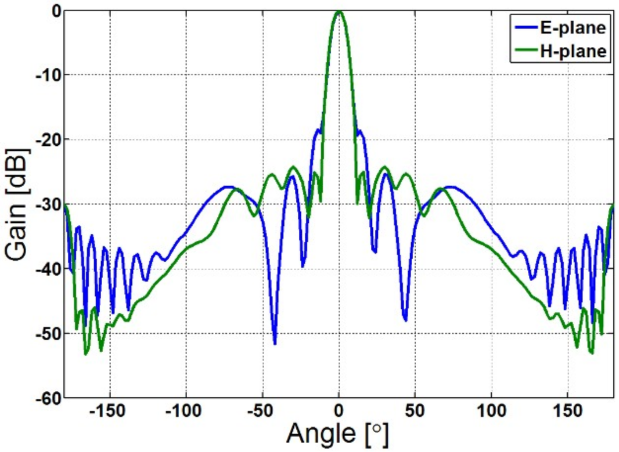

Single-dish (TP) scans to cover long scales

How does ALMA work?

Extended sources with fine structures: Combined approach

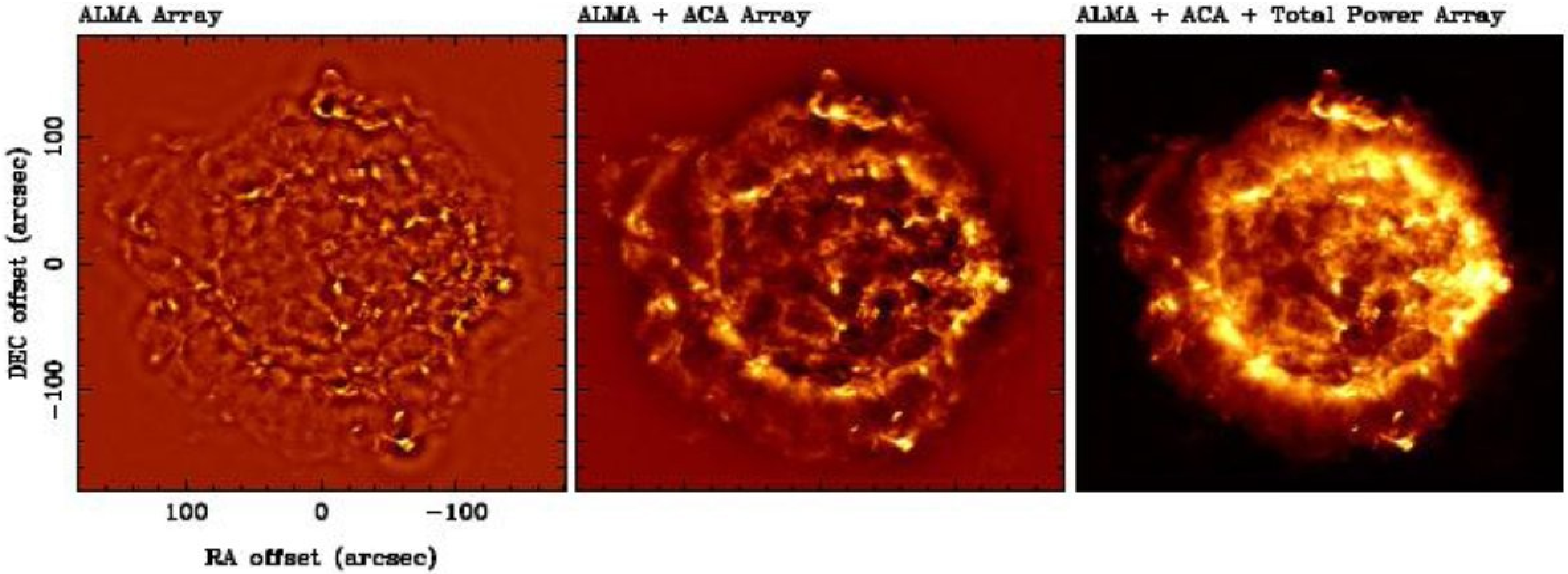

simple simulation of ALMA observation by Y.Kurono

Science with ALMA

1. Cosmology and the high redshift universe
2. Galaxies and galactic nuclei
3. ISM, star formation and astrochemistry
4. Circumstellar disks, exoplanets and the solar system
5. Stellar evolution and the Sun

http://almascience.eso.org
http://www.almaobservatory.org

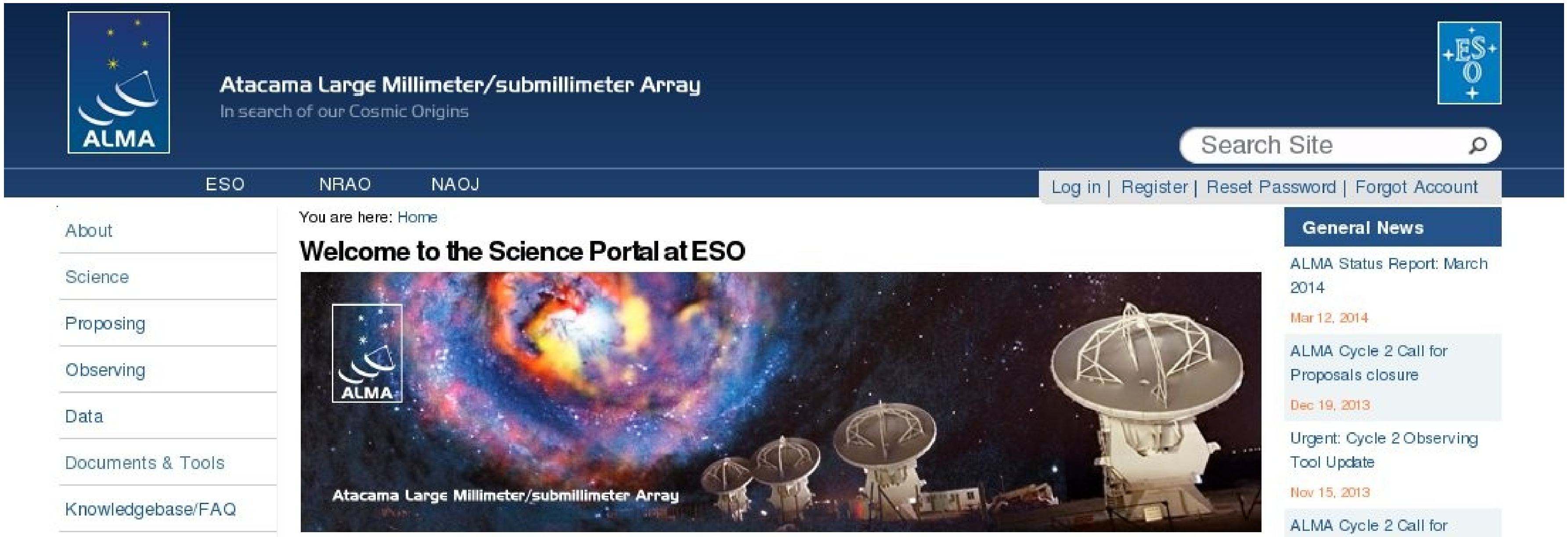

First successes

- Early science since 2012 (observing Cycles 0,1, and 2)
- Consecutively increasing capabilities (N ants, baselines, bands,…)
- Significant discoveries: 10% of ALMA papers are in Nature or Science

ALMA – Early Science

HL Tau

- Formation of a new planetary system
- 450 ly away from Earth
- Resolution better than 5 AU !
- **Many other PP discs** resolved since then.

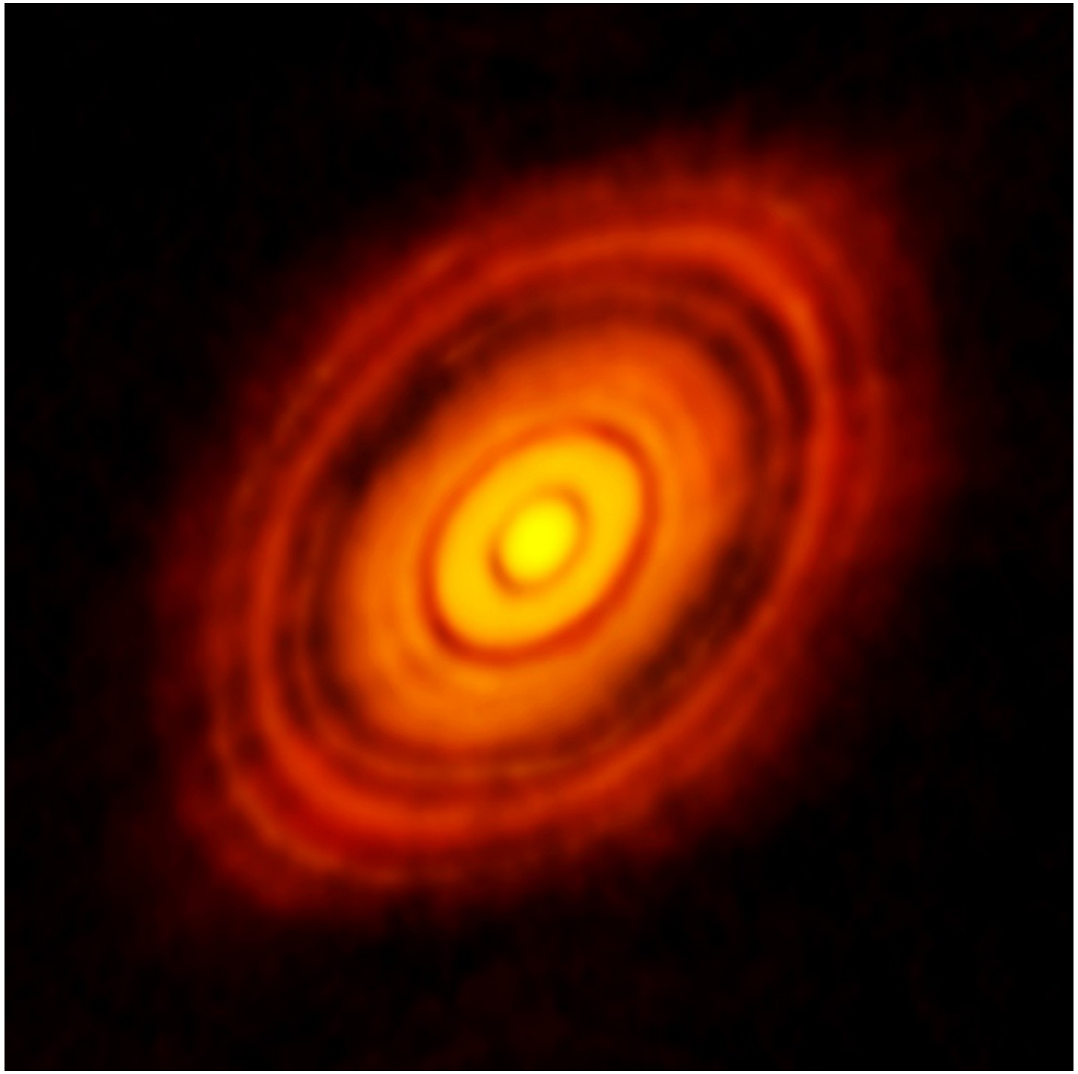

First successes

- Early science since 2012 (observing Cycles 0,1, and 2)
- Consecutively increasing capabilities (N ants, baselines, bands,…)
- **Significant discoveries: 10% of ALMA papers are in Nature or Science**

http://www.almaobservatory.org

Section ‘Multimedia → videos’

First sucesses

ESO/ALMA press-releases related to EU ARC.CZ

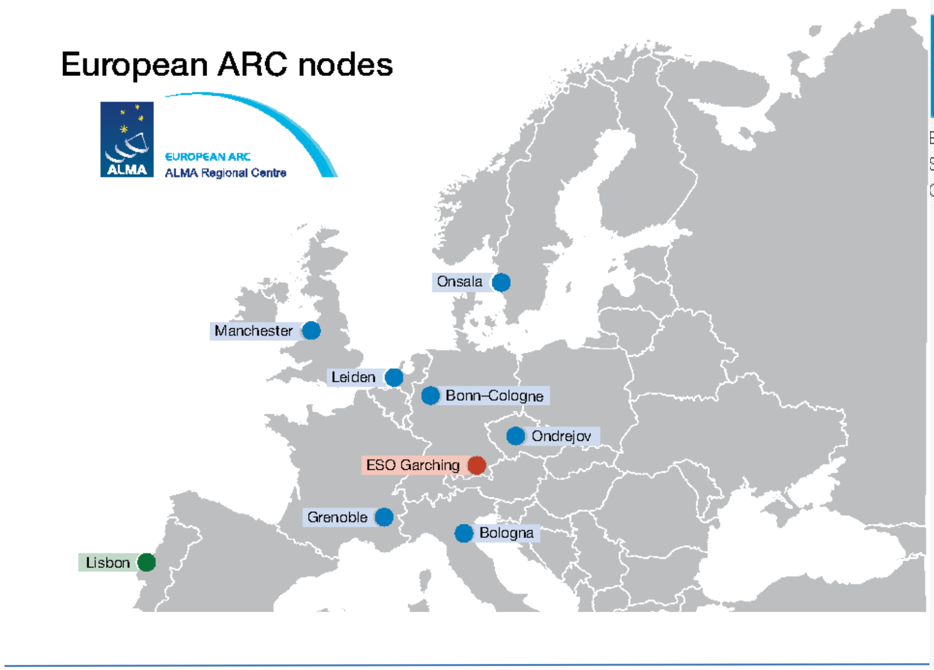

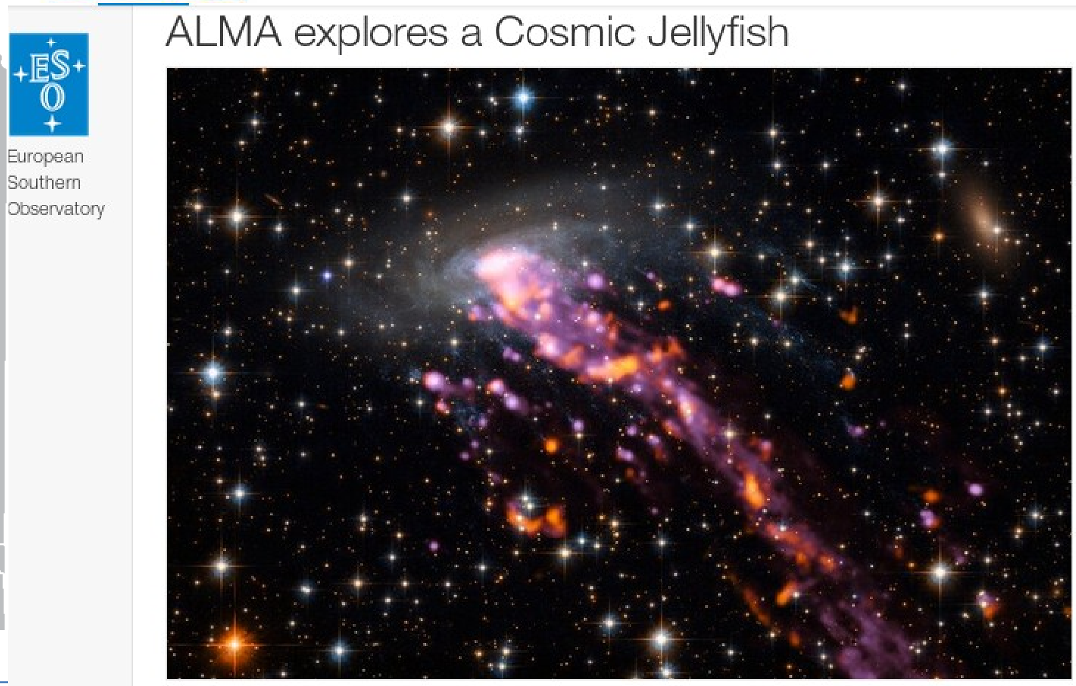

Perspectives

- Long baselines (up to 15km) in Bands 9 and 10 (11), extending the array
- Wider sidebands / spectral windows (2x 8GHz)
- Full polarisation
- VLBI
  - Black Hole Cam
  - Event Horizon Telescope – **expected already in 2018!**

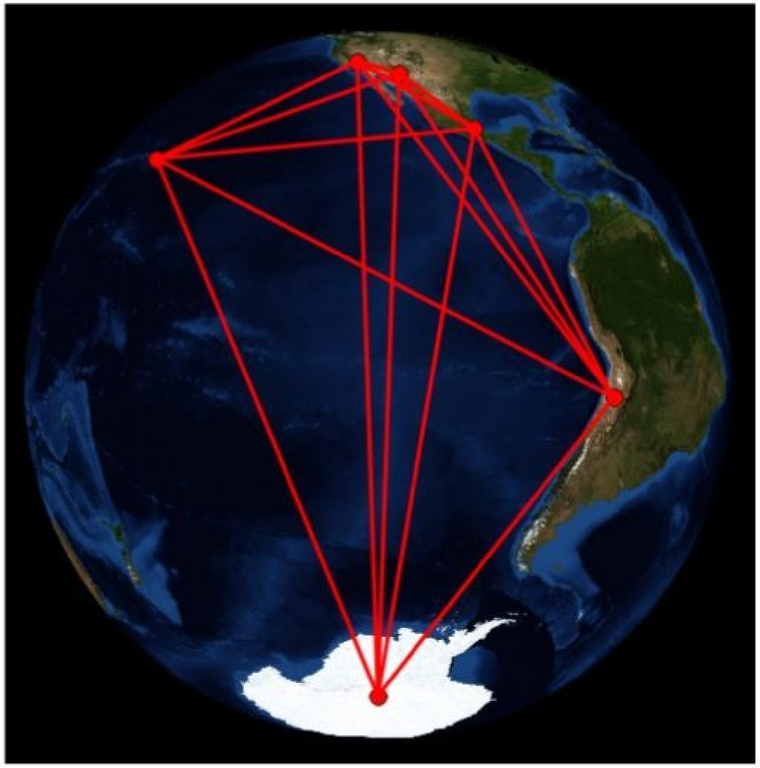

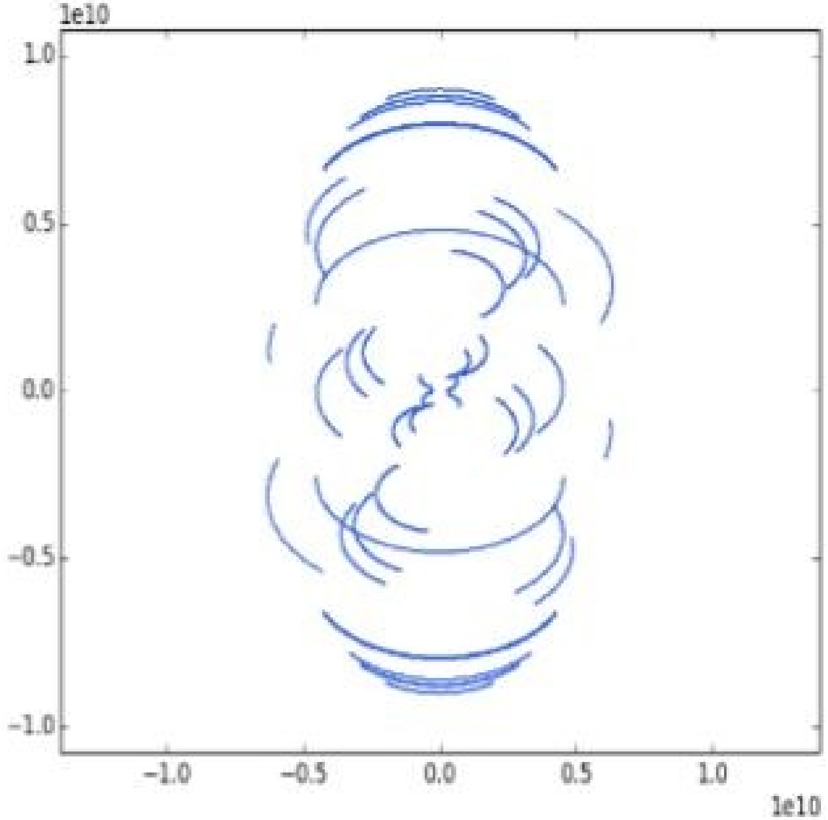

Perspectives

- Long baselines (up to 15km) in Bands 9 and 10 (11), extending the array
- Wider sidebands / spectral windows (2x 8GHz)
- Full polarisation
- VLBI
  - Black Hole Cam
  - Event Horizon Telescope – **expected already in 2018!**

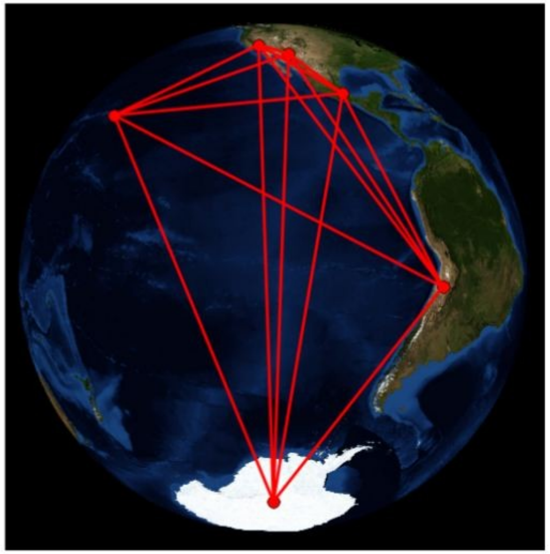

2018 (expected):

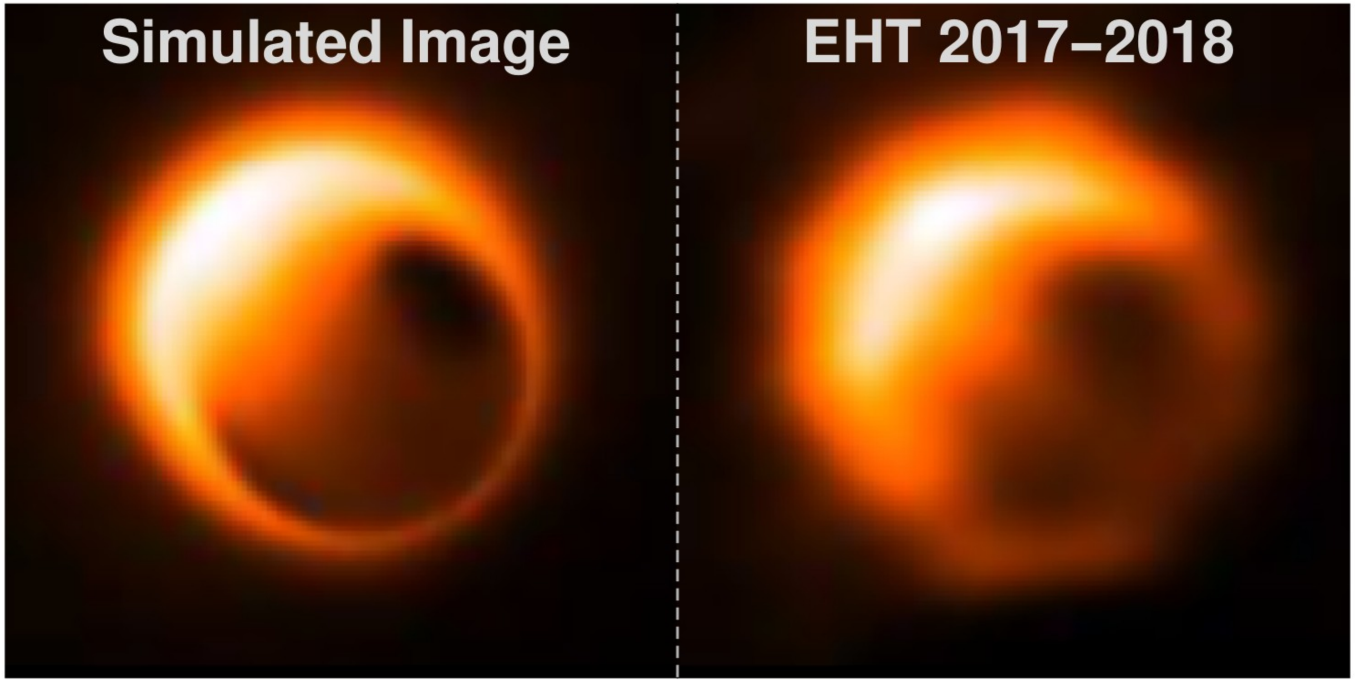

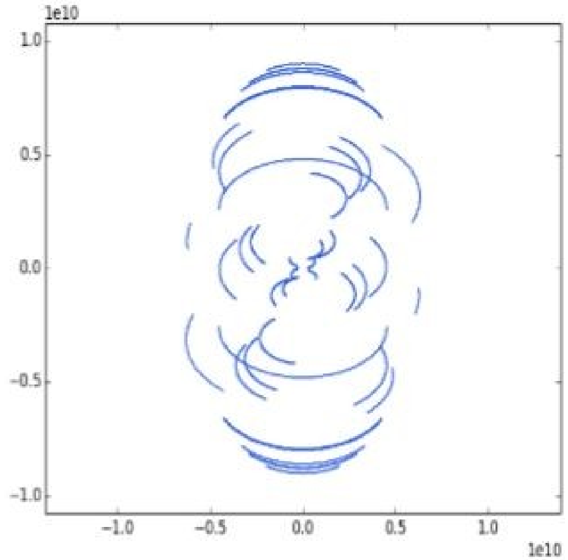

This is the first photo of a black hole

By Ashley Strickland, CNN

Updated 1640 GMT (0040 HKT) April 10, 2019

BH in M87: ALMA contribution to the success

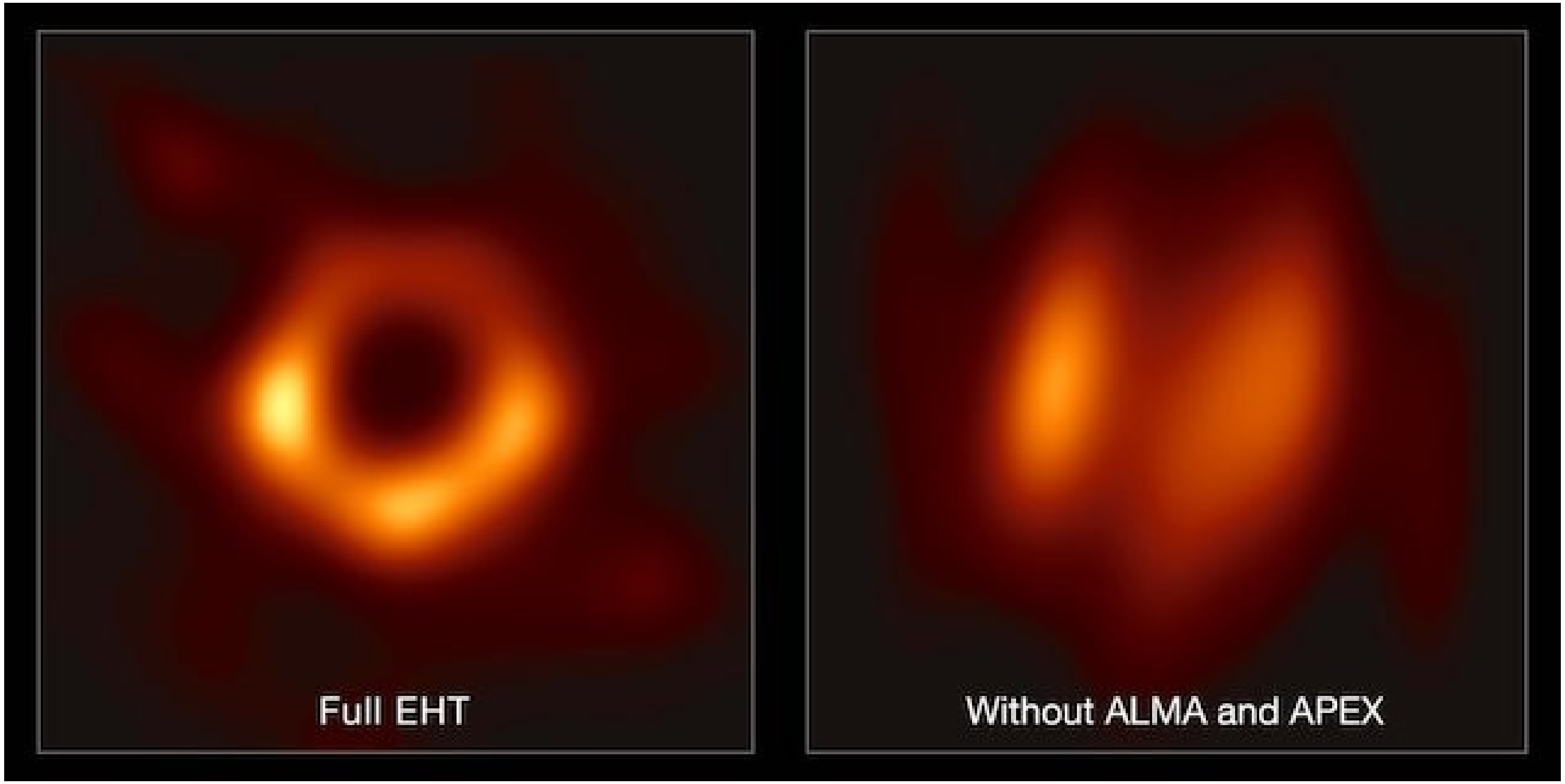

Lifetime of your ALMA observation project: Subsystems, data flow and SW

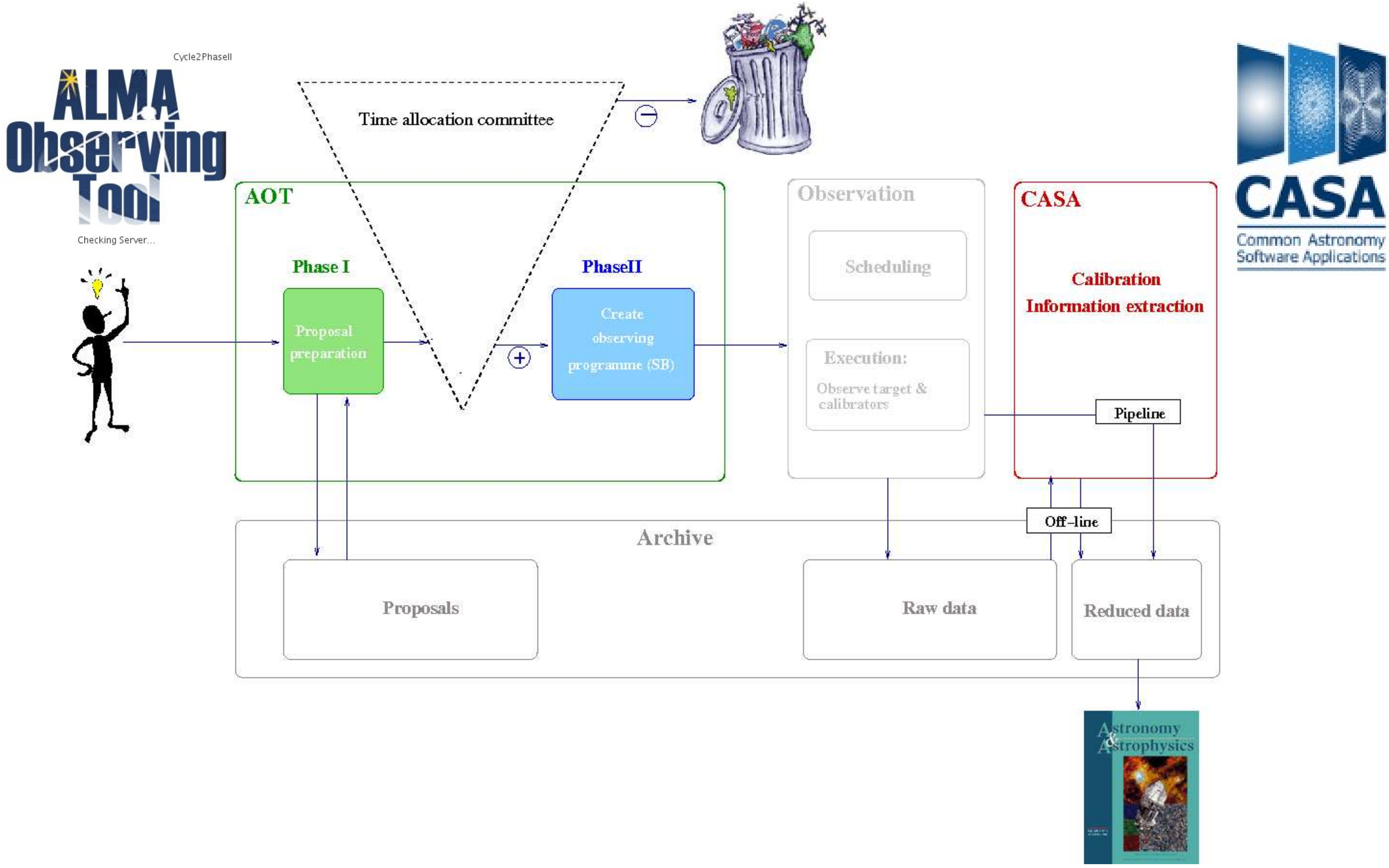

Preparing your project – ALMA OT (Phase I)

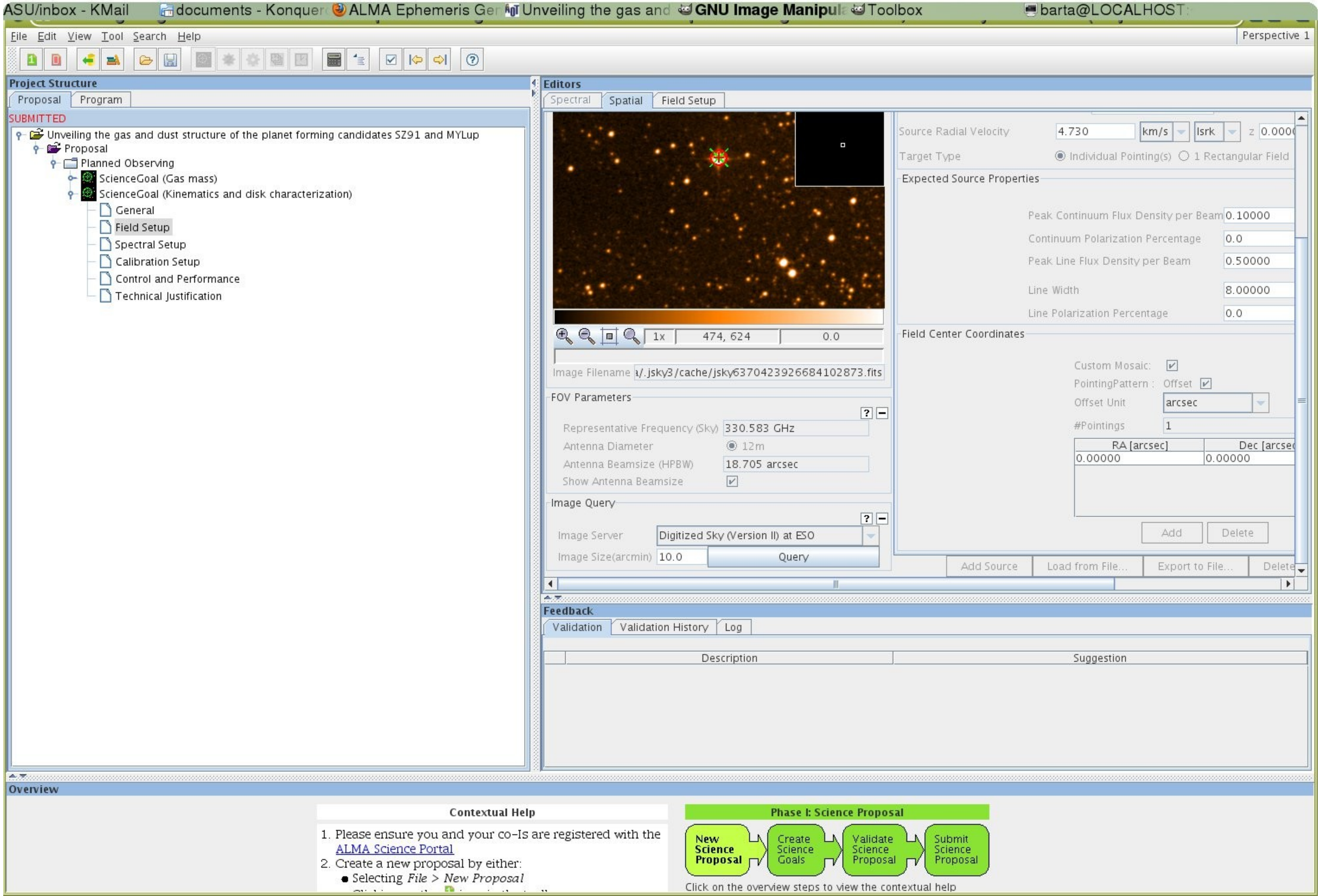

Project execution – typical *Scheduling Block* (OT Phase II)

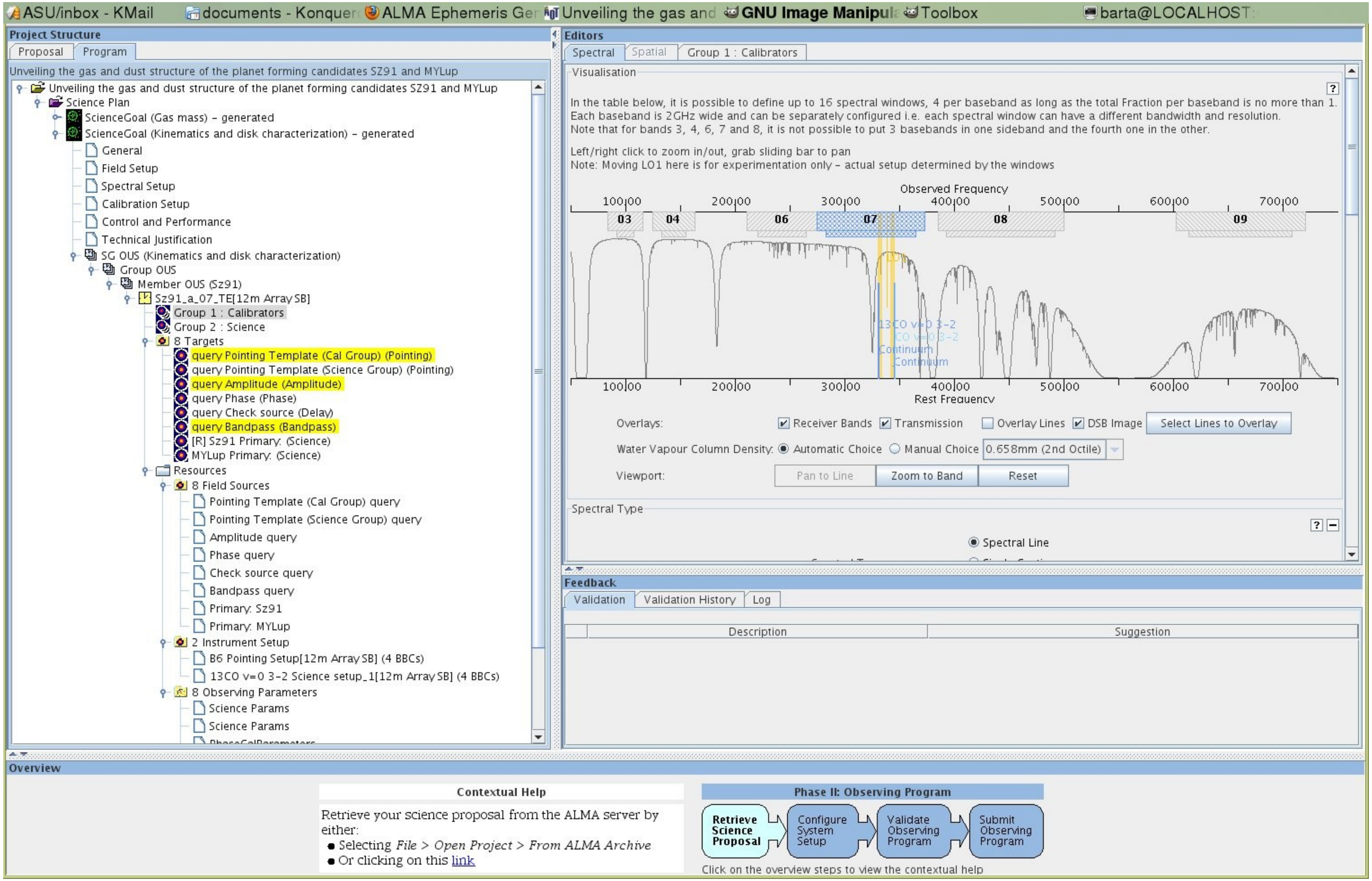

Postprocessing – calibration and imaging in CASA

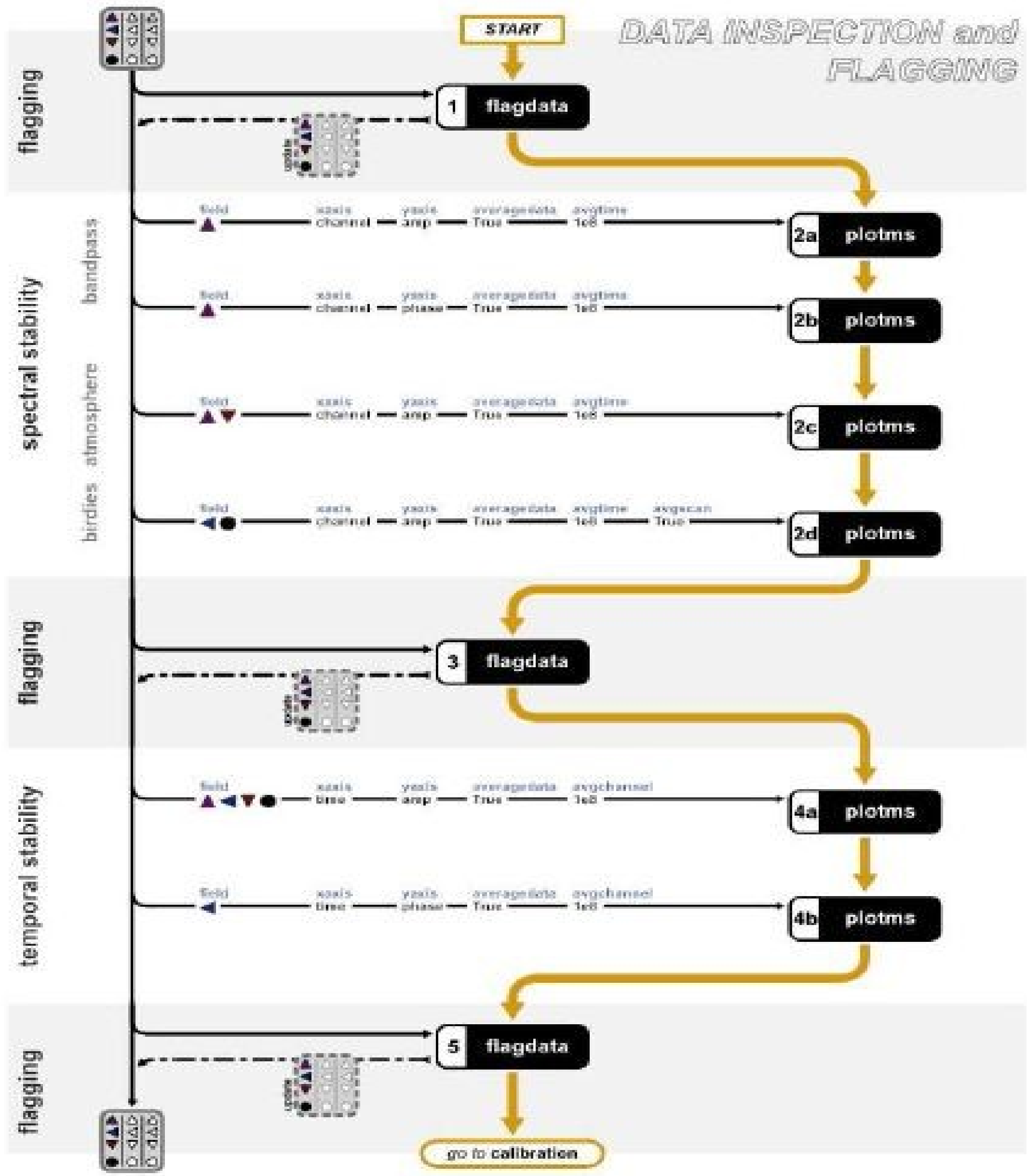

Project execution – typical *Scheduling Block* (ObsSim)

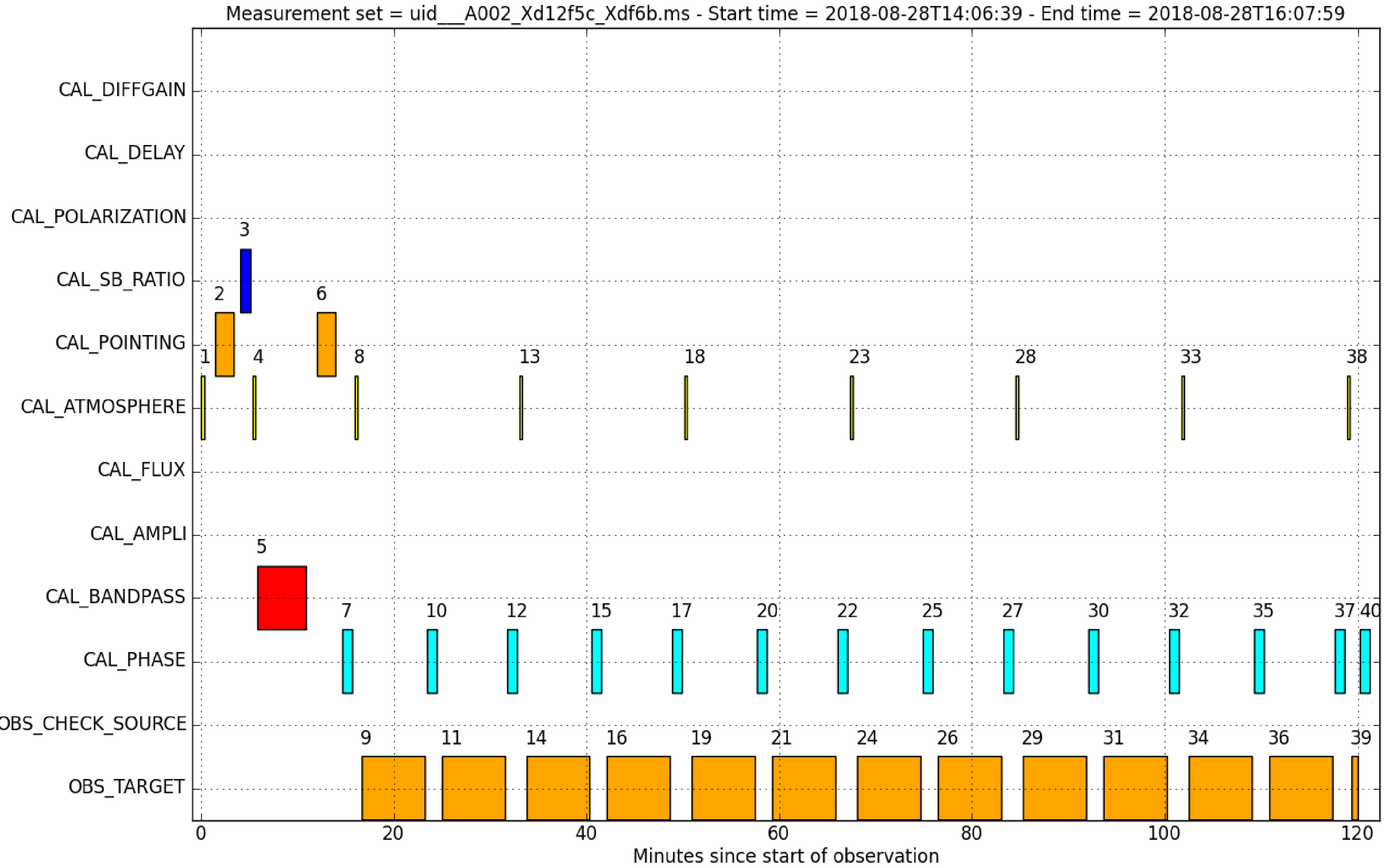

Postprocessing – calibration and imaging in CASA

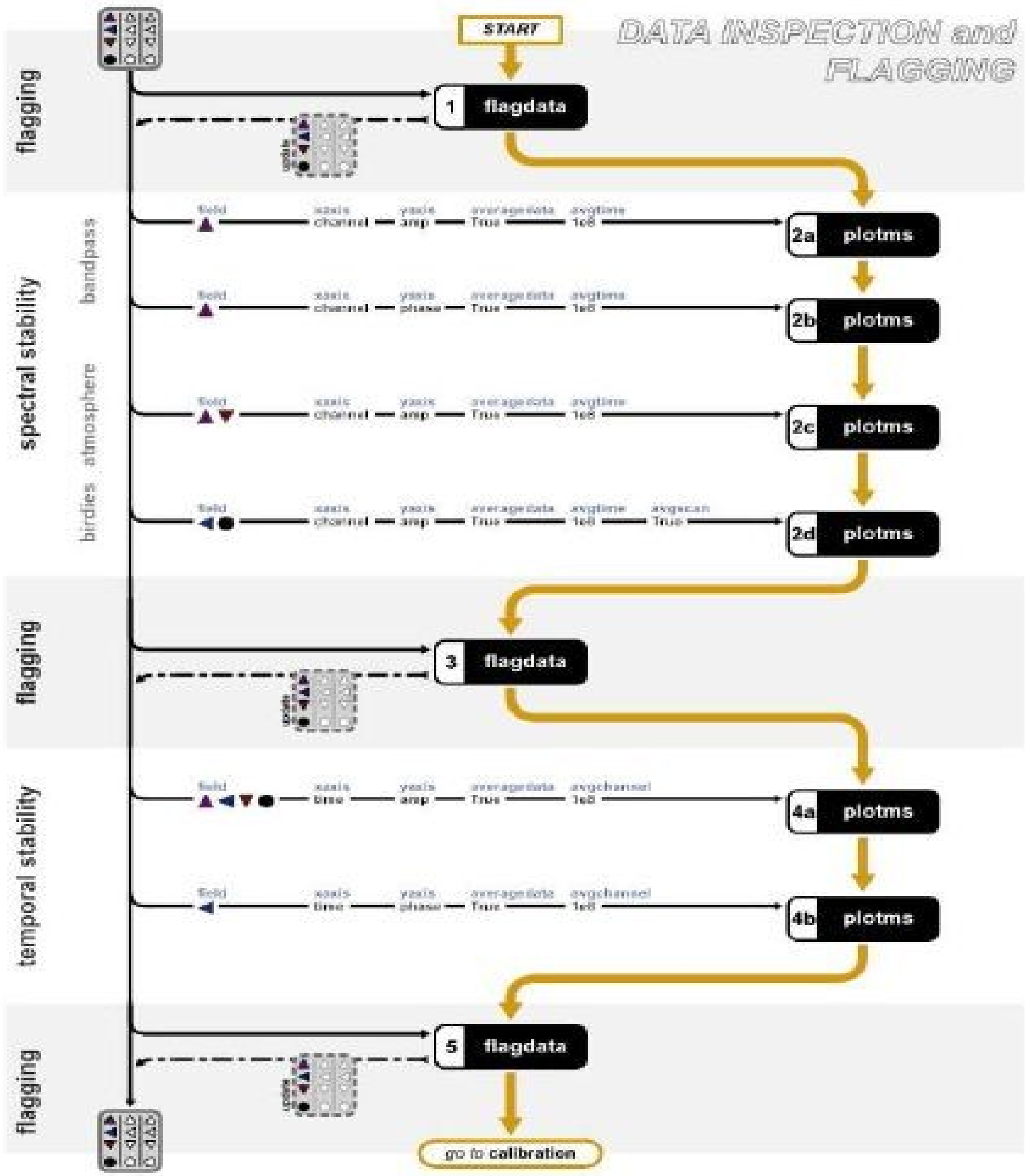

Postprocessing – calibration and imaging in CASA

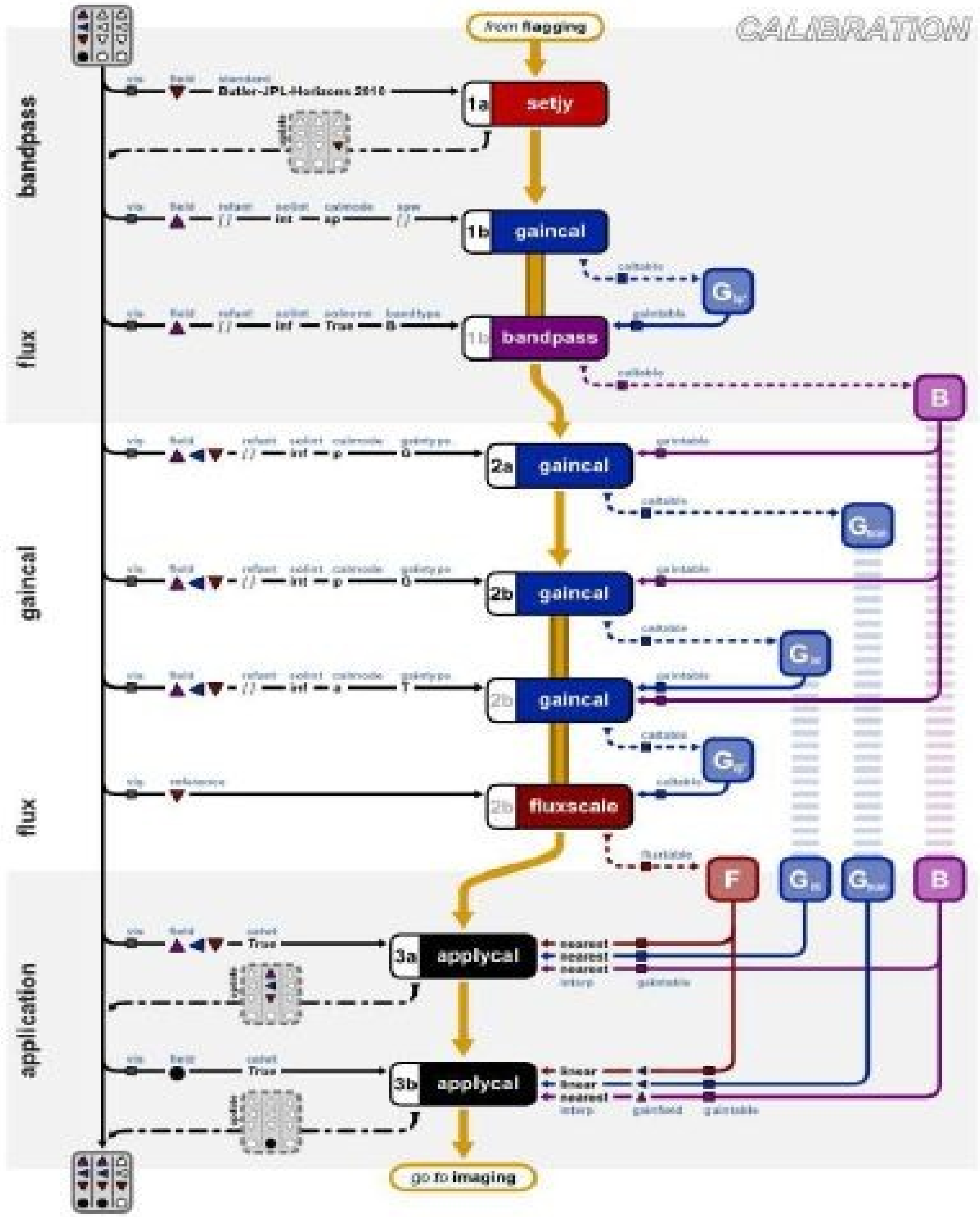

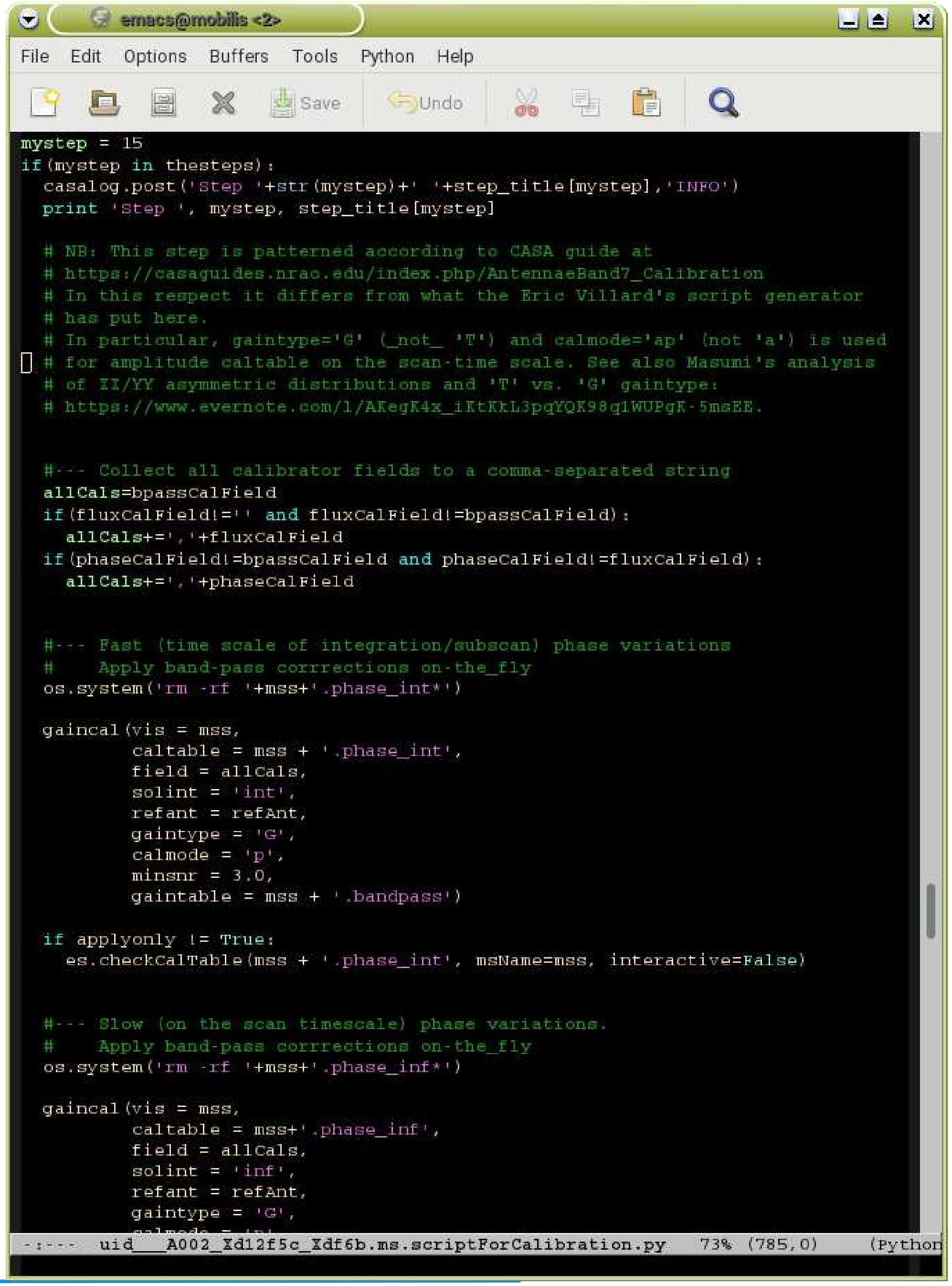

Postprocessing – calibration and imaging in CASA

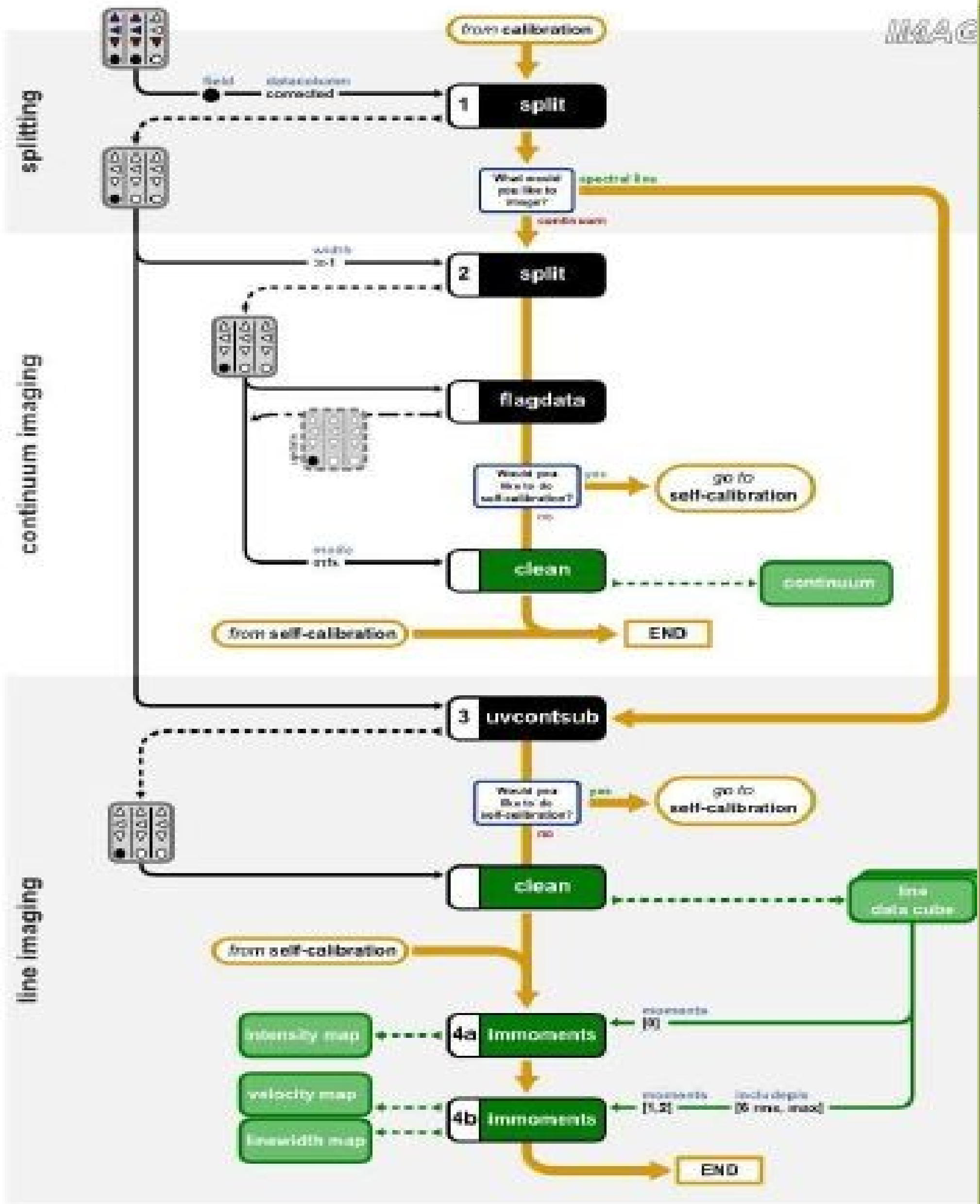

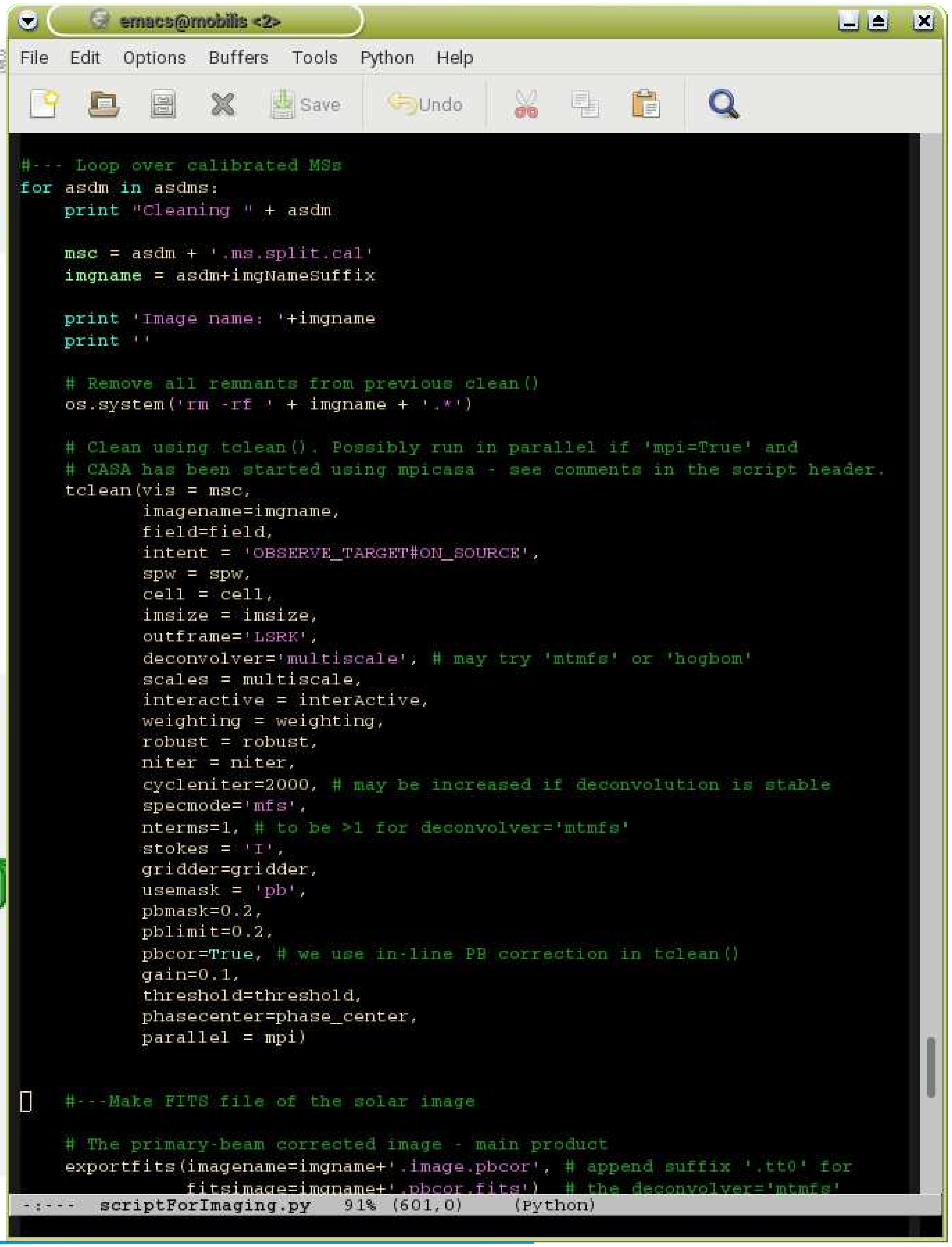

ALMA Regional Centers / ARCs and the ARC nodes

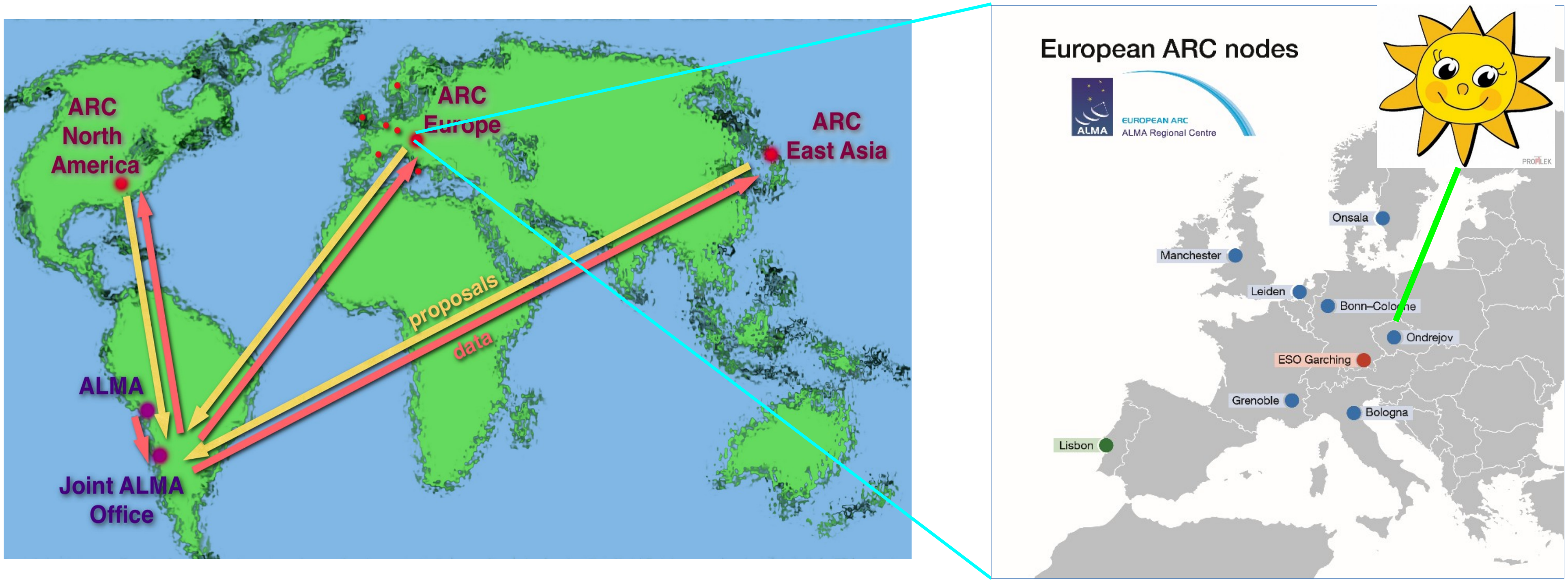

ALMA Regional Centers – ARCs:
Supporting infrastructure – interface between ALMA observatory and user community

Structure of the European ARC:

- Head in ESO Garching
- Seven nodes across Europe
  - **One in Ondřejov (Prague), Czech republic**

EUROPEAN ARC
ALMA Regional Centre

EU ARC – Czech node

ALMA

EUROPEAN ARC
ALMA Regional Centre || Czech

Status

- Hosted by the Astronomical Institute ASCR
- Negotiations with ESO started in 2007, node accepted into EU ARC network in 2009
- Since 2015 ***Research Infrastructure*** (support till 2022, listed in CZ *Roadmap*, one of the 42 in CR)
- Expertise areas: Galactic & extragalactic physics, stars & ISM, **solar physics**, laboratory mw spectroscopy

Mission

- User support, community building & training, help with ALMA development
- Serves the community in CR and entire CE Europe in all its expertise areas
- In **solar physics** it supports community on the **European-wide scale**

Role of the ARC nodes

Towards user community:

- Face-to-face (F2F) support of users in all stages of their ALMA-oriented projects.
- ALMA-system knowledge dissemination
- Spreading awareness of ALMA among scientific community

Towards ALMA observatory and ALMA-system developers:

- Help to the developers of ALMA user software:
- testing of CASA, ALMA OT, ALMA Helpdesk system,
- suggestions for improvement

Connecting users ↔ ALMA developers:

- Definition of new modes of observation – based on scientific community requests:
  → use-case studies, simulations, test observations (CSV/**EOC**),
  assembling requirements for system update => suggestions
  to ALMA observatory and developers.

User support

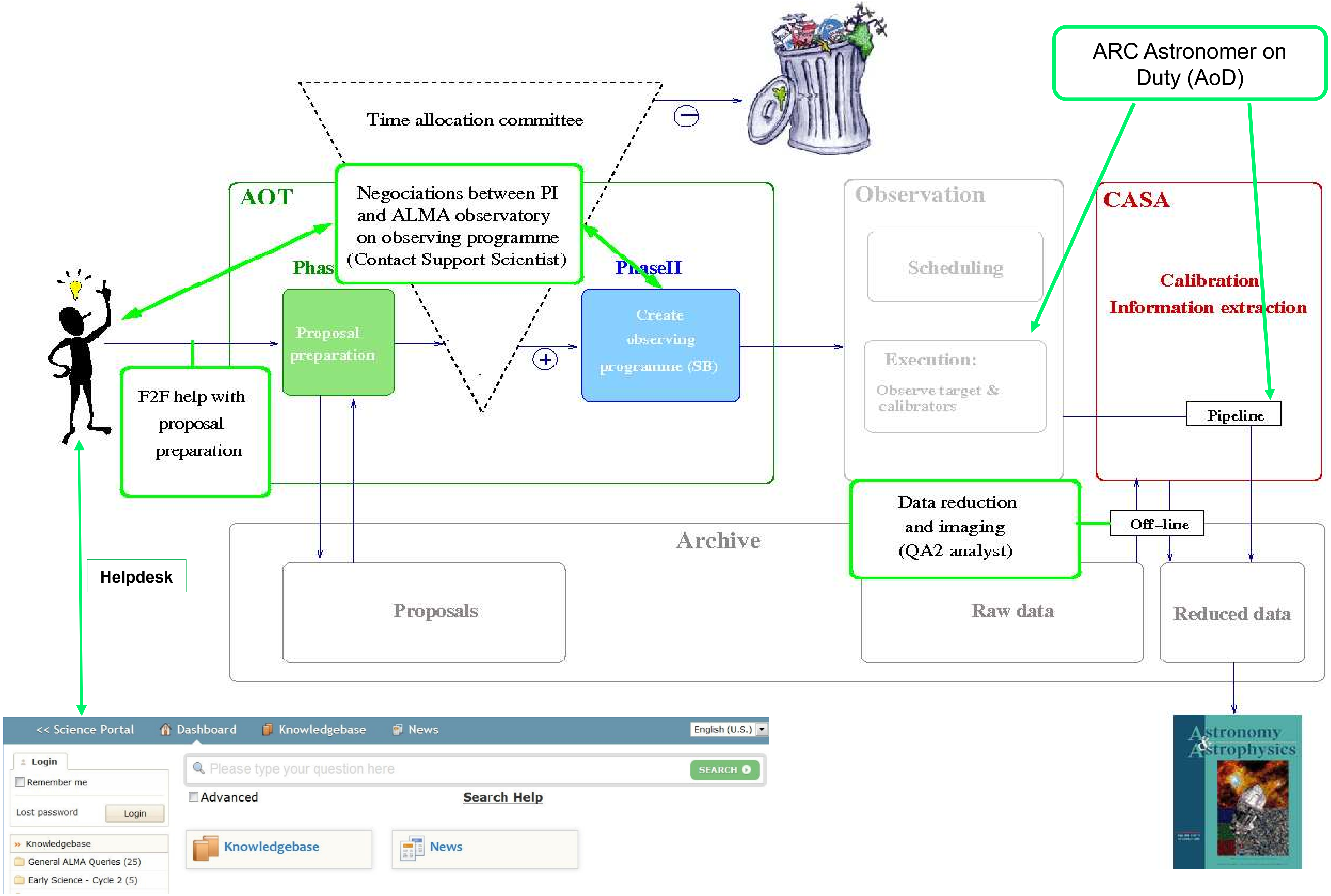

Role of the ARC nodes

Towards user community:

- Face-to-face (F2F) support of users in all stages of their ALMA-oriented projects.
- ALMA-system knowledge dissemination
- Spreading awareness of ALMA among scientific community

Towards ALMA observatory and ALMA-system developers:

- Help to the developers of ALMA user software:
- testing of CASA, ALMA OT, ALMA Helpdesk system,
- suggestions for improvement

Connecting users ↔ ALMA developers:

- Definition of new modes of observation – based on scientific community requests:
  → use-case studies, simulations, test observations (CSV/**EOC**),
  assembling requirements for system update => suggestions
  to ALMA observatory and developers.

The ARC node in Ondrejov is developping the solar ALMA observing mode for entire Europe – manated by ESO: **EOC Project *Solar Research with ALMA***
M. Barta, I. Skokic and R. Brajsa: Members of international Solar ALMA Development Team

Specific solar ALMA ObsMode: Why?

Why to observe the Sun with ALMA?

- A lot of key science questions in solar physics can be addressed with ALMA.
  - → This is reflected in the *Science with ALMA* document (+ Karlicky et al. 2011, S. Wedemeyer et. al 2015, EU ARC.CZ – *EoC* Project Report 2017, …)
- Meaningful use of the day time (‘bad weather’ – higher humidity).
  - → Increase of the ALMA scientific return/efficiency

Solar peculiarities: Why the solar observations need special treatment?

- The Sun is ‘hot’. Solved *apriori* by ‘scraped’ surface of parabolic reflectors.
- The Sun is far brighter in mm/sub-mm than other sources.
  - → Issue of dynamic range (e.g., in comparison with much weaker calibrators).
- Variability on short timescales (down to <1s in solar flares).
  - → Time-domain imaging & self-calibration needed.
  - → Less dense coverage of *uv*-space (Earth rotation cannot be used).
- In addition to apparent celestial motion of the Sun‘s center we have also (differential) solar rotation → complicated pointings / specific ephemeris required.
- Specific coordinate systems used in solar physics.
- Extended sources / emission in entire FOV – TP mapping needed, in a fast-scanning mode.

Specific solar ALMA ObsMode: Why?

Why to observe the Sun with ALMA?

- A lot of key science questions in solar physics can be addressed with ALMA.
  - → This is reflected in the *Science with ALMA* document (+ Karlicky et al. 2011, S. Wedemeyer et. al 2015, EU ARC.CZ – *EoC* Project Report 2017, …)
- Meaningful use of the day time ('bad weather' – higher humidity).
  - → Increase of the ALMA scientific return/efficiency

Solar peculiarities: Why the solar observations need special treatment?

- The Sun is 'hot'. Solved *apriori* by 'scraped' surface of parabolic reflectors.
- The Sun is far brighter in mm/sub-mm than other sources.
  - → Issue of dynamic range (e.g., in comparison with much weaker calibrators).
- Variability on short timescales (down to <1s in solar flares).
  - → Time-domain imaging & self-calibration needed.
  - → Less dense coverage of *uv*-space (Earth rotation cannot be used).
- In addition to apparent celestial motion of the Sun's center we have also (differential) solar rotation → complicated pointings / specific ephemeris required.
- Specific coordinate systems used in solar physics.
- Extended sources / emission in entire FOV – TP mapping needed, in a fast-scanning mode.

Solar ObsMode Commissioning: A project of world-wide collaboration

International Solar ALMA ObsMode Development Team

Shin'ichiro Asayama, East Asia ALMA Support Center, Tokyo, Japan;
Miroslav Barta, Astronomical Institute of the Czech Academy of Sciences, Ondrejov, Czech Republic;
Tim Bastian, National Radio Astronomy Observatory, USA;
Roman Brajsa, Hvar Observatory, Faculty of Geodesy, University of Zagreb, Croatia;
Bin Chen, New Jersey Institute of Technology, USA;
Bart De Pontieu, LMSAL, USA; Gregory Fleishman, New Jersey Institute of Technology, USA;
Dale Gary, New Jersey Institute of Technology, USA;
Antonio Hales, Joint ALMA Observatory, Chile;
Akihiko Hirota, Joint ALMA Observatory, Chile;
Hugh Hudson, School of Physics and Astronomy, University of Glasgow, UK;
Richard Hills, Cavendish Laboratory, Cambridge, UK;
Kazumasa Iwai, National Institute of Information and Communications Technology, Japan;
Sujin Kim, Korea Astronomy and Space Science Institute, Daejeon, Republic of Korea;
Neil Philips, Joint ALMA Observatory, Chile;
Tsuyoshi Sawada, Joint ALMA Observatory, Chile;
Masumi Shimojo (interferometry lead), NAOJ, Tokyo, Japan;
Giorgio Siringo, Joint ALMA Observatory, Chile;
Ivica Skokic, Astronomical Institute of the Czech Academy of Sciences, Ondrejov, Czech Republic;
Sven Wedemeyer, Institute of Theoretical Astrophysics, University of Oslo, Norway;
Stephen White (single dish lead), AFRL, USA;
Pavel Yagoubov, ESO, Garching, Germany
Yihua Yan, NAO, Chinese Academy of Sciences, Beijing, China.

ESO charged the Czech node by leading EU participation in the Solar ObsMode Development

EOC project *Solar Research with ALMA (2014-2017)*

Project strategy translated into *Working Packages*

- WP1: Science use-cases for solar research with ALMA
  - Develop and investigate a set of detailed use cases for solar observing with ALMA
    - Request input from the community
    - Define requirements for spatial/spectral/temporal resolution, FOV, polarisation, …
    - Use CASA simulation package for TA
- WP2: Solar Observing Modes and Calibration
  - Research in possible new solar observing modes and analyse calibration requirements
    - Solar attenuators („filters“)
    - MD1/MD2 w/wo attenuation
    - SD/TP fast-scanning observations
- WP3: Software Requirements
  - Produce requirements for observing preparation, execution and post-processing

Project team

- Core: **M. Bárta (PM), R. Brajša (PI), I. Skokič**, M. Karlický, P. Heinzel
- ESO Coordinator: **R. Laing**
- External collaborators (ESO): A. Hanslmeier, M. Temmer (Uni Graz, AT), A. Benz (FNHW Windisch, CH), E. Kontar (Uni Glasgow, UK), S. Wedemayer-Boehm (Uni Oslo, NO), R. Hills (Cambridge, UK)
- Cooperation with similar activity at NA and EA ARCS: S. White (US Air Force Research Lab, Albuquerque, US), T. Bastian (NRAO, Charlottesville, US), M. Shimojo (NAOJ, JP), A. Kazamusa (NAOJ/Nobeyama)

Specific solar ALMA ObsMode: Why?

Why to observe the Sun with ALMA?

- A lot of key science questions in solar physics can be addressed with ALMA.
  → This is reflected in the *Science with ALMA* document (+ Karlicky et al. 2011, S. Wedemeyer et. al 2015, EU ARC.CZ – *EoC* Project Report 2017, …)
- Meaningful use of the day time ('bad weather' – higher humidity).
  → Increase of the ALMA scientific return/efficiency

Solar peculiarities: Why the solar observations need special treatment?

- The Sun is 'hot'. Solved *apriori* by 'scraped' surface of parabolic reflectors.
- The Sun is far brighter in mm/sub-mm than other sources.
  → Issue of dynamic range (e.g., in comparison with much weaker calibrators).
- Variability on short timescales (down to <1s in solar flares).
  → Time-domain imaging & self-calibration needed.
  → Less dense coverage of *uv*-space (Earth rotation cannot be used).
- In addition to apparent celestial motion of the Sun's center we have also (differential) solar rotation → complicated pointings / specific ephemeris required.
- Specific coordinate systems used in solar physics.
- Extended sources / emission in entire FOV – TP mapping needed, in a fast-scanning mode.

What can ALMA tell us about the Sun? Typical uses cases

- **Particle acceleration in solar flares**
  Ultra energetic electrons can produce synchrotron radiation in mm range. With ALMA we would reach unprecedented spatial imaging of energetic particles.

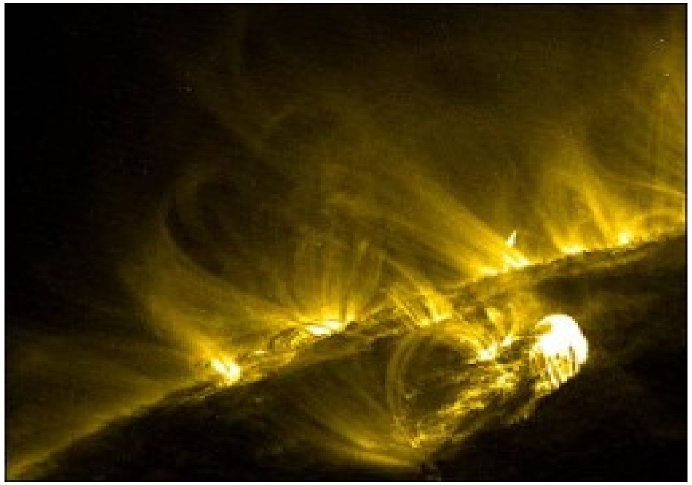

- **Structure and dynamics of solar chromosphere**
  Temperature structure remains unclear.
  What is the role and nature of oscillations and waves?
  Thermal emission in ALMA range can provide an answer.

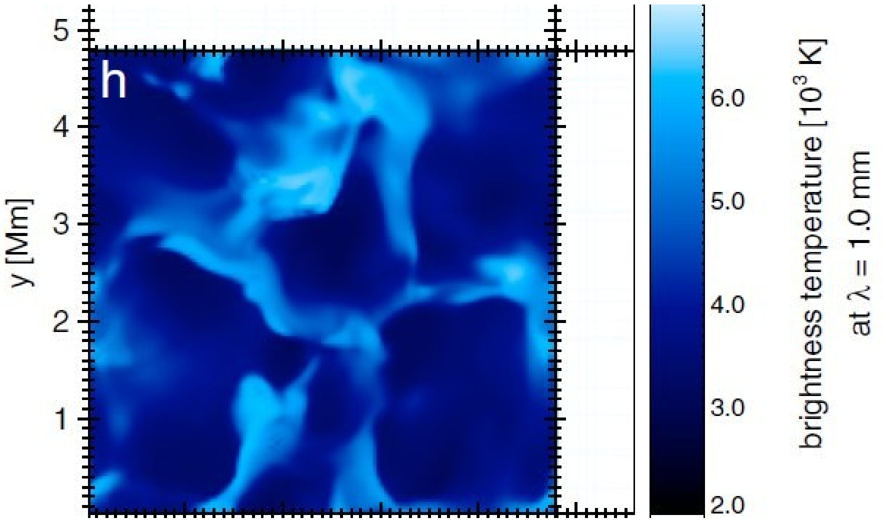

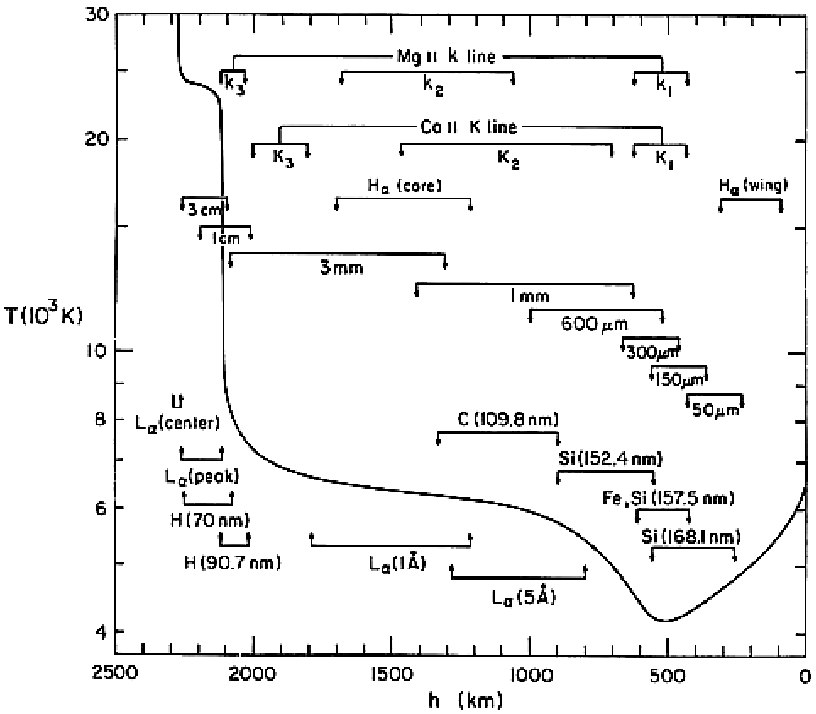

What can ALMA tell us about the Sun? Typical use cases

- **Structure of solar prominences**
  Internal structure of prominences and filaments remain unclear. ALMA can look through with very high resolution.

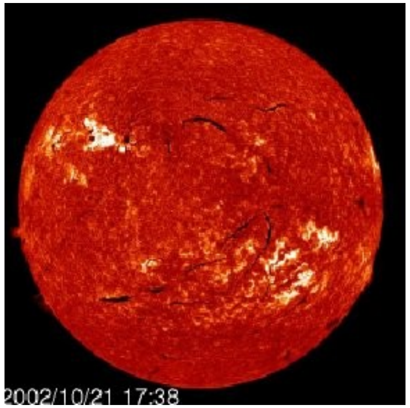

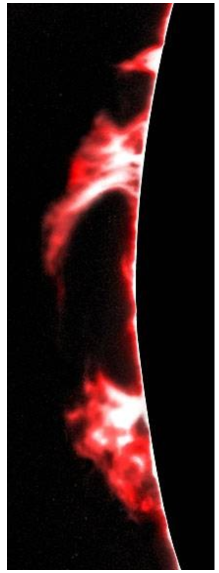

- **Study of recombination lines in solar atmosphere**
  It still unclear whether these can be observed in the mm wavelength range. If yes, an important diagnostic tool for measurement of magnetic field in the part of the solar atmosphere where it is otherwise difficult would emerge.

- **Probably many more open issues...**
  Solar community should look. Numerical modelling combined with CASA simulation tool can represent a way how to find out.

See review by S. Wedemeyer-Boehm et al. at http://arxiv.org/abs/1504.06887 (SSR 2015) and the **Final report of our project** (ESO / Czech node of EU ARC, 2017)

Specific solar ALMA ObsMode: Why?

Why to observe the Sun with ALMA?

- A lot of key science questions in solar physics can be addressed with ALMA.
  → This is reflected in the *Science with ALMA* document (+ Karlicky et al. 2011, S. Wedemeyer et. al 2015, EU ARC.CZ – *EoC* Project Report 2017, …)
- Meaningful use of the day time ('bad weather' – higher humidity).
  → Increase of the ALMA scientific return/efficiency

Solar peculiarities: Why the solar observations need special treatment?

- The Sun is 'hot'. Solved *apriori* by 'scraped' surface of parabolic reflectors.
- The Sun is far brighter in mm/sub-mm than other sources.
  → Issue of dynamic range (e.g., in comparison with much weaker calibrators).
- Variability on short timescales (down to <1s in solar flares).
  → Time-domain imaging & self-calibration needed.
  → Less dense coverage of *uv*-space (Earth rotation cannot be used).
- In addition to apparent celestial motion of the Sun's center we have also (differential) solar rotation → complicated pointings / specific ephemeris required.
- Specific coordinate systems used in solar physics.
- Extended sources / emission in entire FOV – TP mapping needed, in a fast-scanning mode.

Proper motion of solar sources: Ephemeris/pointings

ALMA OT + *Ephemeris Generator Tool*

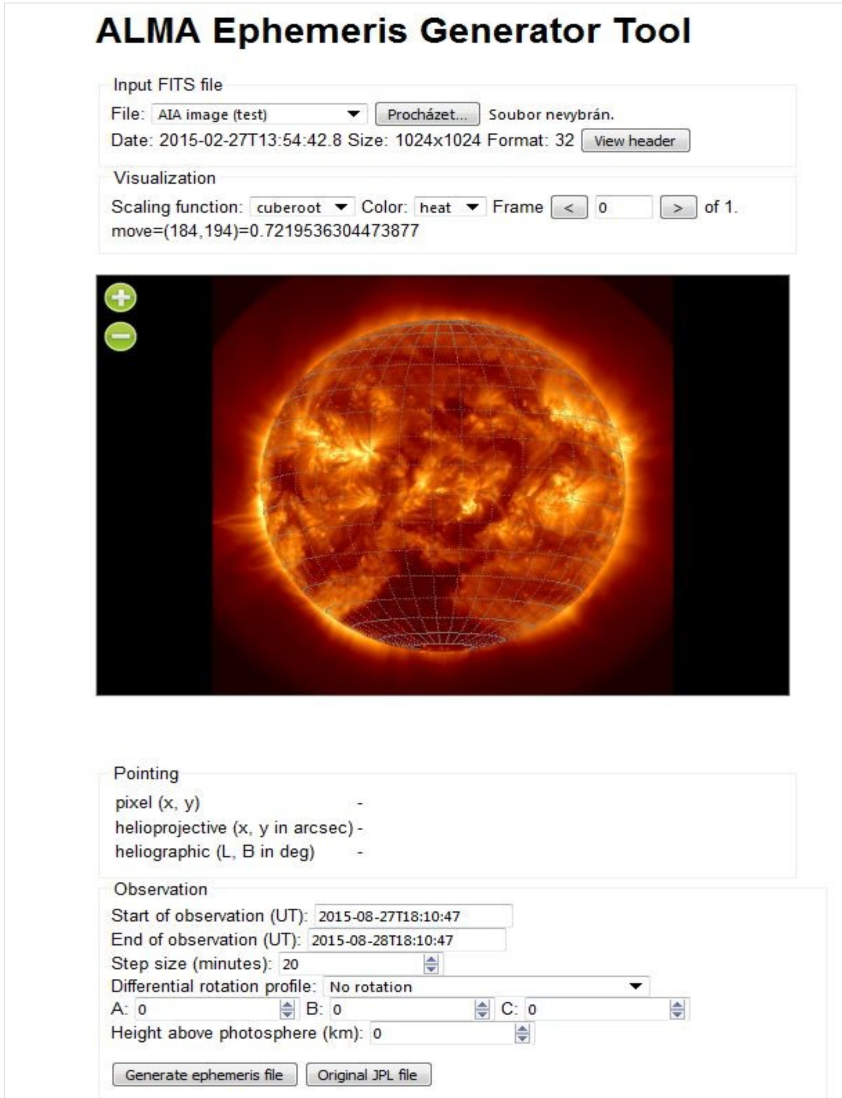

http://celestialscenes.com/alma/coords/CoordTool.html

Accessible from ALMA Science Portal
http://www.almascience.org

Author: **Ivica Skokic**

Nowadays used also for (E)VLA and other observatories

What can ALMA tell us about the Sun? Typical use cases & obs. strategies

Prominences: Simulation using CASA::simobserve(), imaging using CASA::clean(), Heinzel et al. 2015

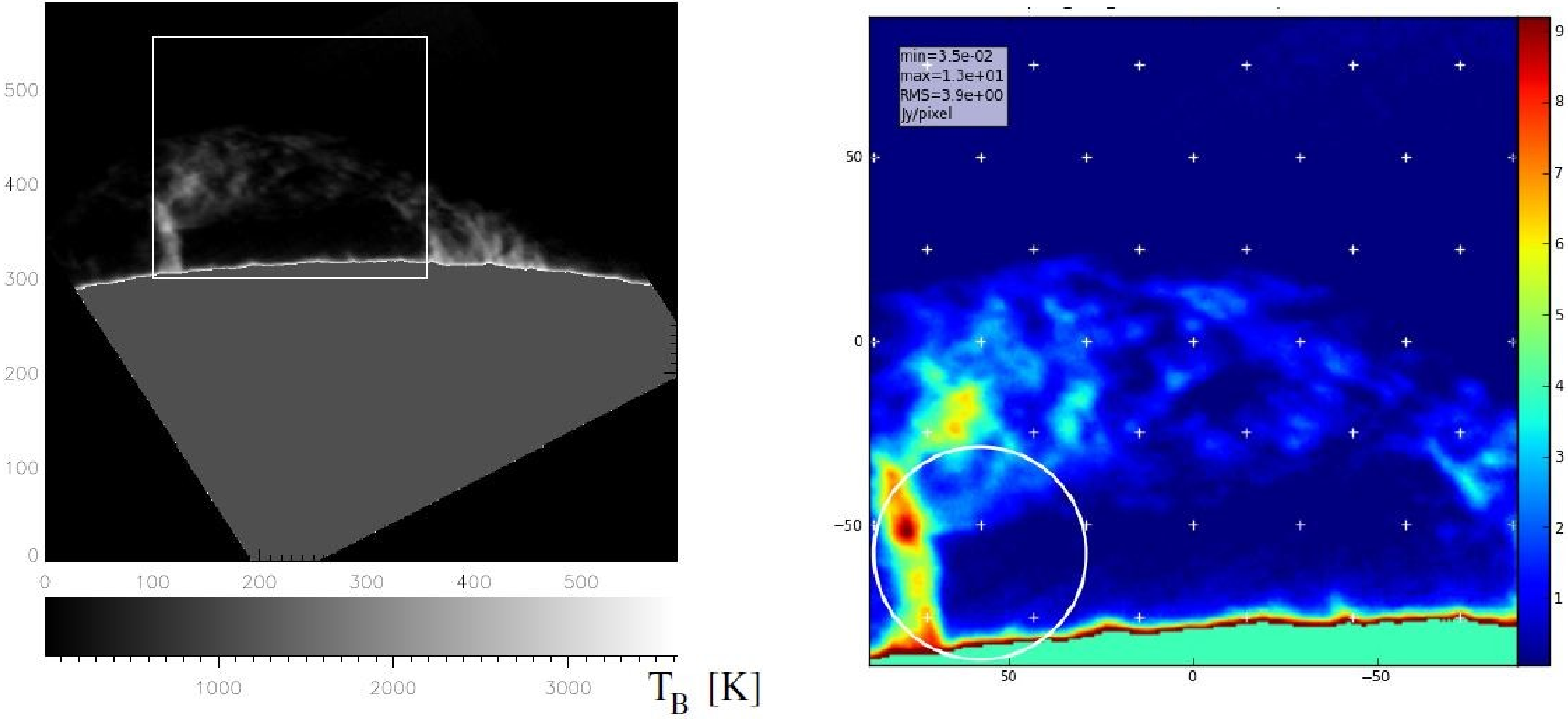

What can ALMA tell us about the Sun? Typical use cases & obs. strategies

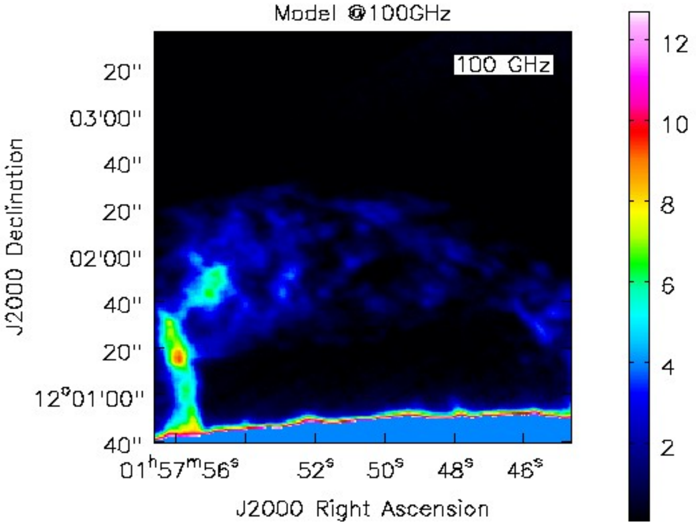

Model data

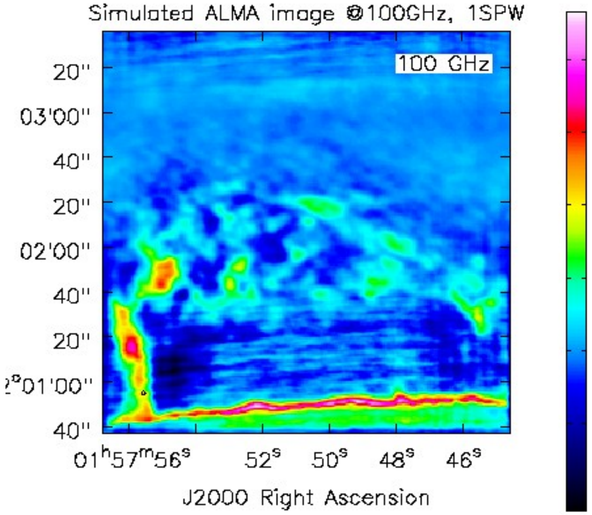

Single continuum:1 SPW

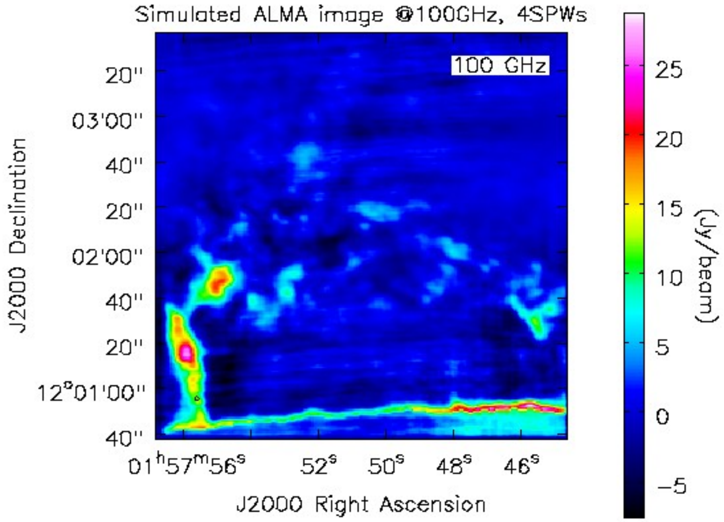

Single continuum: 4 SPWs

<u>Result:</u> MFS improves *uv* Coverage and reconstructed image fidelity even for continuum images

Specifics of solar ALMA observations: Solutions for project execution

Interferometric observations: The Sun is far brighter in mm/sub-mm than other sources

– Issue of dynamic range - e.g., in comparison with phase calibrators

Two suggested solutions:

- Solar attenuators (“filters”)
  - Put them in the optical path for solar target, remove for P-cal (mechanicaly, carousel/robotic arm)
  - Large time overhead
  - Phase delays in filters depending on too many parameters, measurements of phase delays practically unreproducible
  - **Now mostly deprecated** (perhaps will be used in the future flare mode)
- Mixer detuning (+electronic attenuation)
  - **Working approach!** (as found by our tests)

Specifics of solar ALMA observations: Solutions for project execution

„Extended“ Scheduling Block

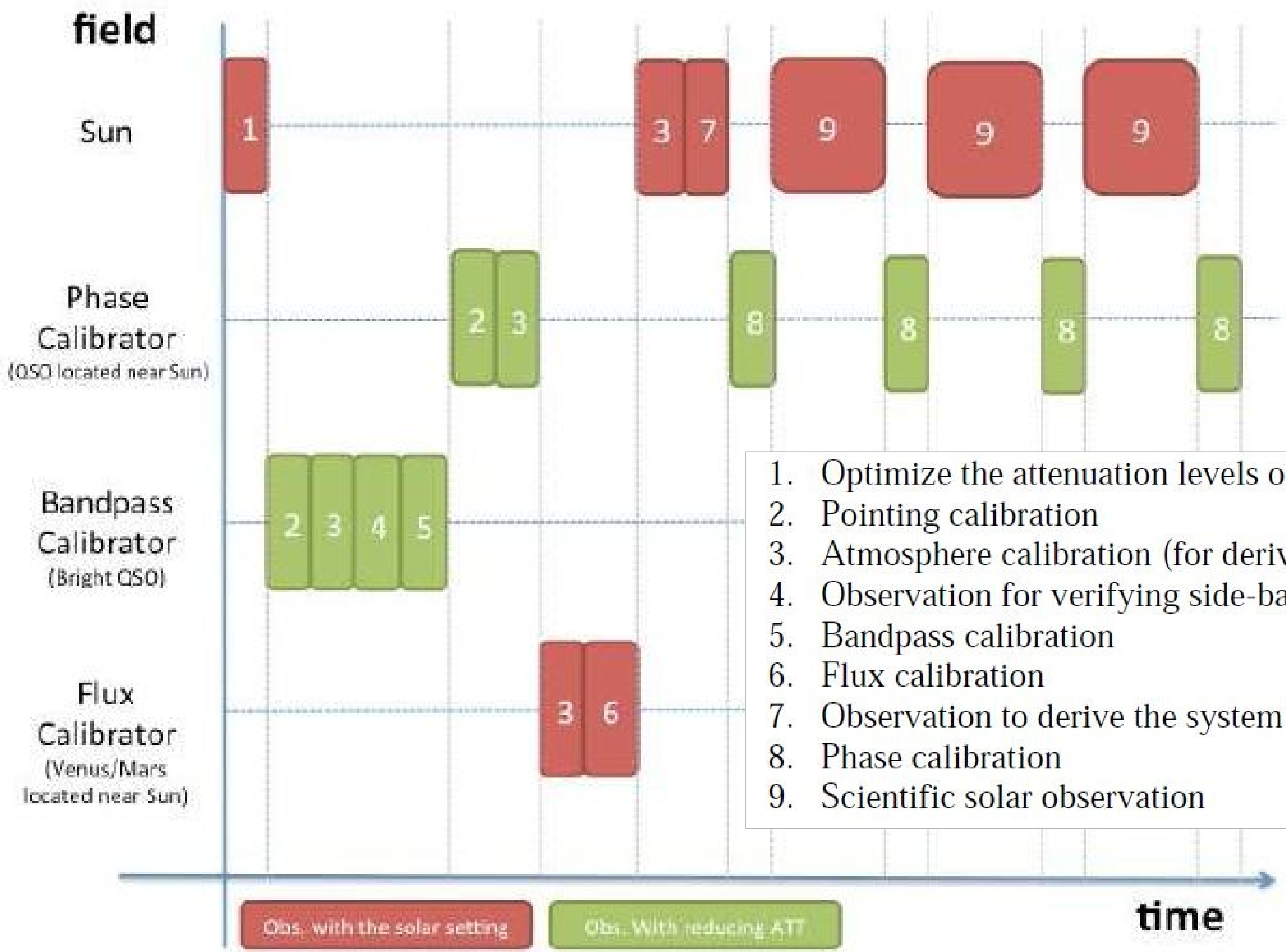

1. Optimize the attenuation levels of the receiver
2. Pointing calibration
3. Atmosphere calibration (for deriving the system temperature on the sky)
4. Observation for verifying side-band separation
5. Bandpass calibration
6. Flux calibration
7. Observation to derive the system temperature on the target region
8. Phase calibration
9. Scientific solar observation

Specifics of solar ALMA observations: Solutions for project execution

TP antenna – double-circle scanning pattern

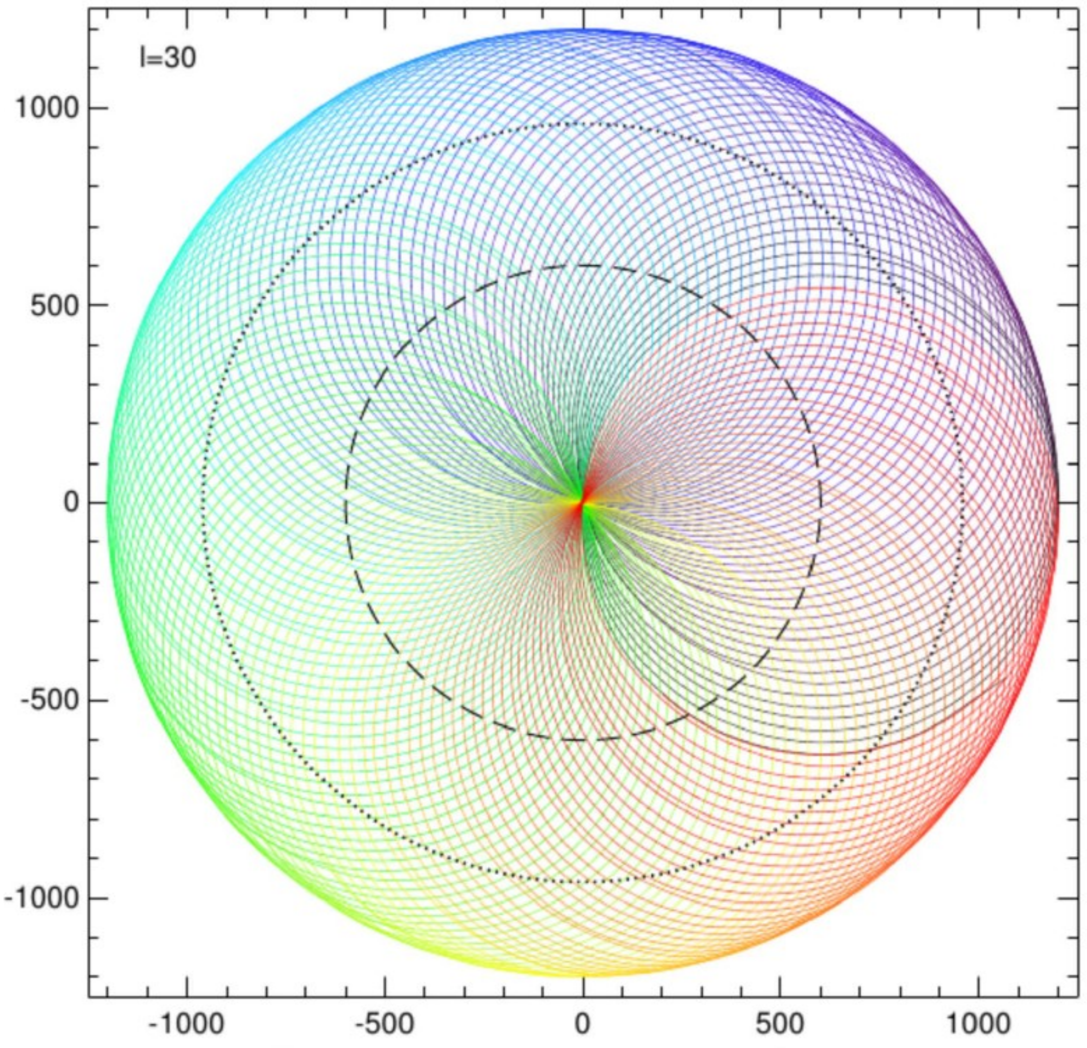

Single-dish scanning

Testing and on-line tuning of suggested procedures: Solar CSV campaigns 2014/15

Team

- EU ARC: M. Bárta (CZ node, Ondrejov), R. Brajša (CZ node, Zagreb), I. Skokic (CZ node Ondrejov)
- NA ARC: T. Bastian (NRAO), S. White (US Air Force Research Lab)
- EA ARC: M. Shimojo (NAOJ), S. Kazamusa (NAOJ/Nobeyama)
  + strong JAO support (T. Remijan, A. Hales, A. Hirota,…)

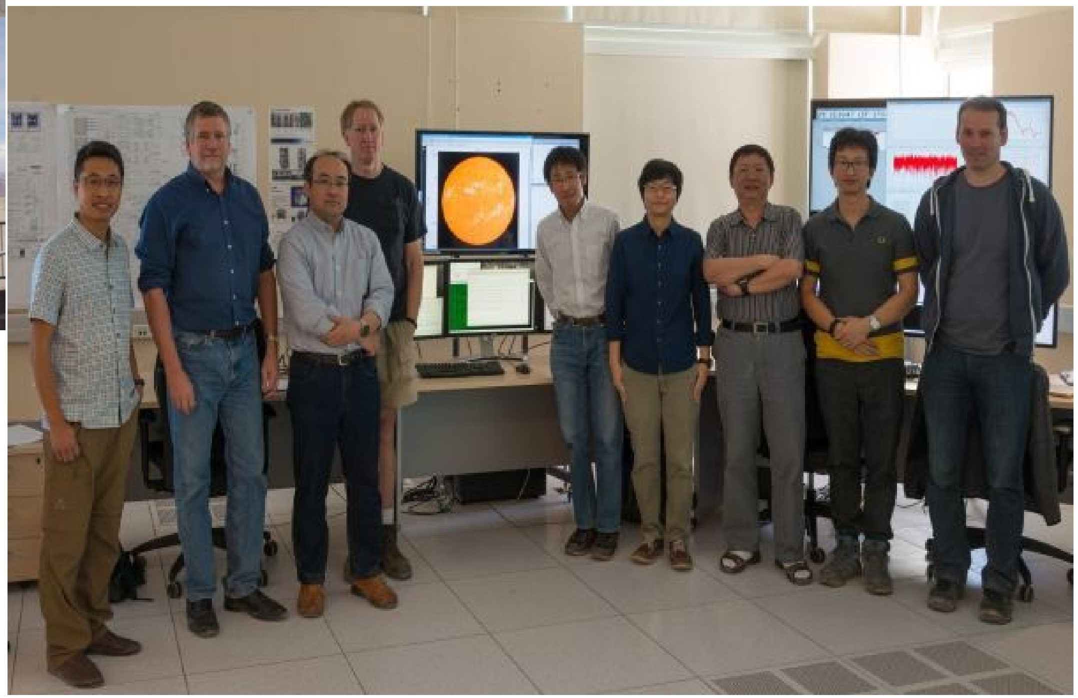

Testing and on-line tuning of suggested procedures: Solar CSV campaigns 2014/15

Results

Whole-disc SD scan in ALMA continuum @240GHz (Band 6, left panel) as compared do Hα image from BBSO (Dec. 2014)

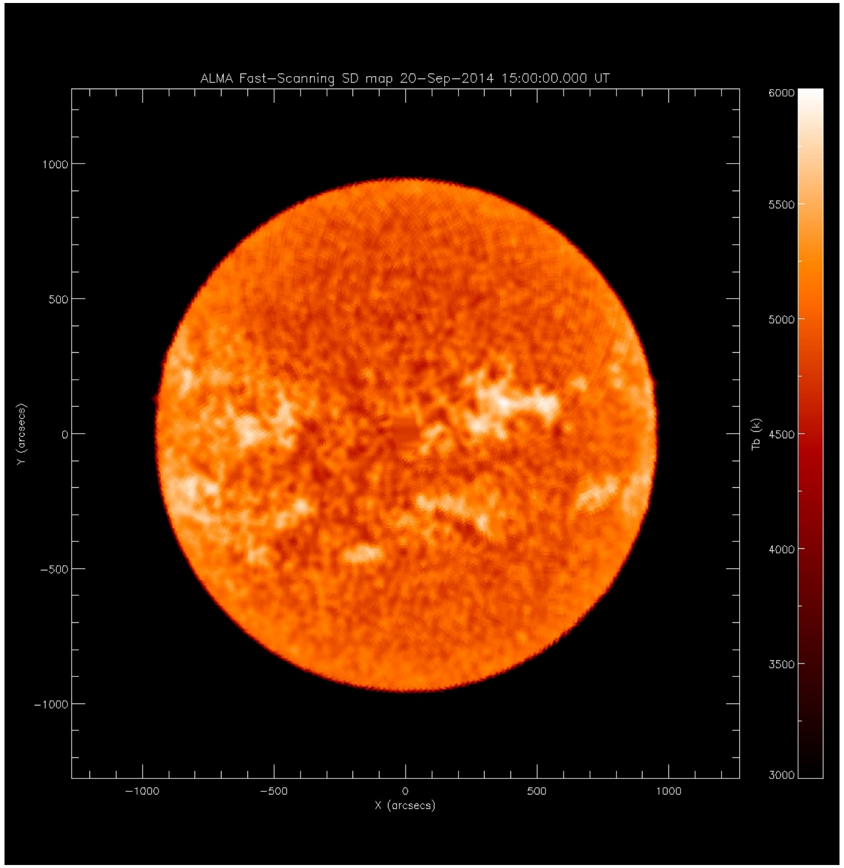

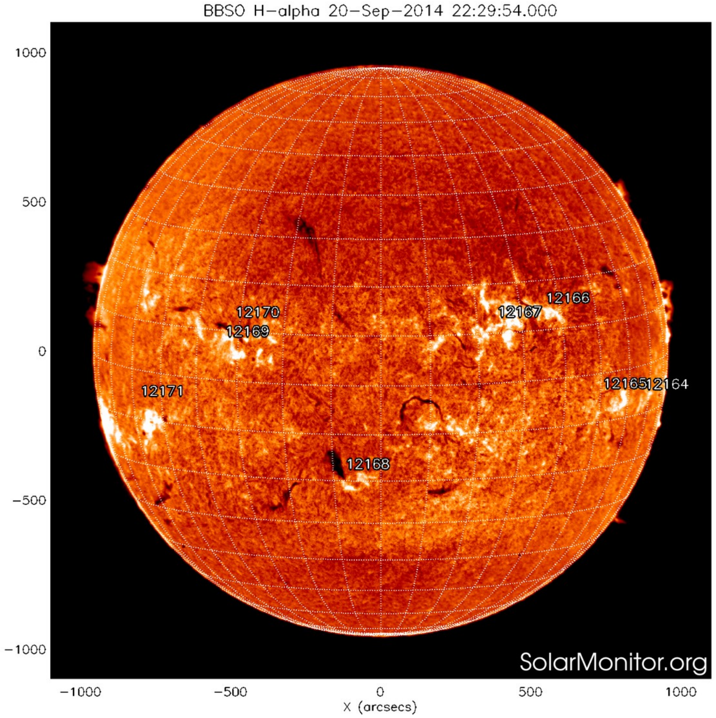

Results

Filament in ALMA continuum @100GHz (Band 3 – middle panel), compared with AIA observations at 304A (left) and 1700A (right). IF image – main array (BL correlator only; Dec 2014)

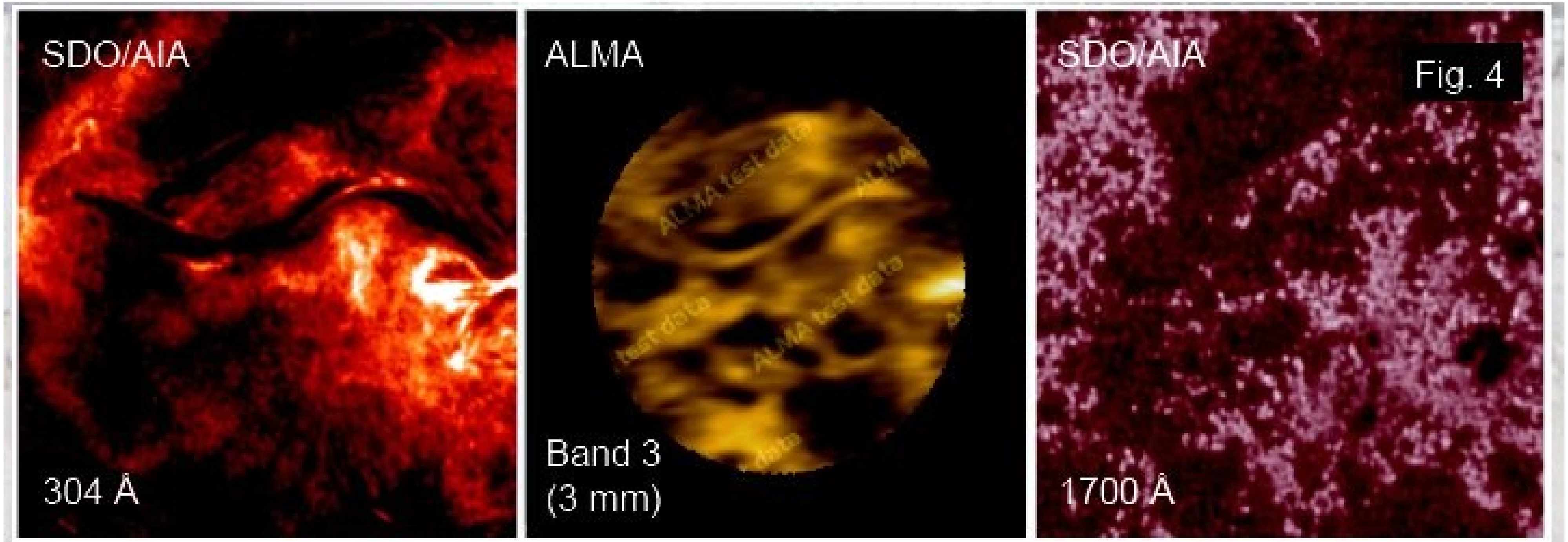

Testing and on-line tuning of suggested procedures: Solar CSV campaigns 2014/15

Results

The sunspot (NOAA 12470) in ALMA continuum Band 3 @100GHz (left), Band 6 @240GHz (middle) and AIA 1700A (right) – **IF images combined with TP scans**.

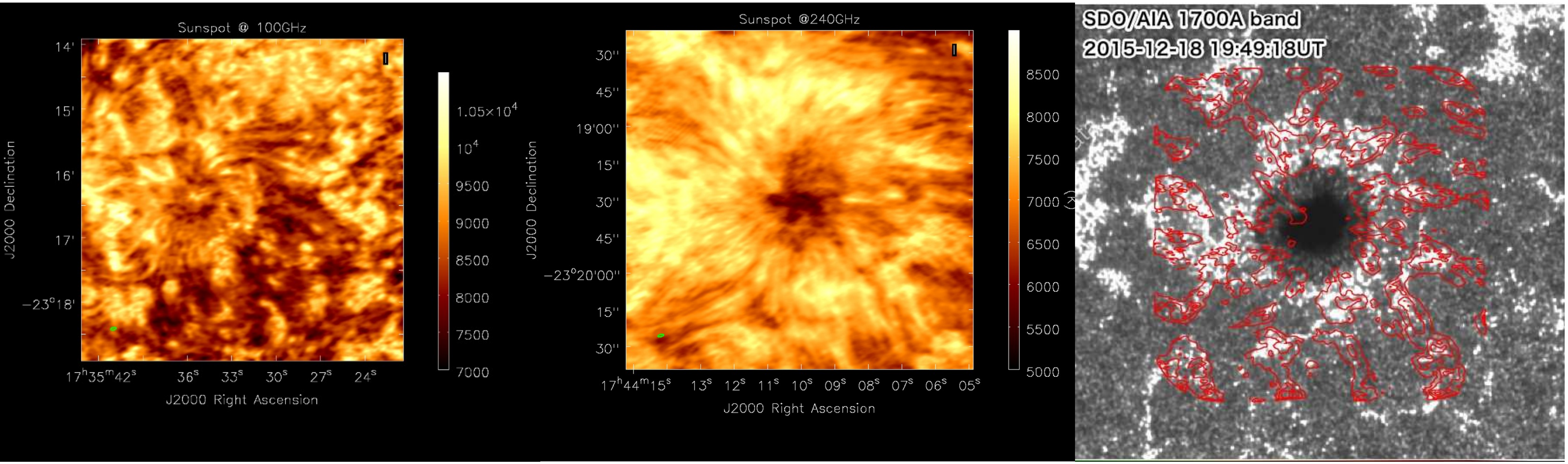

Testing and on-line tuning of suggested procedures: Solar CSV campaigns 2014/15

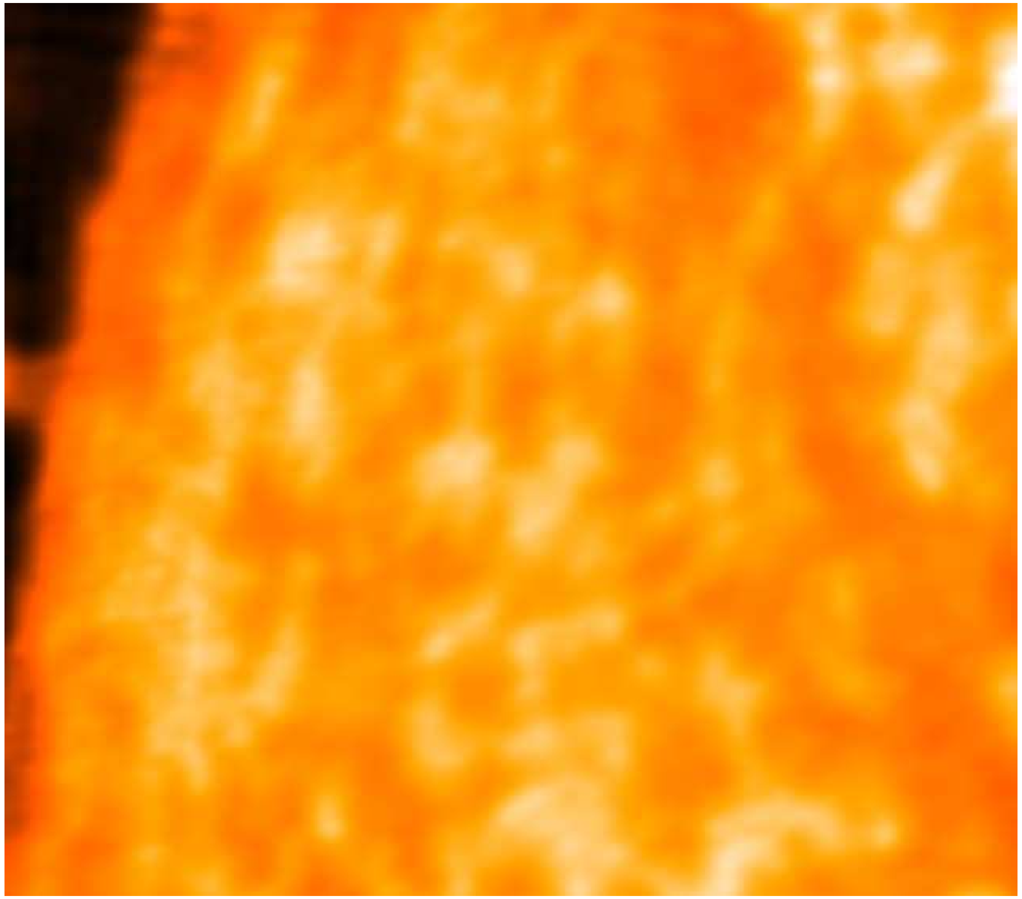

100 GHz, prominence, small mosaic

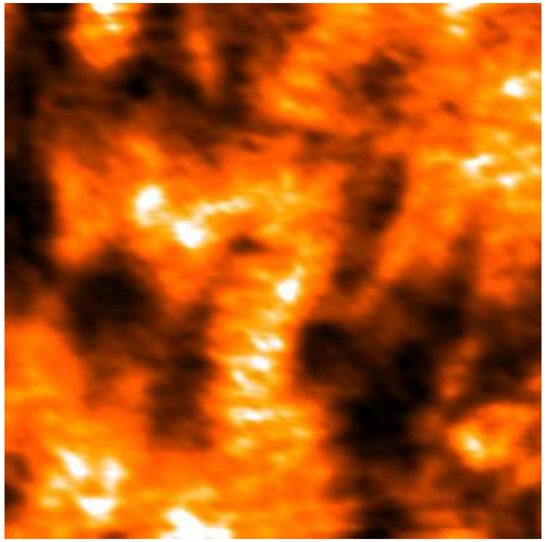

100 GHz, AR, small mosaic

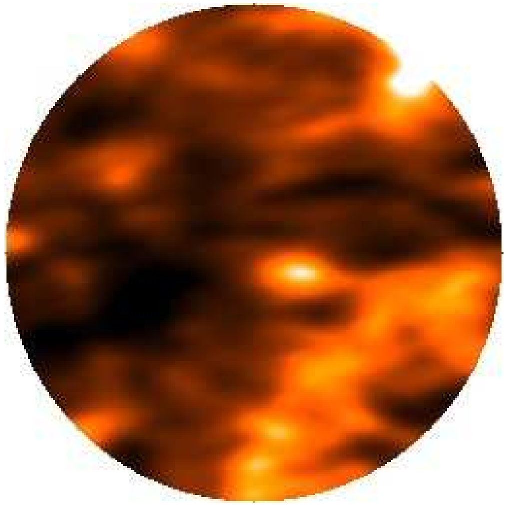

100 GHz, AR, single pointing

CSV data release

https://almascience.eso.org/alma-data/science-verification

Acceptace of the *Solar ObsMode* – Start of solar science with ALMA

Final resolution

- Accepted as a non-standard science mode for Cy 4 with limitations

- Summary of CSV published in two Solar Physics papers
  Fast-scanning TP: http://adsabs.harvard.edu/abs/2017SoPh..292...88W
  Interferometric obs.: http://adsabs.harvard.edu/abs/2017SoPh..292...87S

- ESO press-release no 1703 (also ALMA Science Portal news)

Acceptance of the Solar ObsMode: Results of the project

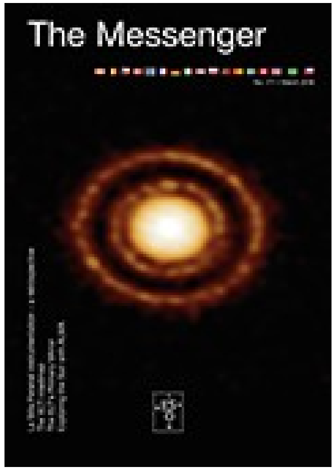

Exploring the Sun with ALMA

ESO Messenger
No. 171, March 2018

Timothy S. Bastian[1]
Miroslav Bárta[2]
Roman Brajša[3]
Bin Chen[4]
Bart De Pontieu[5,6]
Dale E. Gary[4]
Gregory D. Fleishman[4]
Antonio S. Hales[1,7]
Kazumasa Iwai[8]
Hugh Hudson[9,10]
Sujin Kim[11,12]
Adam Kobelski[13]
Maria Loukitcheva[4,14,15]
Masumi Shimojo[16,17]
Ivica Skokić[2,3]
Sven Wedemeyer[6]
Stephen M. White[18]
Yihua Yan[19]

[1] National Radio Astronomy Observatory, Charlottesville, USA
[2] Astronomical Institute, Czech Academy of Sciences, Ondřejov, Czech Republic
[3] Hvar Observatory, Faculty of Geodesy, University of Zagreb, Croatia
[4] Center for Solar-Terrestrial Research, New Jersey Institute of Technology, Newark, USA
[5] Lockheed Martin Solar & Astrophysics Lab, Palo Alto, USA
[6] Rosseland Centre for Solar Physics, University of Oslo, Norway
[7] Joint ALMA Observatory (JAO), Santiago, Chile
[18] Space Vehicles Directorate, Air Force Research Laboratory, Albuquerque, USA
[19] National Astronomical Observatories, Chinese Academy of Sciences, Beijing, China

The Atacama Large Millimeter/submillimeter Array (ALMA) Observatory opens a new window onto the Universe. The ability to perform continuum imaging and spectroscopy of astrophysical phenomena at millimetre and submillimetre wavelengths with unprecedented sensitivity opens up new avenues for the study of cosmology and the evolution of galaxies, the formation of stars and planets, and astrochemistry. ALMA also allows fundamentally new observations to be made of objects much closer to home, including the Sun. The Sun has long served as a touchstone for our understanding of astrophysical processes, from the nature of stellar interiors, to magnetic dynamos, non-radiative heating, stellar mass loss, and energetic phenomena such as solar flares. ALMA offers new insights into all of these processes.

ALMA solar science

Radiation from the Sun at millimetre and ... and to gain an understanding of how mechanical and radiative energy are transferred through that atmospheric layer.

Much of what is currently known about the chromosphere has relied on spectroscopic observations at optical and ultraviolet wavelengths using both ground- and space-based instrumentation. While a lot of progress has been made, the interpretation of such observations is complex because optical and ultraviolet lines in the chromosphere form under conditions of non-local thermodynamic equilibrium. In contrast, emission from the Sun's chromosphere at millimetre and submillimetre wavelengths is more straightforward to interpret as the emission forms under conditions of local thermodynamic equilibrium and the source function is Planckian. Moreover, the Rayleigh-Jeans approximation is valid ($hn/kT \ll 1$) and so the observed intensity at a given frequency is linearly proportional to the temperature of the (optically thick) emitting material. By tuning across the full suite of ALMA's frequency bands it is possible to probe the entire depth of the chromosphere.

Wedemeyer et al. (2016) comprehensively discuss the potential of ALMA in this context. In brief, observations of thermal emission from material at chromospheric

Solar ALMA science observations: Cycle 4 & 5

Cycle 5

- World-wide End-to-End test in mid March 2018 (PI M. Barta – CZ node, CSS A. Hales – JAO, QA2 analyst W. Liu – CZ node)
- Observations: 01/04/2018 – 05/05/2018 in the config C43-3; a few projects during June with lower resolution; return to C43-3 in mid August
- We are working as remote AoDs assistants via *Target of Opportunity Trigger Tickets*
- QA2 & more: Right now working on that – most datasets delivered, working on late-August observations.
  - More automated procedure – towards the Script Generator/auto-pipeline used in non-solar data.
  - Self-calibration and time-domain imaging (calibrated movies)

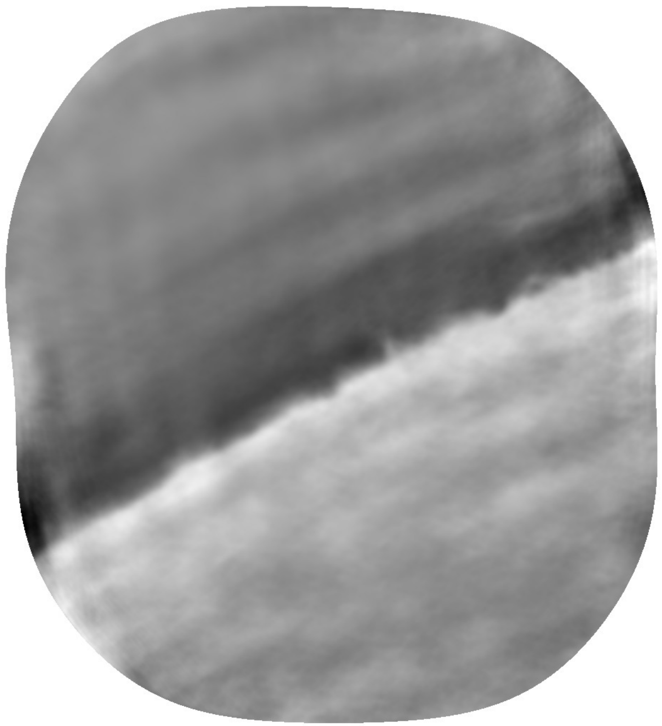

Solar AR - movie

Solar ALMA science observations: Cycle 4 & 5

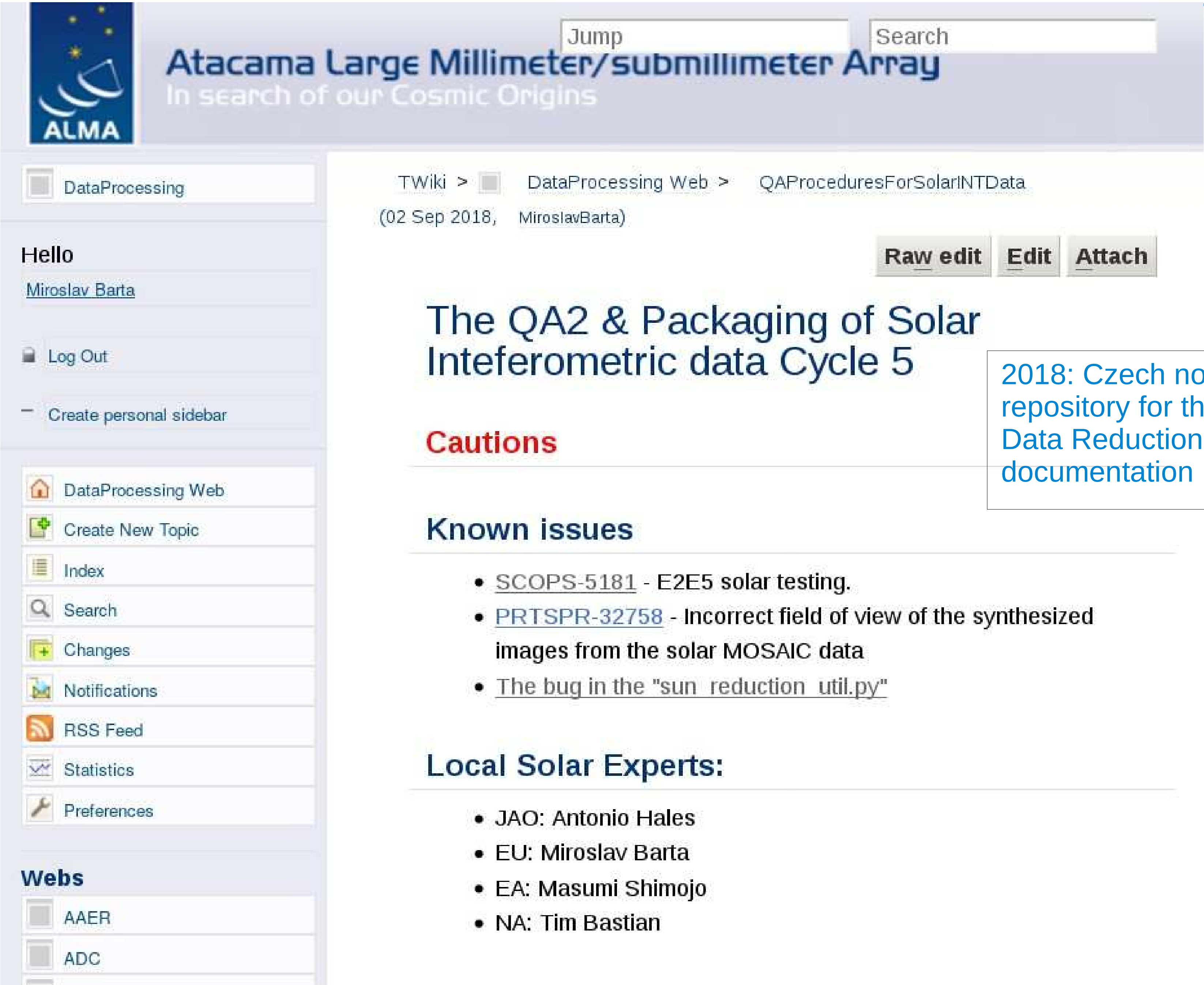

2018: Czech node maintains central repository for the Solar Science Data Reduction procedure and its documentation

Sluneční pozorovací kampaň v Chile, prosinec 2014: Dojmy z cesty

EXTREMO
PELIGROSO
ALTO
MEDIO
BAJO
SOLMAFORO
UV Rays Indicator
Alert
Maximum time of exposure (Minutes)
White tone skin
Matte tone Skin
Suggestion
Extreme 11 - 22 20 - 33
Dangerous 15 - 30 27 - 45
High 21 - 40 38 - 60
Medium 30 - 80 54 - 120
Low 75 - 240 135 - 360
SOLMAFORO
INDICADOR DE RAYOS ULTRAVIOLETA
Alerta
Tiempo máximo de exposición (minutos)
Piel Blanca
Piel Mate
Sugerencia
EXTREMO 11 - 22 20 - 33 Evite el sol, use protección
PELIGROSO 15 - 30 27 - 45 Busque sombra, use manga larga y gorro
ALTO 21 - 40 38 - 60 Use bloqueador y gorro
MEDIO 30 - 80 54 - 120 Puede tomar sol con precaución
BAJO 75 - 240 135 - 360

100
OXIGENO
MEDICINAL
INDURA
100
OXIGENO
MEDICINAL
OXIGENO MEDICINAL COMPRIMIDO
Las Américas 585
INDURA S.A.
Cerrillos – Santiago


DV-02

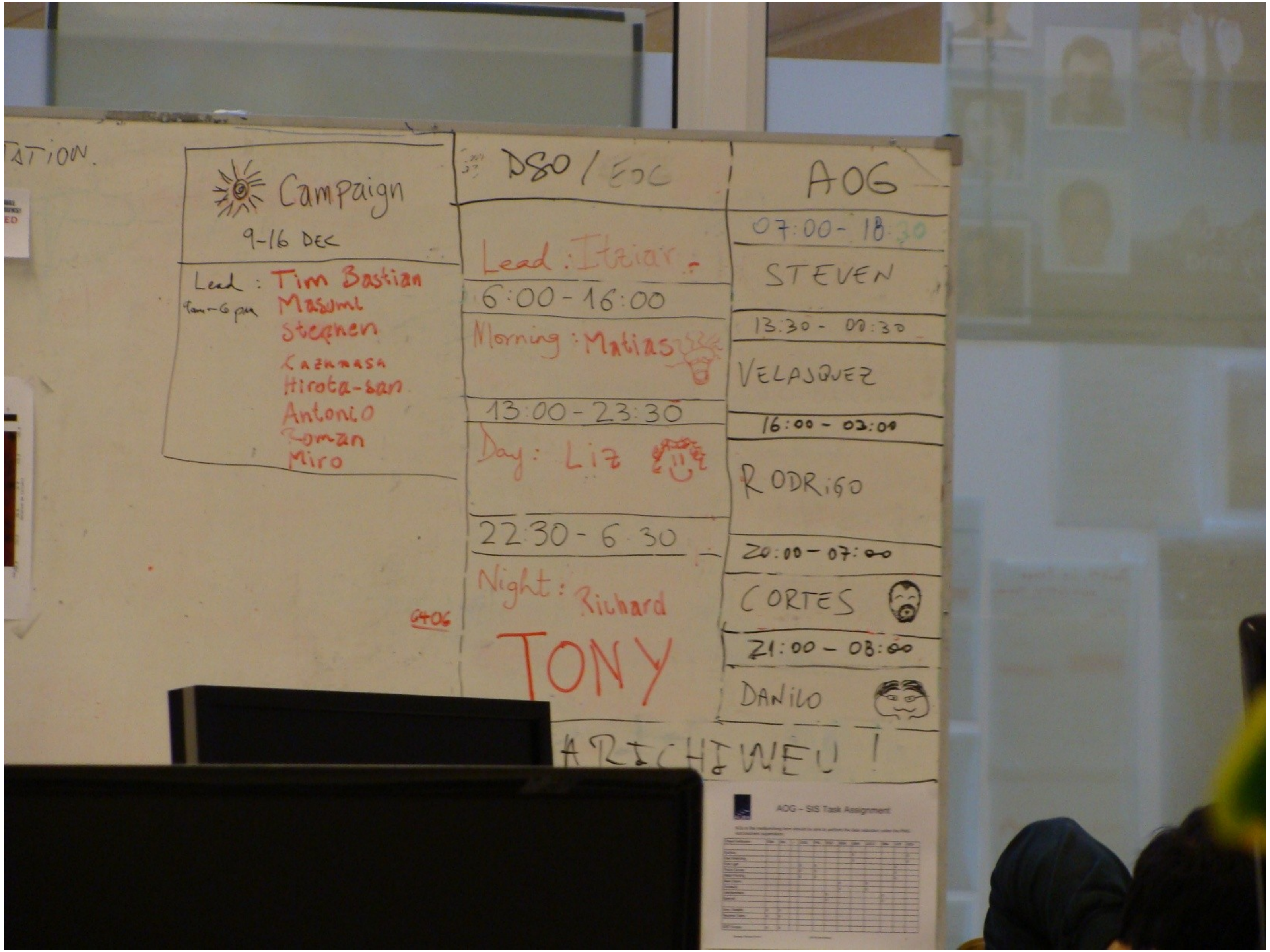

Campaign
9-16 DEC
Lead : Tim Bastian
Masumi
Stephen
Hirota-san
Antonio
Roman
Miro
DSO / EOC
Lead : Itziar
6:00 - 16:00
Morning : Matias
13:00 - 23:30
Day : Liz
22:30 - 6:30
Night : Richard
TONY
AOG
07:00 - 18:30
STEVEN
13:30 - 00:30
VELASQUEZ
16:00 - 03:00
RODRIGO
20:00 - 07:00
CORTES
21:00 - 08:00
DANILO
AOG – SIS Task Assignment


SCHEUERLE
Otto

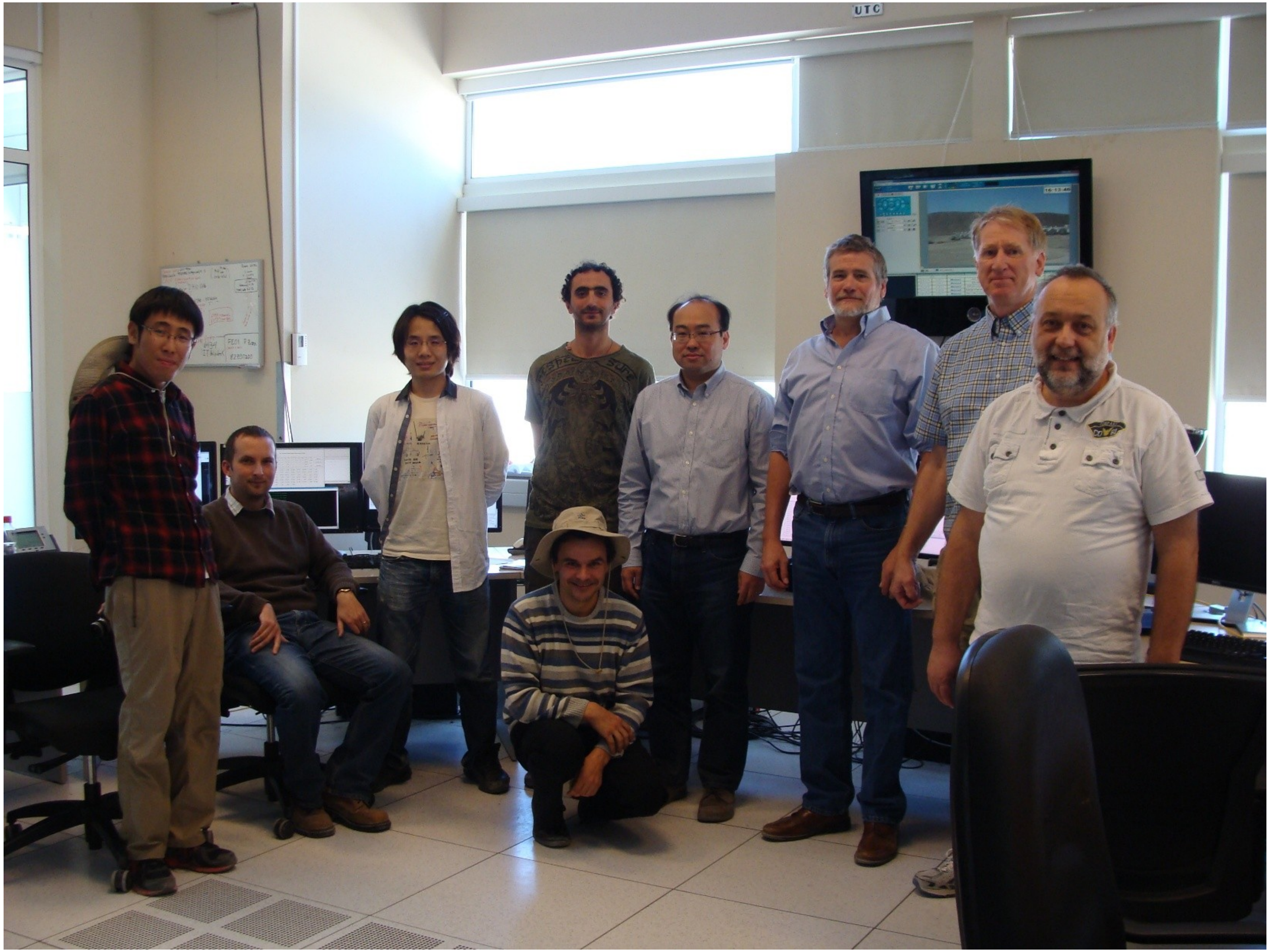
UTC

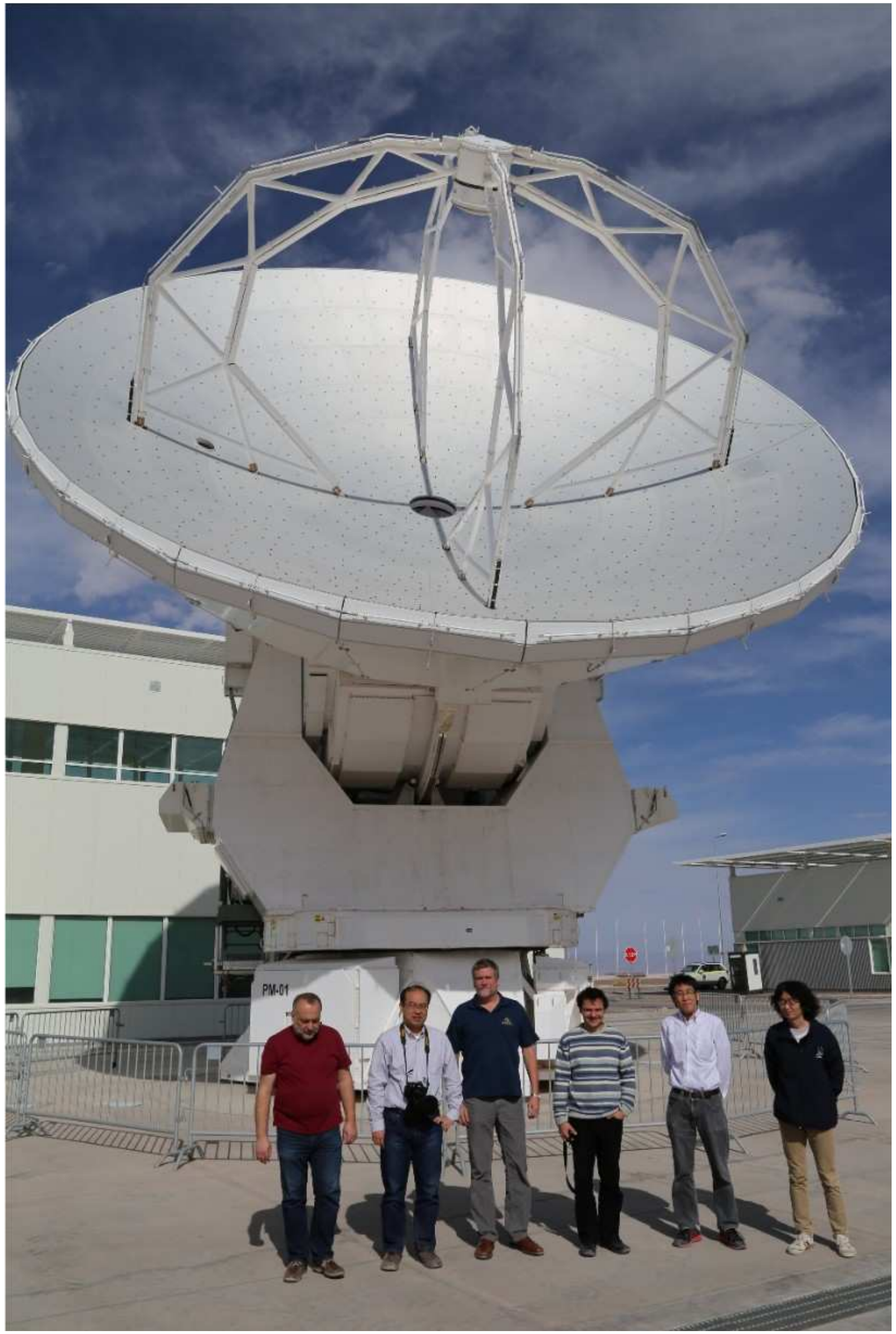
PM-01

Díky za pozornost!